RADC-TDR-63-302

August 1963

SUPPRESSION OF SPURIOUS FREQUENCIES

By

L. Young, E. G. Cristal, B. M. Schiffman, L. A. Robinson

Stanford Research Institute
Menlo Park, California

SRI Project 4096

Contract AF 30(602)-2734

Prepared for

Rome Air Development Center
Research and Technology Division
Air Force Systems Command
United States Air Force
Griffiss Air Force Base, New York

FOREWORD

This is the Final Report issued on Contract AF 30(602)-2734, SRI Project 4096. It summarizes research on the suppression of spurious frequencies, conducted by the Electromagnetic Techniques Laboratory of Stanford Research Institute on behalf of the Electromagnetic Vulnerability Laboratory of the Rome Air Developmemt Center. The detailed description of this work is given in four quarterly progress reports issued by Stanford Research Institute. (The contents of these reports are listed in the appendix.) The program covered the period 26 March 1962 to 15 May 1963. Captain Owen Allen served as the technical monitor on this contract.

ABSTRACT

This report summarizes the work done on several experimental components and theoretical topics, all concerned with the problem of suppressing spurious frequency emissions from high-power transmitters.

New and improved waffle-iron filters are described. A substantial improvement is obtained in the pass-band VSWR, the bandwidth, and the power-handling capacity.

Experimental data on the performance of a high-power, low-pass, coaxial leaky-wave filter are reported. The filter is absorptive rather than reflective in the stop-band, which exceeds 8 octaves.

The attenuation constant of a waveguide leaky-wave filter structure is solved for analytically over a two-to-one frequency range. The solutions show the dependence of the attenuation constant on the various design parameters of the filter.

Several 0-db and 3-db couplers were tested as harmonic pads. The best results were obtained with the short-slot sidewall coupler.

A new band-stop filter design technique for suppressing harmonic frequencies is described. A strip-line version was constructed, and measurements on it bore out the theory.

The relationship between attenuation and time delay of filters is investigated analytically, and several useful formulas are given.

The transient responses of four different types of filters (both with and without dissipation loss) to rectangular and sine-squared pulses of different lengths are presented.

Thin-film bolometers were investigated and found to be capable of measuring power over a wide frequency range without regard to mode.

PUBLICATION REVIEW

This report has been reviewed and is approved

Approved: for Robert Powers

OWEN W. ALLEN
Capt., USAF
Interference Reduction Branch

Approved: Samuel D. Zaccari

SAMUEL D. ZACCARI, Chief
Electromagnetic Vulnerability Lab
Directorate of Communications

FOR THE COMMANDER: for Fred J. Brainard

IRVING J. GABELMAN
Director of Advanced Studies

CONTENTS

CONTENTS

ILLUSTRATIONS

ILLUSTRATIONS

TABLES

I INTRODUCTION

The research described in this report covers several aspects of the fight to suppress the emission of spurious energy from high-power transmitters: waffle-iron filters to provide high reactive attenuation; harmonic pads to protect the transmitter and prevent arcing from harmonic resonances; leaky-wave filters to provide high dissipative attenuation; band-stop filters to provide high attenuation at particular frequencies; and wide-band bolometers to measure the combined power of many harmonic frequencies. The analytical investigation included the effect of filter bandwidth and filter type on the attenuation and group delay, and on the transient response to both rectangular and shaped pulses.

The work on the waffle-iron filter (Sec. II) has produced a number of very successful designs, which represent a considerable improvement on the earlier versions. Improvements were obtained in the pass-band width and in the power-handling capacity.

Performance data of a high-power, $1\frac{5}{8}$-inch, low-pass, coaxial leaky-wave filter are presented in Sec. III. A $1\frac{5}{8}$-inch, coaxial leaky-wave filter was constructed and its attenuation and mismatch loss were measured for an incident TEM wave from 1 to 10 Gc. Also, the attenuation and mismatch loss were determined for the next-higher-order propagating mode, the TE_{11} mode. High-power tests were conducted to determine the peak power capacity of the filter. Methods for improving the attenuation rate of the leaky-wave filter about its cutoff frequency, and also for increasing the attenuation of the TE_{11} mode of a particular polarization are discussed.

Leaky-wave absorption filters have been found advantageous for the suppression of spurious energy of high-power transmitters. However, although there are experimental data on the properties of several specially constructed leaky-wave filters, there are apparently few data relating the effect upon filter attenuation of varying one or more of the possible design parameters. In Sec. IV, a filter structure that retains the basic geometry of waveguide leaky-wave filters is analyzed theoretically over a finite frequency range. The complex propagation constant for the least-attenuated leaky-wave mode was obtained by reducing the fundamental integral equation to a transverse resonance equation and solving the reduced equation.

The attenuation constant of the least-attenuated mode was obtained for values of $2a/\lambda$ (*i.e.*, the ratio of waveguide width to one-half the free-space wavelength) ranging from 0 to 2. Its dependence on various design parameters of leaky-wave filters, such as main waveguide height, spacing of the coupling slots, width of coupling slots, and height of the absorbing waveguides, is presented. Good correspondence between theoretically computed curves and experimental data was obtained.

Work on harmonic pads, using directional couplers with 0-db coupling at the fundamental frequency, is still at an early stage. Several branch guide couplers have been constructed and tested, and commercial, 3-db, sidewall couplers have been purchased and tested. Early results, as explained in Sec. V, are promising, and point to possible further improvements.

The most troublesome spurious frequencies are often harmonics of the carrier frequency. Such undesired radiation can be very effectively suppressed by means of band-stop filters designed to strongly reject narrow frequency bands. This problem was considered (Sec. VI) with the added stipulation that the filter be very well-matched in the pass band, and a relatively new design technique was used to solve this problem.

The connection between attenuation and group delay in the pass band of transmission-line and lumped-constant filters has been investigated (Sec. VII). If the group delay varies with frequency in the pass-band of narrow-band filters, the input signal emerges distorted at the output. Hence it is important to maintain fairly constant group delay in such filters.

The transient responses to rectangular and sine-squared pulses of four types of filters are presented in Sec. VIII. The four types of filters are the equal-ripple filter, the maximally flat filter, the maximally flat time-delay filter, and the equal-element filter. The cases of the filters having three- and six-resonators are considered. All filters have the same bandwidth, measured to the points of 30-db attenuation, which is well within the the stop-band. The effect of varying the filter bandwidth relative to the pulse-spectrum is shown. The effect of dissipation loss is also demonstrated for the usual situation in microwave filters where all of the resonators have the same unloaded Q.

The useful power that a transmitter generates is ordinarily confined to a narrow frequency range, whereas the spurious emissions usually cover

an extremely wide frequency range. Adequate power-measuring equipment is usually available to measure the useful transmitter power, but little equipment has been developed to monitor the wide-band spurious emission. Yet it is important to keep the level of the latter low, just as it is important to raise the transmitter power. Thin-film bolometers appear to have desirable characteristics for monitoring the spurious power output and a number of these devices were investigated (Sec. IX).

II WAFFLE-IRON FILTERS*

A. GENERAL DESCRIPTION AND HISTORY

A waffle-iron filter is a waveguide low-pass filter with a wide stop-band, in which there are no spurious pass-bands such as usually arise with other types of waveguide filters in which higher-order modes may propagate. It is a passive, reciprocal (ideally) lossless filter in which attenuation is caused only by reflection above the cutoff frequency. This form of filter is compact, with a low VSWR and generally negligible loss in the pass-band, and with a high attenuation per unit length in the stop-band.

The waffle-iron filter was invented by S. B. Cohn, and has been developed progressively at Stanford Research Institute.[1-9]† The filter was first described by B. M. Schiffman in a 1957 SRI Report.[1] All the filters described previously[1-6] were modeled closely on the original designs of Cohn and Schiffman.

A new generation of waffle-iron filters has recently been investigated, based on a suggestion by Young.[7] These new types have a wide pass-band, as well as a wide stop-band, and handle several times the peak power handled by the earlier filters. The new filters typically have a VSWR less than 1.15 over almost the entire *L*-band; they have the same stop-band attenuation and frequency limits as the previously mentioned filter; when four filters were paralleled in a single compact design, it had a peak power handling capacity of over five times that of the earlier version.[4]

B. SUMMARY OF DESIGN PRINCIPLES

The waffle-iron filter is based on the wideband corrugated rectangular-waveguide filter with a uniform *E*-plane cross section, which has been treated by Cohn.[10,11] The analysis takes into account the fringing fields at the two ends of each high-impedance region. To facilitate

---

* The work reported herein is described in more detail in Quarterly Progress Reports 1, 2 and 4.

† References are listed at the end of the section

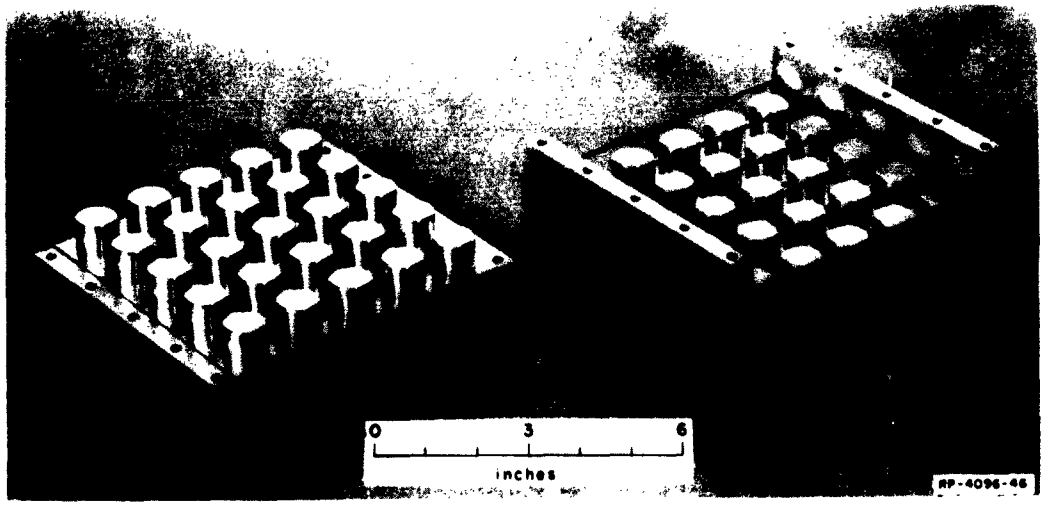

SOURCE: Quarterly Progress Report 2, Contract AF 30(602)-2734, SRI (See Ref. 43 by L. Young)

FIG. II-1 EXPLODED VIEW OF WAFFLE-IRON FILTER WITH ROUND TEETH AND HALF--INDUCTANCES AT THE ENDS

the explanation, picture the filter lying with its broad wall horizontal, as shown in Fig. II-1. In the frequency band of interest the fringing fields are of two main types. First, there are essentially vertical lines of force, bridging the gap between two opposite teeth (one vertically above the other); these fields form the shunt capacitances of the low-pass filter, storing electric energy. Similarly, there is a series-inductance effect due to magnetic energy stored between (horizontally) neighboring teeth. The product of the shunt capacitance and series inductance determine the filter cutoff frequency. Second, there are electric lines of force that are essentially horizontal, bridging the gap between two neighboring teeth set in the same block (Fig. II-1); these electric fields result in a bridging capacitance across the series inductance, forming a parallel resonant circuit that causes infinite attenuation (theoretically) at some frequency. This infinite-attenuation frequency is above the cutoff frequency of the filter because the filter structure is designed so that the fields between neighboring teeth are weaker than the fields between opposite teeth.

C. DESIGN OF FILTERS WITH VERY WIDE PASS-BANDS

The improved matching of the new filter in the pass-band may be readily understood qualitatively by reference to Figs. II-2 and II-3. The low-frequency approximation to a waffle-iron filter is the *L-C* circuit shown in Fig. II-2, with the capacitances shown approximating the gaps between opposite teeth, and the inductances approximating the longitudinal or transverse slots. For clarity the (smaller) bridging capacitances across the inductances (mentioned in Part B) have been omitted in Fig. II-2. Such a filter consists of a number of identical sections whose image impedances Z_I match (on the image-impedance basis) section-to-section.[15] The individual sections of which the filter is made up may be considered as π-sections [Fig. II-2(a)] or as T-sections

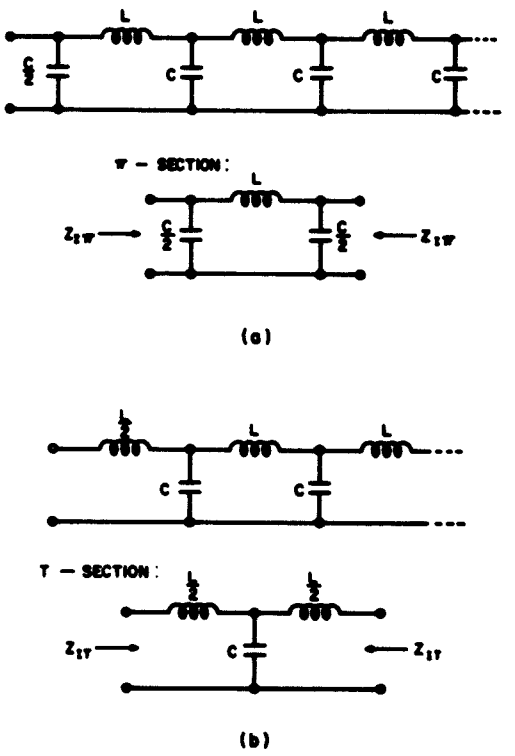

FIG. II-2 LUMPED-CONSTANT LOW-PASS FILTER (Pass-Band Approximation):
(a) Starting with Half-Capacitance,
(b) Starting with Half-Inductance

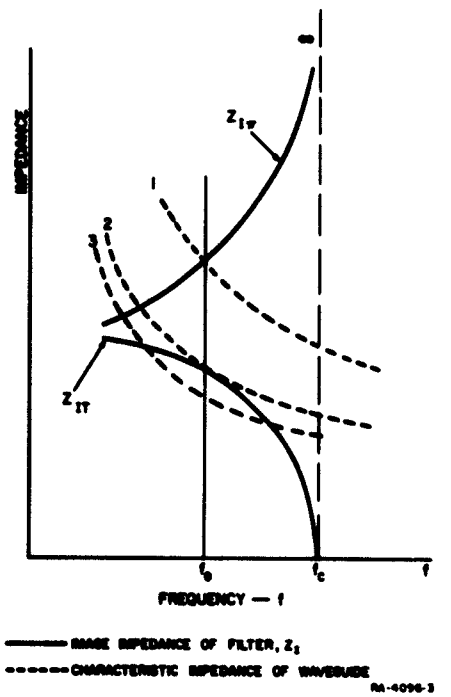

FIG. II-3 IMAGE IMPEDANCE OF LOW-PASS FILTER AND CHARACTERISTIC IMPEDANCES OF WAVEGUIDES OF VARIOUS HEIGHTS

[Fig. II-2(b)]. This does not affect the interior elements of the filter, but determines whether the first and last elements are to be half-capacitances [Fig. II-2(a)] or half-inductances [Fig. II-2(b)]; it also determines whether the image impedance is to be $Z_{I\pi}$ or Z_{IT} (Fig. II-2). These two image impedances vary differently with frequency, $Z_{I\pi}$ increasing and Z_{IT} decreasing with frequency, as shown in Fig. II-3. On the same figure are three typical curves (broken lines) showing how the waveguide characteristic impedance changes with frequency. If it is required to match the π-section waffle-iron filter (which begins and ends with a half-capacitance, as in the earlier filters[1-6]) at the design frequency f_0, then a waveguide must be chosen corresponding to Curve 1 in Fig. II-3. It is readily appreciated that this results in a relatively narrow pass-band, since $Z_{I\pi}$ and the waveguide impedance diverge quite rapidly. On the other hand Z_{IT} runs tangential to the waveguide impedance, leading to the possibility of good match over a wide pass-band. Such a filter must begin with a half-inductance.

The filter shown in Fig. II-1 was derived from an earlier filter,[4] whose dimensions have already been given. However, the new filter begins and ends on a transverse plane half-way between two rows of teeth. Such an end-section is equivalent to one beginning with a half-inductance. The only other change made was to replace the square teeth by circular teeth (to increase the power-handling capacity); in making this change, the area of the top of each tooth was kept approximately constant (so that the capacitances would remain approximately the same); the diameter of each new round tooth was made equal to 0.893 inch. The center-to-center spacing is still 1.300 inch (five teeth to a row). The b-dimension[7] is still 1.610 inch, and the b''-dimension[7] between teeth is also 0.210 inch. The exposed circular edge of the teeth is rounded to a radius R = 0.063 inch.

The image impedance of this filter was determined experimentally by Dawir's method[12,13] and was found to correspond to the impedance of a waveguide of height 0.375 inch. The VSWR was then measured with the filter between three successive pairs of similar waveguides, each pair of a different height, 0.350 inch, 0.375 inch, and 0.400 inch. It is evident from Fig. II-4 that 0.400 inch is slightly too high, corresponding to a Curve-1 situation in Fig. II-3. There is a tendency for all VSWR curves to come down to unity at about 1225 Mc and again at about 1635 Mc. This was shown by separate measurements (not reproduced here) to be due to

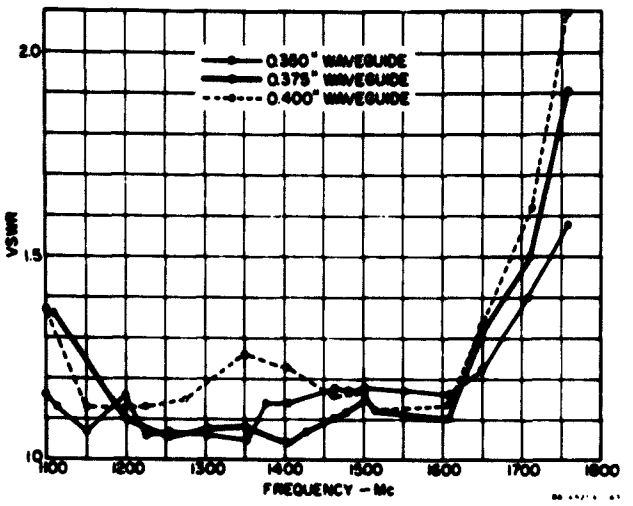

FIG. II-4 PASS-BAND VSWR OF SINGLE-LAYER WAFFLE-IRON FILTER WITH ROUND TEETH AND HALF-INDUCTIVE END-SECTIONS (Fig. II-1) OPERATING BETWEEN WAVEGUIDES OF VARIOUS HEIGHTS

the filter's being one wavelength long at 1225 Mc and one-and-one-half wavelengths long at 1635 Mc. It is seen from Fig. II-4 that the average image impedance over *L*-band corresponds closely to a waveguide height of between 0.350 inch and 0.375 inch.

D. FOUR-LAYER FILTER

One of the prime objectives of this investigation was to increase the power-handling capacity of the previously built filters. The change from square to round teeth[7] helps appreciably (see below). Dividing the power among *n* identical waffle-iron filters, and then combining their outputs, raises the power-handling capacity *n* times. It is mechanically simplest to parallel only two filters: This results in a structure that can generally be fitted into standard waveguide, and which can be matched with especial mechanical simplicity. Paralleling four filters leads to a structure that is approximately square in cross section, and that handles four times the peak power of a single filter. The waffle-iron filter shown in Fig. II-5 consists of four filters of the type shown in Fig. II-1. To match into and out of this filter, two binary power dividers were constructed as shown in Fig. II-5. (Notice that the

electrical length from the input of a power-divider to any one of its four outputs has been kept the same.) The over-all length of the filter and two power dividers shown in Fig. II-5 is 24 inches.

The low-power performance of the two filters (that shown in Fig. II-1, and the composite filter unit shown in Fig. II-5) were found to be nearly the same. The second filter should handle four times as much peak power as the first. However, there is a possibility of resonances around the plates of the composite filter, if there should be electrical path differences or other unbalancing effects between the four parallel paths. No such resonance was ever observed in this filter, which had been carefully constructed. To forestall the possibility of such a resonance in less well constructed filters, coupling can be introduced between the layers by, for instance, cutting large circular holes between the circular teeth.[8]

The VSWR of the four-layer filter, with or without coupling holes, including both power dividers and tapers to WR-650 waveguide, is better than 1.20 from 1100-1650 Mc, *i.e.*, over almost the whole of *L*-band.

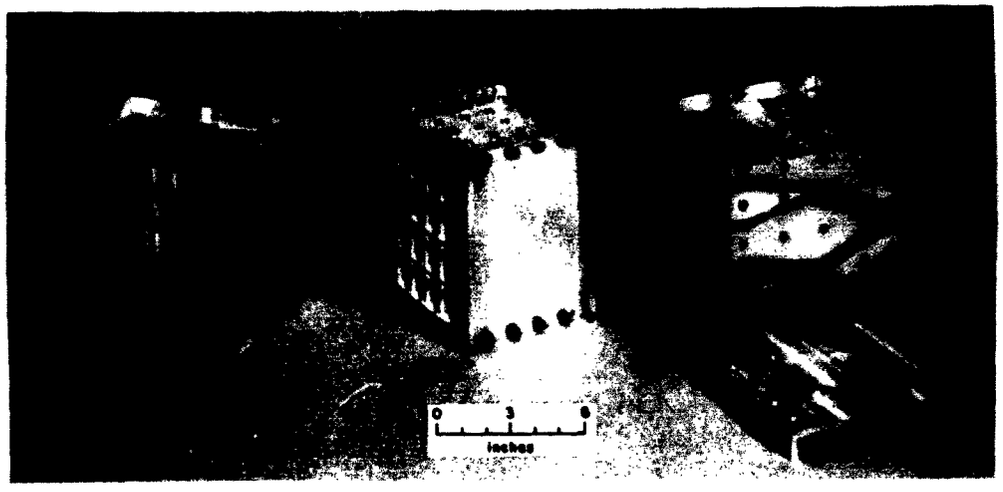

FIG. II-5 FOUR-LAYER WAFFLE-IRON FILTER WITH POWER DIVIDERS

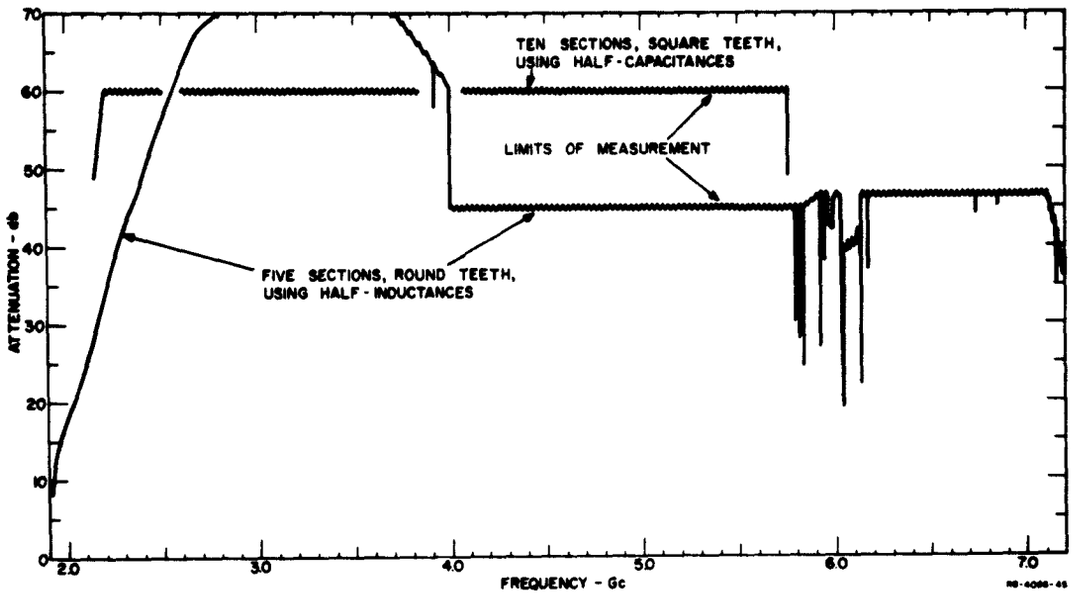

SOURCE: Quarterly Progress Report 2, Contract AF 30(602)-2734, SRI
(See Ref. 43 by L. Young)

FIG. II-6 STOP-BAND ATTENUATION CHARACTERISTICS OF WAFFLE-IRON FILTER IN FIG. II-1

E. ATTENUATION MEASUREMENTS IN THE STOP-BAND

The filter tested had five sections, round teeth, and half-inductance end-sections; its stop-band attenuation characteristic is plotted in Fig. II-6. The wriggly lines indicate the limits of measurement, determined by the available signal-generator power and the receiver sensitivity. The measurements were made with a continuously (mechanically) swept signal generator, and the filter output was measured by a broad-band bolometer connected to a chart recorder. (It would have been impractical to take point-by-point measurements with a superheterodyne receiver, since the spurious responses are very sharp and would probably have been missed.)

A traveling-wave-tube amplifier was available from 2 to 4 Gc, thus giving additional sensitivity. For instance, the attenuation of both filters at the second and third harmonics of 1.3 Gc (the nominal band-center) is greater than 60 db. It may be more than 60 db up to 5.8 Gc, but without the TWT amplifier the limit of measurement was 45 db. The humpbacked appearance of the curve is not due to the filter, but is due to the extra available power from the TWT. There were several spurious responses in the region 5.8-6.2 Gc (not shown in Fig. II-6), but another

clear stop-band (which had not been predicted) existed from 6.2 to 7.1 Gc, where the attenuation was at least 40 db.

F. HIGH-POWER PERFORMANCE

Tests at power levels sufficiently high to induce breakdown were made on four different waffle-iron filters designed for the *L*-band. The results of these tests, together with the results of tests made earlier,[4] are summarized in Table II-1. Two of the four filters tested are shown in the photographs, Figs. II-1 and II-5, as indicated in Table II-1. The other two filters are the ones referred to as Waffle-Iron Filters I and II in Ref. 4. (Tests 1 and 2 were on Waffle-Iron Filter I, and Test 3 was on Waffle-Iron Filter II.) The two columns of Table II-1 with the common heading "Peak Power, Mw" gives, first, the value of peak power (in megawatts) observed after arcing was induced and then quenched by reducing the power. The reduced power at which the arc is quenched, called the *all-clear power*, is the value listed. The second column under the same heading gives the all-clear power that might be expected when the filter is perfectly matched at its output. This value of power is calculated by applying a small correction factor equal to the load VSWR.

Table II-1

SUMMARY OF HIGH-POWER TESTS ON WAFFLE-IRON FILTERS

TEST NO.	WAFFLE-IRON FILTER			TEST FREQUENCY (Gc)	PULSE LENGTH (μsec)	PULSE REPETITION FREQUENCY (cps)	PEAK POWER (Mw)		TESTED BY
	Fig. No.	Description	Filter Cutoff (Gc)				Measured All-Clear	Corrected for Load VSWR	
1	--	Square Tooth[4]	2.0	1.3	2	60	1.26	1.64	E. D. Sharp[4]
2	--	Square Tooth[4]	2.0	1.3	110	30	0.48	0.51	Authors
3	--	Square Tooth[4]	5.0	1.3	110	30	0.68	--	Authors
4	II-1	Round Tooth	2.0	1.3	110	30	0.56	0.66	Authors
5	II-5	Round Tooth, 4-Layer	2.0	1.35	2.5	200	6.3*	--	Authors

*This value is believed to have been limited by the system capability rather than the filter. A value of 8.5 Mw was predicted. See the text.

By comparing Tests 2 and 4, one can see that the filter with round teeth can carry 1.3 times as much power as the square-tooth filter, with 110-microsecond pulse length. If we extrapolate this relationship to calculate the 2-microsecond pulse power capability of a round-tooth filter, we obtain a value of $1.3 \times 1.61 = 2.1$ Mw. For a four-layer

filter with round teeth, and still with 2-microsecond pulses, we obtain a predicted pulse power capability of (1.3 × 1.64 × 4) ≈ 8.5 Mw. Test 5 shows that this four-layer filter actually carried 6.3 Mw power with a 2.5-microsecond pulse. It is considered unlikely, however, that breakdown occurred in the waffle-iron filter, because the waveguide system without the filter was later found to break down at 6 Mw peak power, and because no burn marks were found on the four-layer filter. For comparison, the computed power handling capacity[14] of full-height *L*-band waveguide at 1.3 Gc is 14 Mw, assuming a voltage gradient at breakdown of 15 kv per cm.

G. TWO-LAYER WAFFLE-IRON FILTER

In order to increase the power-handling capacity of the waffle-iron filter, a number of such filters can be paralleled, as already described in connection with the four-layer high-power filter. In some applications it will be desirable to fit the filter into a waveguide cross section; this is not possible with four filters in parallel, but works out very conveniently for two filters in parallel, at least with the present waffle-iron filter design.

A two-layer filter, complete with matching transformer-power dividers and with twice the theoretical peak power capability of a single-layer filter was constructed for the *L*-band. The filter portion is shown in Fig. II-7. Its performance is similar to the other filters.[8]

H. MODIFIED CASCADED WAFFLE-IRON FILTERS[15]

The waffle-iron filter developed on Contract AF 30(602)-2392 was modified so that its pass-band bandwidth was approximately doubled, while at the same time its length was reduced by about one-third. This results in an electrically improved and mechanically more compact filter.

The original filter consisted of three separate waffle-iron filters designed for separate and slightly overlapping stop-bands. They were cascaded, with quarter-wave transformers placed between them to match their different image impedances.

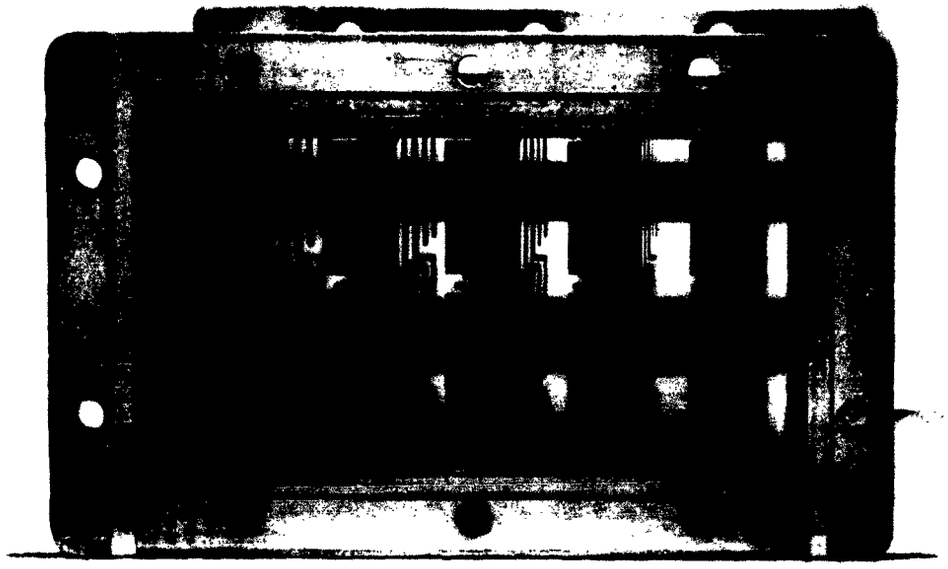

RP-4000-04

FIG. II-7 PHOTOGRAPH OF TWO-LAYER WAFFLE-IRON FILTER

Two design modifications were undertaken:

(1) A half-section was removed at each end of the three separate filters,[4] thus turning the half-capacitance end sections into half-inductance end sections,[7] in order to widen the pass-band of each filter.

(2) The dimensions of the teeth were adjusted to make the image impedances of the three separate filters equal to one another, so that no matching transformers would be required between them when they were cascaded.

The three filters are shown connected in Fig. II-8. The over-all length of the filter is 18.494 inches compared with a little over 30 inches for the earlier filter[4] (9.5 inches is accounted for by the intermediate transformers, and about 2 inches by the removal of one section per filter).

The pass-band VSWR is shown in Fig. II-9. The heavy solid line is the final VSWR obtained with matching posts and bars.[15] It is seen that the three waffle-iron filters, cascaded as shown in Fig. II-7, have a VSWR of less than 1.15 from 1190 to 1560 Mc, and remain below 1.4 over the whole of *L*-band (1120-1700 Mc). The performance compares favorably with the earlier filter,[4] whose VSWR is also shown in Fig. II-9 for comparison.

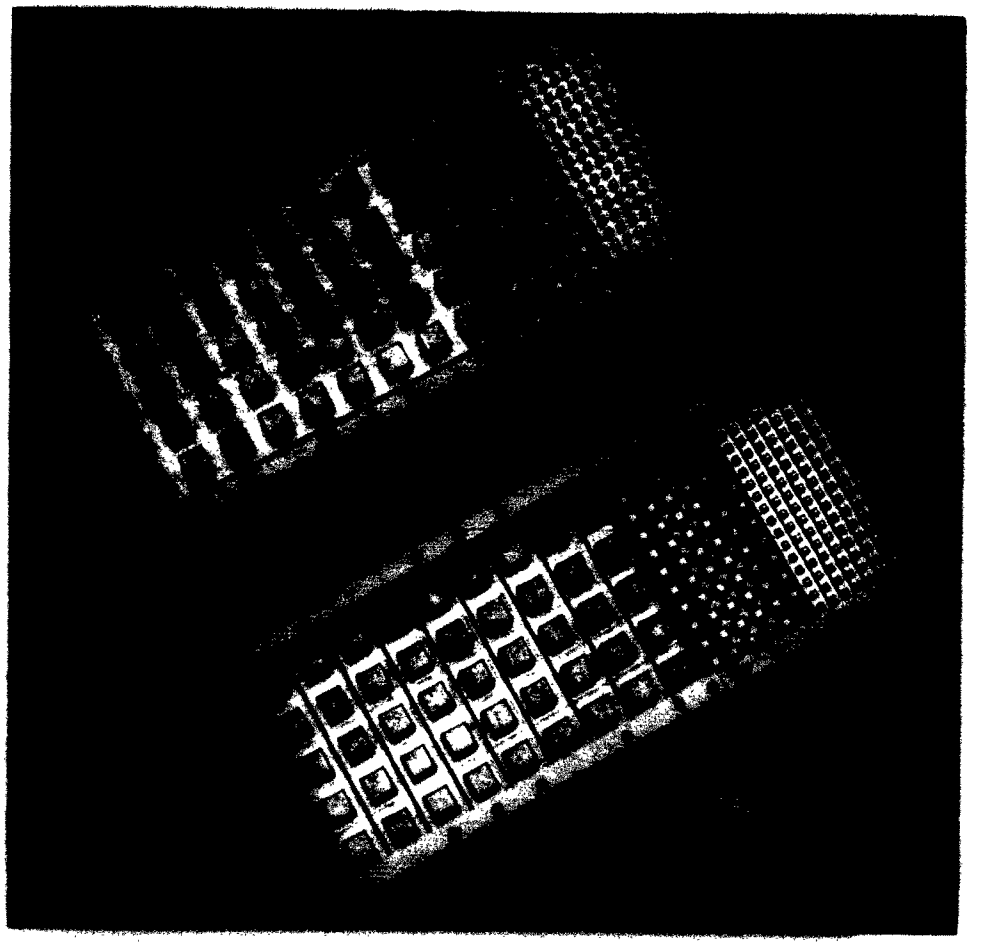

FIG. II-8 EXPLODED VIEW OF THREE WAFFLE-IRON FILTERS IN CASCADE

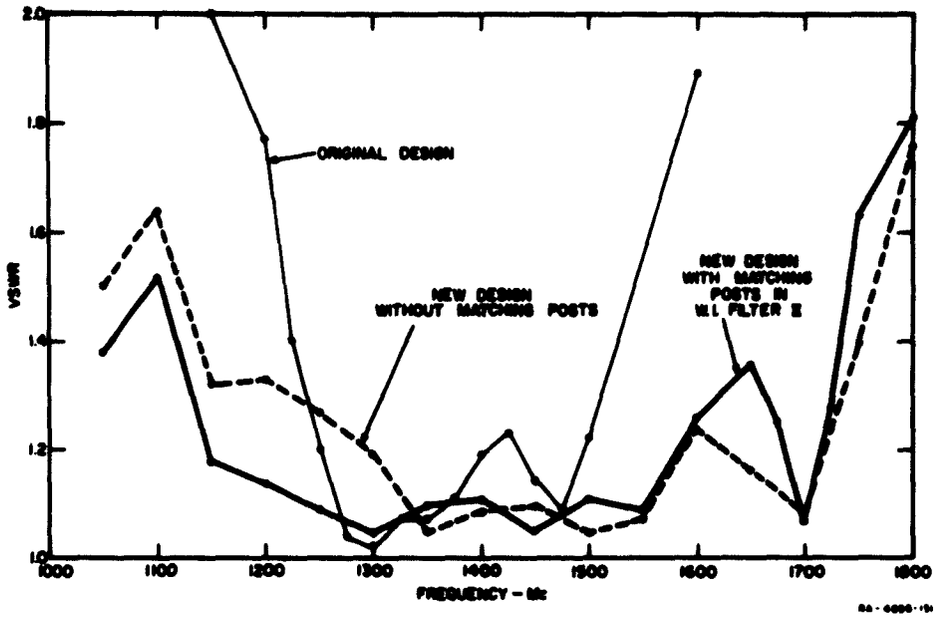

FIG. II-9 VSWR OF THREE WAFFLE-IRON FILTERS IN CASCADE
(The original waffle-iron filter with half-capacitance end sections is also shown for comparison.)

The attenuation measurements in the stop-band were made as described before[4,8] and were limited by the sensitivity of the equipment. No deterioration in the stop-band was observed compared with the previously published curves.[4] The attenuation was at least 60 db from 2.1 to 13.8 Gc, except in two regions: the sensitivity fell from 60 db to 55 db between 6.8 to 7.5 Gc, so that it is not known for certain whether it exceeded 60 db in this region; and the attenuation dropped measurably, but remained better than 55 db in the region 9.7 to 10.3 Gc. With these exceptions it thus remained above 60 db from the second to the tenth harmonic of 1.3 Gc. These results are consistent with Fig. 13 of Ref. 4.

Figure II-10 is a photograph of the seven-section quarter-wave transformers[15] used to match the waffle-iron filter to WR-650 waveguide. The transformer alone had a VSWR of less than 1.01 over and beyond the *L*-band.

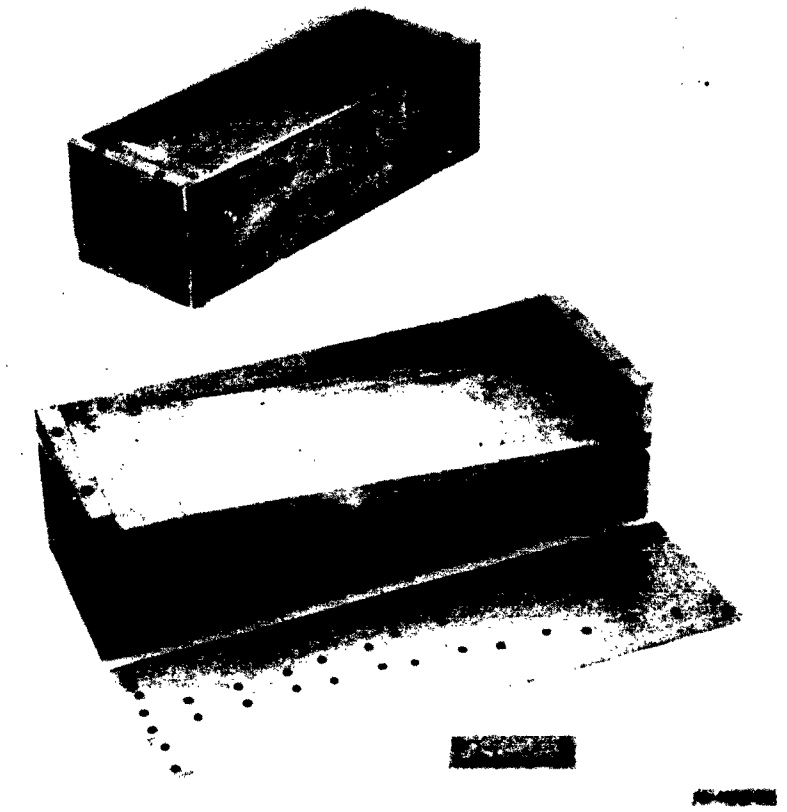

FIG. II-10 PHOTOGRAPH OF SEVEN-SECTION QUARTER-WAVE TRANSFORMER

REFERENCES

1. S. B. Cohn, E. M. T. Jones, O. Heinz, J. K. Shimizu, H. M. Schiffman, and F. S. Coale, "Research on Design Criteria for Microwave Filters," Final Report, SRI Project 1331, Contract DA-36-039 SC-64625, Stanford Research Institute, Menlo Park, California (June 1957).

2. S. B. Cohn, C. Flammer, E. M. T. Jones, and H. M. Schiffman, "Design Criteria for Microwave Filters and Coupling Structures," Technical Report 2, SRI Project 2326, Contract DA 36-039 SC-74062, Stanford Research Institute, Menlo Park, California (June 1958).

3. H. Guthart and E. M. T. Jones, "A High-Power S-Band Waffle-Iron Filter," Technical Note 4, SRI Project 2797, Contract AF 30(602)-1998, Stanford Research Institute, Menlo Park, California (March 1961). RADC TN-61-121.

4. E. Sharp, "A High-Power Wide-Band Waffle-Iron Filter," Technical Note 2, SRI Project 3478, Contract AF 30(602)-2398, Stanford Research Institute, Menlo Park, California (January 1962). RADC-TDR-62-182. To be published in the *IRE Trans. PGMTT*.

5. H. M. Schiffman and S. B. Cohn, "Wide-Band Waveguide Filters," PGMTT National Symposium, Harvard University, Cambridge, Massachusetts (1959).

6. H. Guthart and E. M. T. Jones, "High-Power *S*-Band Filter," *IRE Trans.* MTT-10, pp. 148-149 (March 1962).

7. Leo Young, "Suppression of Spurious Frequencies," Quarterly Progress Report 1, SRI Project 4096, Contract AF 30(602)-2734, Stanford Research Institute, Menlo Park, California (July 1962).

8. L. A. Robinson, E. G. Cristal, B. M. Schiffman, and Leo Young, "Suppression of Spurious Frequencies," Quarterly Progress Report 2, SRI Project 4096, Contract AF 30(602)-2734, Stanford Research Institute, Menlo Park, California (October 1962).

9. G. L. Matthaei, L. Young, and E. M. T. Jones, "Design of Microwave Filters, Impedance Matching Networks, and Coupling Structures," SRI Project 3527, Contract DA 36-039 SC-87398, Stanford Research Institute, Menlo Park, California (January 1963).

10. S. B. Cohn, "Analysis of a Wide-Band Waveguide Filter," *Proc. IRE* 37, pp. 651-656 (June 1949).

11. S. B. Cohn, "Design Relations for the Wide-Band Waveguide Filter," *Proc. IRE* 38, pp. 799-803 (July 1950).

12. H. N. Dawirs, "Graphical Filter Analysis," *IRE Trans.* MTT-3, pp. 15-21 (January 1955).

13. H. N. Dawirs, "A Chart for Analyzing Transmission-Line Filters from Input Impedance Characteristics," *Proc. IRE* 43, pp. 436-443 (April 1955).

14. G. L. Ragan (Editor), *Microwave Transmission Circuits*, Chapter 4 (McGraw-Hill Book Co., Inc., New York, 1948).

15. L. Young, B. M. Schiffman, E. G. Cristal, and L. A. Robinson, "Suppression of Spurious Frequencies," Quarterly Progress Report 4, SRI Project 4096, Contract AF 30(602)-2734, Stanford Research Institute, Menlo Park, California (June 1963).

III COAXIAL LEAKY-WAVE FILTERS*

A. GENERAL

This section describes a $1^5/_8$ inch coaxial leaky-wave filter which was designed for the suppression of harmonic and spurious frequency energy of high-power sources. A schematic diagram of the filter is given in Fig. III-1. It consists of a modified coaxial line having periodically spaced slot-pairs on the outer conducting wall. Each slot couples the coaxial line to a single waveguide that is terminated in a matched wide-band load. At frequencies in the filter pass-band, the side waveguides are cut off and energy in the coaxial line passes to the load unattenuated. However, at frequencies in the filter stop-band, the waveguides support propagation; hence, the energy within the coaxial line at these frequencies is coupled into the side waveguides, absorbed in loads, and thus greatly attenuated.

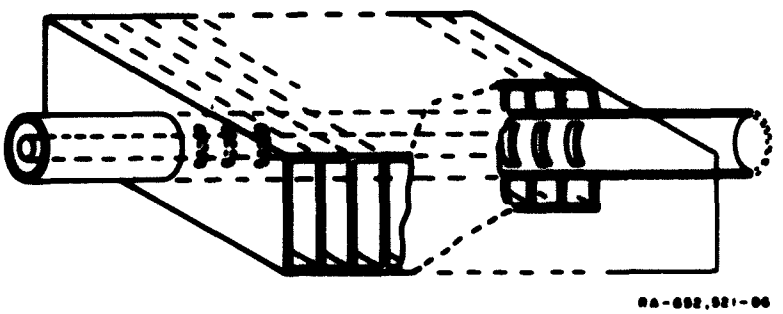

FIG. III-1 A COAXIAL LEAKY-WAVE FILTER FOR THE SUPPRESSION OF SPURIOUS ENERGY

* This investigation is reported in more detail in Ref. 1. (References are listed at the end of the section.)

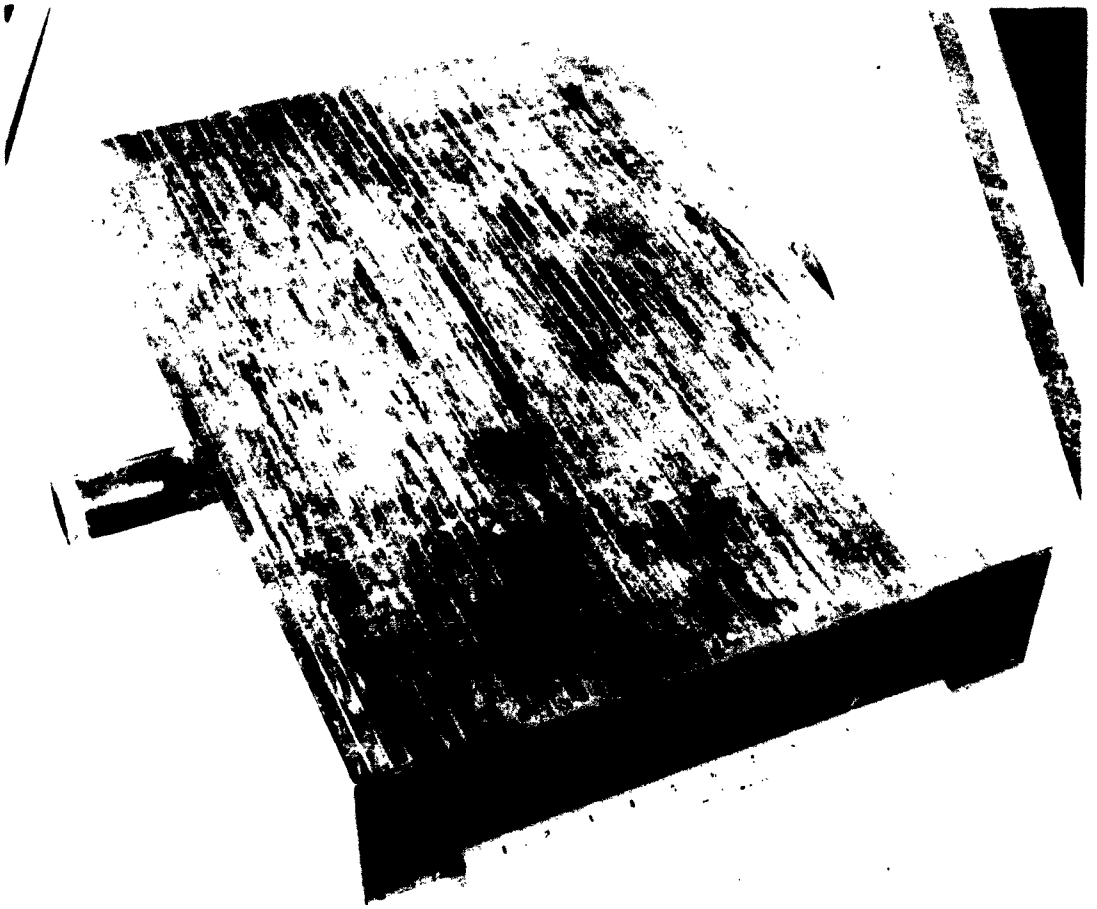

FIG. III-2 PHOTOGRAPH OF THE 1-5 8-INCH COAXIAL LEAKY-WAVE FILTER

A photograph of the actual filter is given in Fig. III-2. The filter has a cutoff frequency of 1.7 Gc. It is 16.5 inches long measured from the first slot to the last. There are a total of 41 slot-pairs: 10 slot-pairs at each end of the filter are gradually tapered in arc length in order to match the filter to the 50-ohm coaxial line. The remaining 21 slot-pairs subtend a 150-degree arc at the center of the coaxial line.

B. ATTENUATION AND MISMATCH LOSS OF THE 1 5/8-INCH COAXIAL LEAKY-WAVE FILTER FOR AN INCIDENT TEM WAVE

The filter shown in Fig. III-2 was tested for transducer loss* and mismatch loss† for an incident TEM wave over the frequency band 1.2 to 10 Gc. An electrically long, linear taper was used as a TEM-mode launcher. In the tests, a "50-ohm center conductor"§ was initially used with the filter. In addition to this center conductor, three other center conductors, whose impedances gradually tapered from 50 ohms at the input of the filter to smaller values of 40, 30 and 20 ohms, were also used with the filter. The smaller impedance center conductors were tapered from one end only. Therefore a single section quarter-wave impedance matching transformer was used at the low-impedance end of each center conductor in order to match the filter to the 50-ohm line in the pass-band. The purpose of using the tapered center conductors was to reduce the filter impedance in order to achieve greater attenuation per unit length. The attenuation of the filter using 50-, 40-, 30-, and 20-ohm center conductors is given in Fig. III-3. The data show that the filter has a wide stop-band and provides high attenuation throughout most of the stop-band.

An approximate relationship for the dependence of the attenuation of the filter on the center-conductor impedance is

$$[(L_a)_2/(L_a)_1] \approx [Z_1/Z_2] \qquad \text{(III-1)}$$

where $(L_a)_1$ is the attenuation of the filter in dbs when a center conductor of Z_1 ohms is used within the leaky-wave filter. In words, (Eq. (III-1) states that the attenuation is approximately inversely proportional to the center-conductor impedance and is independent of frequency. It is emphasized, however, that Eq. (III-1) is most reliable

---

* Transducer loss is defined as $10 \log_{10} (P_{avail}/P_L)$ db, where P_{avail} is the power available from the generator when the load presents a conjugate match to the generator, and P_L is the power delivered to the load resistance when the filter is in place. The transducer loss is always greater than or equal to zero db. Herein, when attenuation is referred to, the decibel transducer loss will be understood.

† Mismatch loss is the loss of incident power due to reflection. It is equal to $10 \log_{10} [(r+1)^2/4r]$ db, where r is the VSWR of the filter.

§ This notation signifies a center conductor having a diameter such that the characteristic impedance of the unperturbed coaxial line is 50 ohms. In this discussion, the impedance of the filter will often be associated with the center conductor in the above manner.

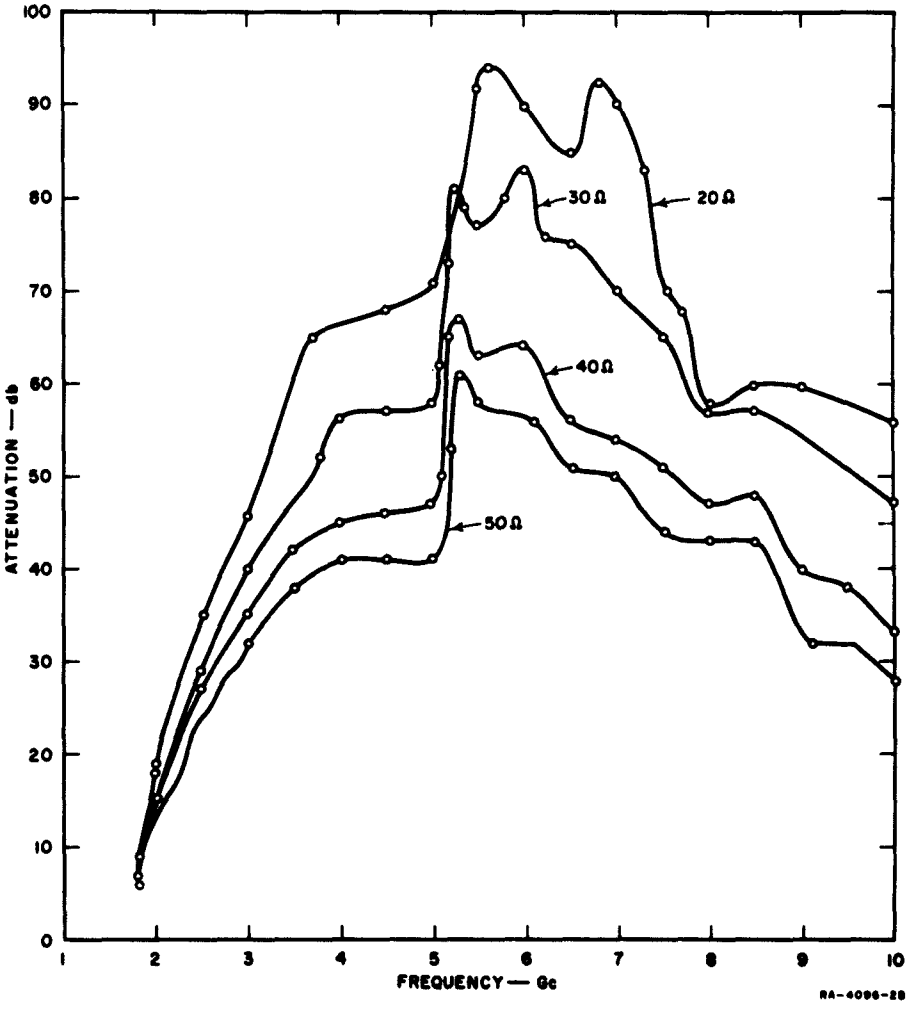

FIG. III-3 ATTENUATION OF THE 1-5/8-INCH COAXIAL LEAKY-WAVE FILTER FOR AN INCIDENT TEM WAVE

for moderate change in center-conductor impedance, and can be in considerable error either for large-percentage reductions in the center-conductor impedance, or if the center-conductor impedance is small to begin with.

The mismatch loss of the filter was determined from 1.7 to 9.5 Gc, using the four center conductors. The differences of the results obtained for the four conductors were small. In general, the mismatch loss was typically less than 0.1 db.

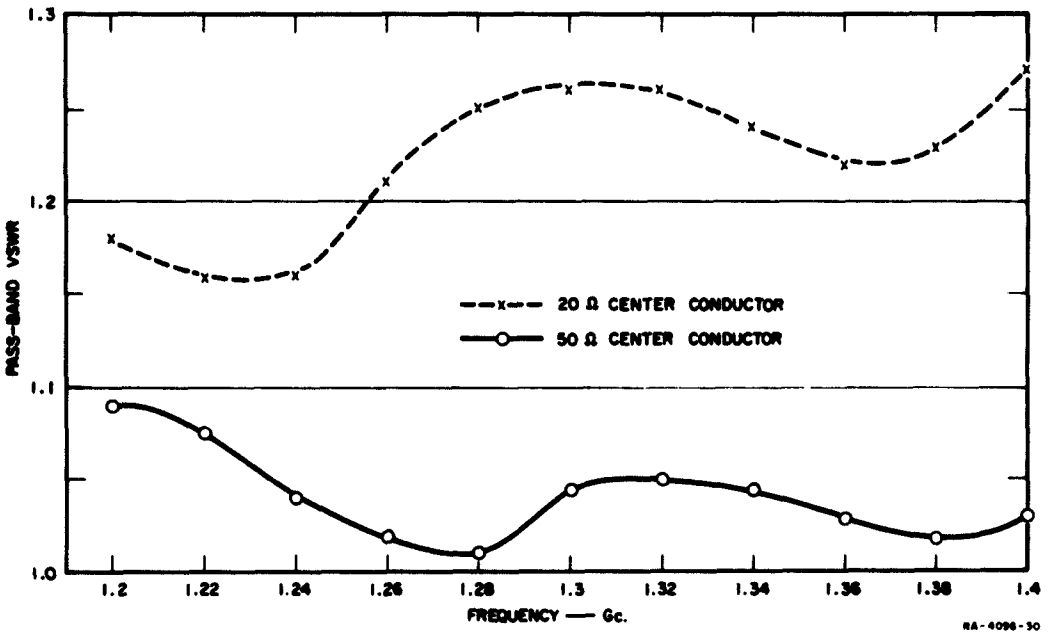

FIG. III-4 VSWR OF THE 1-5/8-INCH COAXIAL LEAKY-WAVE FILTER IN THE PASS-BAND

The VSWR in the pass-band of the filter for the cases of the 50- and 20-ohm center conductors is given in Fig. III-4. The pass-band in this instance is arbitrarily taken as 1.2 to 1.4 Gc, although the coaxial leaky-wave filter passes all frequencies below approximately 1.7 Gc. The VSWR curves of the 40- and 30-ohm center conductors are not shown in Fig. III-4; however, they generally lie between the 50- and 20-ohm center-conductor curves. The VSWR of the filter using the 20-ohm center conductor is less than 1.28. This VSWR could be reduced, if it were necessary, by

using a better matching section at the output of the filter. The VSWR for the 50-ohm center conductor was better than 1.08. The attenuation of the filter in the pass-band was also determined for the cases of the 50- and 20-ohm center conductors and found to be less than 0.2 db in both cases.

C. ATTENUATION AND MISMATCH LOSS OF THE $1^5/_8$-INCH COAXIAL LEAKY-WAVE FILTER FOR AN INCIDENT TE_{11} WAVE

The leaky-wave filter was also tested for attenuation and mismatch loss for an incident TE_{11} wave over the frequency interval 3.6 to 6.7 Gc. This frequency band approximately covers the interval in which only TEM and TE_{11} modes may propagate in a $1^5/_8$-inch, 50-ohm coaxial line.

The coaxial TE_{11} mode was generated by a waveguide-TE_{10}-mode-to-coaxial-TE_{11}-mode transducer. Two transducers were used in the measurement system; one for initiating and the other for capturing the mode. Details of the construction of the transducers and their manner of operation are given elsewhere.[2]

Figure III-5 shows an arbitrary angle coordinate, its direction relative to the orientation of the coaxial filter, and a particular orientation of the transverse electric field of the coaxial TE_{11} mode. A TE_{11} electric field having this particular orientation will be said to be of $\theta = 0$ *polarization*. The TE_{11} electric field of this polarization may be partially characterized by the fact that it has no θ-component at $\theta = 0$ and π, and no R-component at $\theta = \pi/2$ and $-(\pi/2)$.

Next, we define the $\theta = \pi/2$ *polarization* of the TE_{11} mode. This polarization is achieved by rotating the $\theta = 0$ polarized field by $\pi/2$ in the counterclockwise direction. In the $\pi/2$ polarization, the electric field has no θ-component at $\theta = \pi/2$ and $-(\pi/2)$, and no R-component for $\theta = 0$ and π. It can be shown that any other orientation of the TE_{11} mode can be obtained from a linear sum of the $\theta = 0$ and $\theta = \pi/2$ polarizations. Conversely, any arbitrary polarized TE_{11} field may be resolved into a combination of $\theta = 0$ and $\theta = \pi/2$ polarized fields. Further, the energies of the $\theta = 0$ and $\theta = \pi/2$ polarized fields are uncoupled. For these reasons, it is convenient to refer to the orientation of the TE_{11} electric field by the above nomenclature.

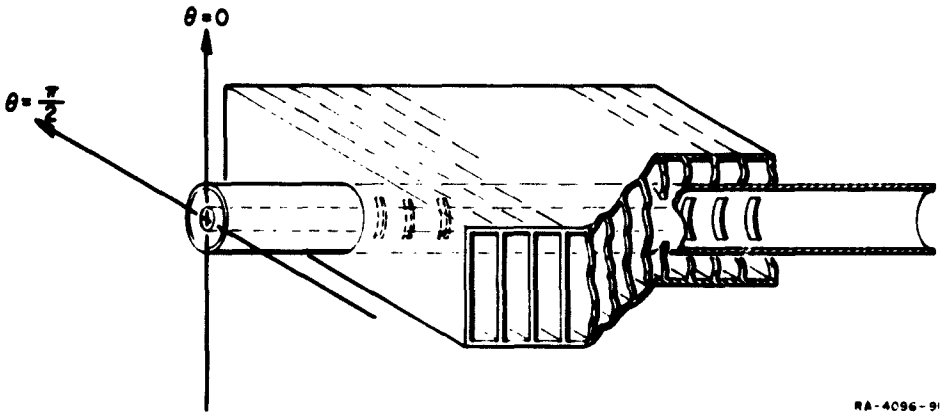

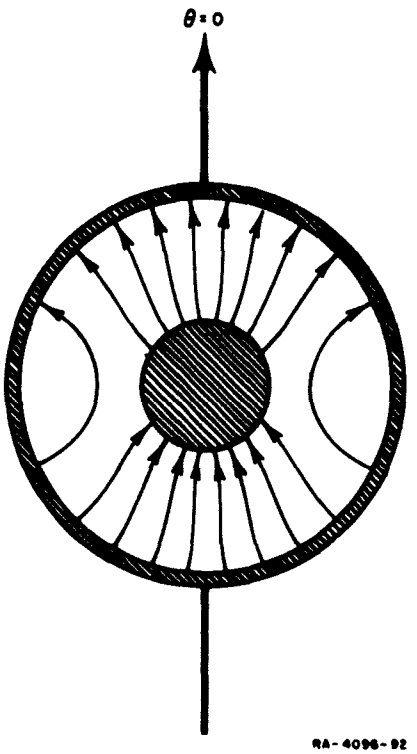

FIG. III-5 THE TRANSVERSE ELECTRIC FIELD CONFIGURATION OF THE COAXIAL TE_{11} MODE WITH AN ANGLE COORDINATE DESIGNATION AND THE COORDINATE DIRECTIONS RELATIVE TO THE ORIENTATION OF THE COAXIAL LEAKY-WAVE FILTER

Using the waveguide-TE_{10}-mode-to-coaxial-TE_{11}-mode transducers, attenuation and mismatch loss measurements of the coaxial leaky-wave filter were made over the frequency interval 3.6 to 6.7 Gc. The measurements were made for both the $\theta = 0$ and $\theta = \pi/2$ polarizations using the 50- and 20-ohm center conductors. No measurements were made using the 40- and 30-ohm center conductors because the results of the TEM attenuation measurements indicate that their responses would be bounded by those of the 50- and 20-ohm cases. The attenuation of the TE_{11} mode is given in Fig. III-6. Figure III-6 shows that fields of $\theta = \pi/2$

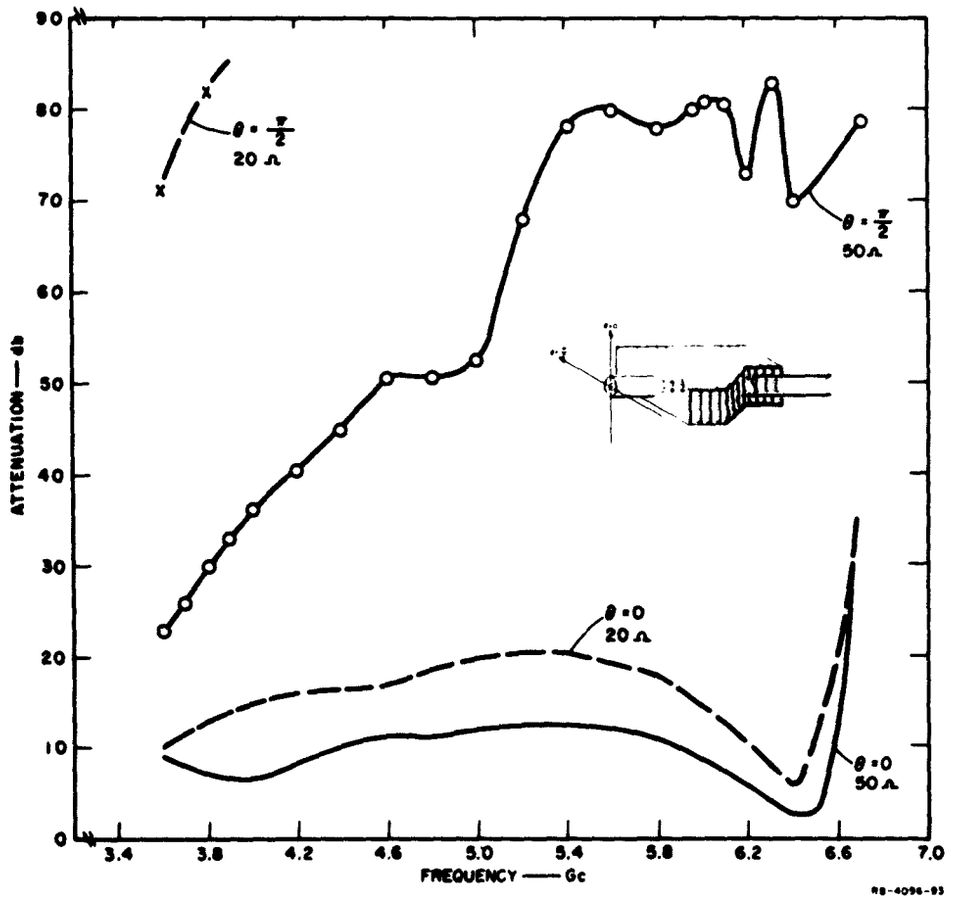

FIG. III-6 ATTENUATION OF THE 1-5 8-INCH COAXIAL LEAKY-WAVE FILTER FOR AN INCIDENT TE_{11} WAVE OF θ = 0 AND π 2 POLARIZATION USING A 50- AND 20-OHM CENTER CONDUCTOR

polarization are strongly attenuated, while fields of $\theta = 0$ polarization are much less attenuated. The reason for this result lies in the different current density distributions on the outer coaxial wall for the two polarizations. The interested reader may find a discussion of this outcome elsewhere.[3]

The mismatch loss of the leaky-wave filter using 50-ohm and 20-ohm conductors for an incident TE_{11} wave of both polarizations was also determined from 3.8 to 6.7 Gc. It was found that for both center conductors and both polarizations the mismatch loss was generally less than 0.1 db from 5.0 to 6.7 Gc; and generally less than 0.3 db from 3.9 to 5.0 Gc.

D. PEAK-POWER TEST RESULTS OF THE COAXIAL LEAKY-WAVE FILTER

Tests to determine the peak power capacity of the coaxial leaky-wave filter were conducted at the Eitel-McCullough facilities in San Carlos, California. A cobalt-60 source of 3.5 millicuries rate was used to irradiate the filter.* The tests were conducted at 1.3 Gc. Rectangular pulses of 2.4 microseconds duration, at a rate of 333 pulses per second, and of variable amplitude were used to attempt to achieve electrical breakdown within the filter. The tests began by initially setting the pulse amplitude to obtain a peak power of 75 kilowatts. After an interval of approximately 5 minutes without breakdown, the pulse amplitude was increased. The cycle was repeated until a peak power of 225 kilowatts (which was the maximum permissible output of the particular tube being used) was obtained. The test was run using all four center conductors within the filter. In no case was breakdown, or sputtering, detected.

A survey of the peak power specifications of $1\frac{5}{8}$-inch, 50-ohm, commercially available coaxial line shows it to be rated at between 140 and 280 kilowatts at unity VSWR. A VSWR of greater than unity will de-rate the peak power capacity by a factor equal to the VSWR. Thus, under the test conditions stated in the previous paragraph, the coaxial leaky-wave filter did not de-rate the peak power capacity of the coaxial line.

* The cobalt-60 source was provided by the Nuclear Physics Laboratory of Stanford Research Institute.

REFERENCES

1. E. G. Cristal, L. Young, and B. M. Schiffman, "Suppression of Spurious Frequencies," Quarterly Progress Report 3, SRI Project 4096, Contract AF 30(602)-2734, Stanford Research Institute, Menlo Park, California (January 1963).

2. *Ibid.*, pp. 49-51.

3. *Ibid.*, pp. 56-57.

4. *Ibid.*, pp. 60-65.

IV ANALYTICAL SOLUTION TO A WAVEGUIDE LEAKY-WAVE FILTER STRUCTURE*

A. GENERAL

In recent years, waveguide structures that support leaky-wave modes[1,2†] have been used to advantage for the suppression of spurious energy of high-power transmitters. These structures are generally referred to as leaky-wall or leaky-wave filters.[3,4,5] They are absorption rather than reflection filters, and exhibit the following characteristics:

(1) They generally provide high attenuation throughout a wide stop-band.

(2) They are reasonably well matched to the transmitter in the stop-band as well as in the pass-band.

(3) They are able to support large peak power levels.

Because of these properties it is expected that leaky-wave filters will play an important part in the suppression of spurious energy, particularly in view of the anticipated increased crowding of the radio spectrum, the development of more sensitive receivers, and the expected greater power output of new transmitting tubes.[6] Consequently, there is a need for a greater understanding of these filters and for quantitative data regarding their design.

Although there are experimental data on the properties of several specially constructed leaky-wave filters,[7,8,9] there are apparently little data relating to the effect on filter attenuation of varying one or more of the possible parameters of the filter design. In this section this particular aspect is considered theoretically over a limited frequency range.

Basically, leaky-wave filters consist of a waveguide that is modified by having closely spaced periodic slots cut on the walls (outer wall for coaxial leaky-wave filters). Each slot couples the waveguide to a side waveguide that is terminated in a wide-band matched load. At frequencies in the filter pass-band, the side waveguides are cut off and the energy in

* This investigation is reported in more detail in Quarterly Progress Report 3.

† References are listed at the end of the section.

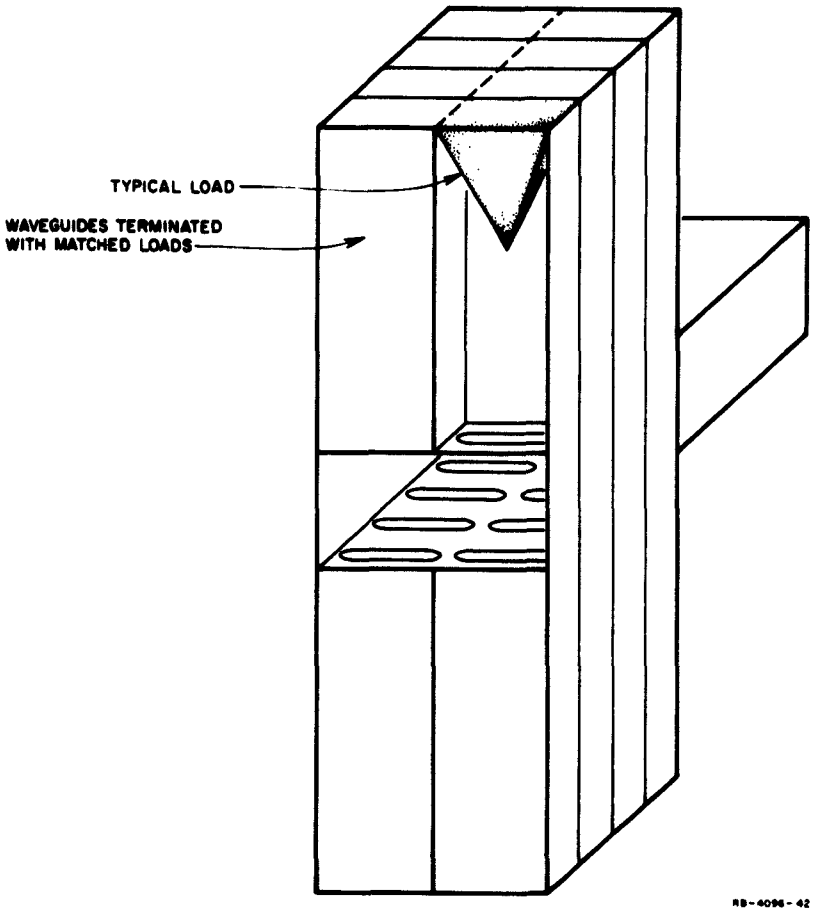

FIG. IV-1 SKETCH OF A POSSIBLE TYPE OF WAVEGUIDE LEAKY-WAVE FILTER

the transmission line passes to the output unattenuated. However, at frequencies in the filter stop-band, the side waveguides support propagation and hence the energy at these frequencies is coupled into the absorbing waveguides and is thus severely attenuated. A sketch of one possible type of waveguide leaky-wave filter is shown in Fig. IV-1.

These structures are not readily amenable to theoretical study; for this reason, an idealized structure that retains the basic geometry of a leaky-wave filter was used in this analysis. The structure is shown in Fig. IV-2. It consists of a waveguide that has closely spaced periodic slots cut in one of the broad walls. Each slot couples the main waveguide

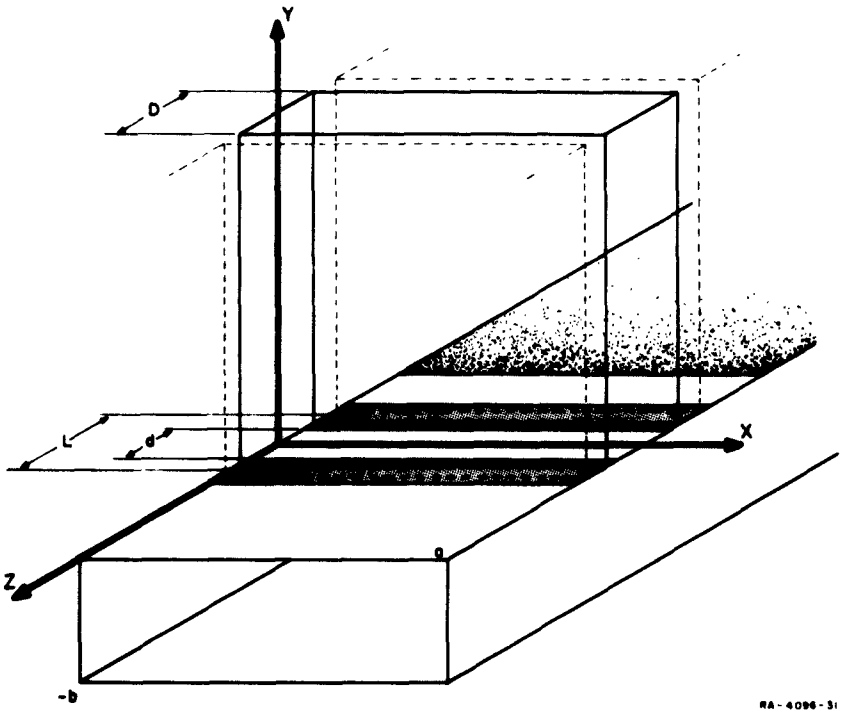

(a)

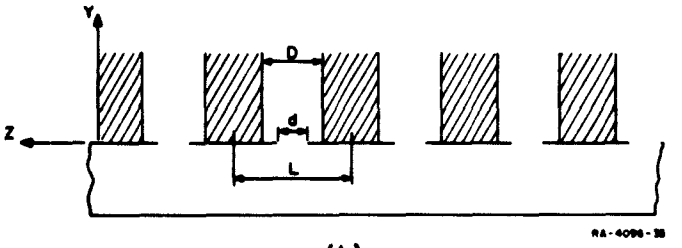

(b)

FIG. IV-2 WAVEGUIDE LEAKY-WAVE FILTER STRUCTURE
(a) Orthogonal Projection
(b) Longitudinal-Section View

to a single side waveguide that is assumed to be terminated in its characteristic impedance. As can be perceived from Fig. IV-2(a) this structure has no pass-band, since both the main waveguide and side waveguides have the same cutoff frequencies. Nevertheless, the analysis which follows is believed to be pertinent to leaky-wave filter design for the following reasons:

(1) Assume a TE_{20} mode incident to the leaky-wave filter of Fig. IV-1. Then, from the symmetry of the structure and the mode of excitation, it can be seen that a conducting (electric) wall could be placed in the *E*-plane between the slots without disturbing the fields. If this were done, the resulting configuration would bear a very close resemblance to the structure of Fig. IV-2. Thus, the results obtained from the analysis may provide useful quantatitive data for the attenuation of this mode. A similar argument applies for filters haveing three slots abreast on the broad wall and incident TE_{30} modes, or for *n* slots abreast on the broad wall and incident TE_{n0} modes.

(2) In the frequency intervals where the coupling slots of practical leaky-wave filters are past resonance, their frequency dependence is similar to that of the capacitive slots of the structure in Fig. IV-2(a). Also, the frequency dependence of the absorbing waveguides for both cases is similar. Therefore, it is believed that while the quantitative data resulting from this analysis may not apply directly to actual leaky-wave filters propagating the TE_{10} mode, the dependence of the attenuation constant on the various design parameters will behave in the same general way. Hence, which parameters should be varied to maximize the attenuation constant, or to make it less frequency sensitive, can be ascertained from this work.

(3) The analysis can easily be extended by symmetry considerations to the case where slots are cut on both broad walls.

(4) The analysis of the periodic structure automatically accounts for all mutual coupling effects of the slots.

B. ATTENUATION OF THE WAVEGUIDE LEAKY-WAVE FILTER STRUCTURE

It is shown elsewhere[10] that the normalized attenuation constant, αa, of the structure of Fig. IV-2 is given in nepers by

$$\alpha a = \mathrm{Re}\left[\pi\sqrt{1 - \epsilon^2 - \left(\frac{\epsilon}{\pi h}\right)^2}\right] \quad \text{nepers,} \qquad \text{(IV-1)}$$

where z is the solution to

$$\frac{\coth z}{z} = -\frac{1}{\pi h}\left\{\frac{\delta^{-1}}{\sqrt{1-\theta^2}} + \epsilon\left[\ln \csc\frac{\pi}{2}\sigma + \ln \csc\frac{\pi}{2}\frac{\sigma}{\delta}\right]\right\} = w = -u + jv \quad , \tag{IV-2}$$

and

$$\left.\begin{aligned} h &= b/a, \text{ ratio of transmission waveguide height to width} \\ \theta &= 2a/\lambda, \text{ ratio of transmission waveguide width to one-half the freespace wavelength} \\ \epsilon &= L/a, \text{ ratio of slot period to waveguide width} \\ \sigma &= d/L, \text{ ration of slot width to slot period} \\ \delta &= D/L, \text{ ratio of side waveguide height to slot period} \end{aligned}\right\} \quad \text{(IV-3)}$$

Solutions of Eq. (IV-2), for specific values of the parameters and of the frequency variable θ, were obtained using the Burroughs Datatron 220 digital computer. The method of solution was to use an iterative equation based on Newton's method[11] as applied to real functions of a complex variable. Convergence was found to be very rapid, usually two or three iterations. Details of the method and choice of initial guess are given in another report.[12] The iterative equation is

$$z_{i+1} = \frac{\coth z_i + z_i \operatorname{csch}^2 z_i}{w + \operatorname{csch}^2 z_i} \quad , \quad \text{for } i = 1,2, \ldots \quad .$$

C. DISCUSSION OF RESULTS

In order to investigate the dependence of the attenuation constant on the several design parameters and frequency, Eq. (IV-2) was solved as a function of θ for various values of ϵ, σ, δ, h. The following cases, which assume a waveguide of fixed width a, were of particular interest:

(1) For a given slot period ϵ, slot width σ, and main waveguide height h, determine the dependence of the attenuation constant on the absorbing waveguide height δ.

(2) For a given slot period ϵ, absorbing waveguide height δ, and main waveguide height h, determine the dependence of the attenuation constant on the slot width σ.

(3) For a given slot period ϵ, absorbing waveguide height δ, and slot width σ, determine the dependence of the attenuation constant on the main waveguide height h.

(4) For a given slot width σ, absorbing waveguide height δ, and main waveguide height h, determine the dependence of the attenuation constant on the slot period ϵ.

The graphs of Figs. IV-3 through IV-6 pertain to Cases 1 through 4. They show plots of αa, the normalized attenuation constant, versus $2a/\lambda$, the ratio of waveguide width to one-half the free-space wavelength. The region $0 \leq (2a/\lambda) \leq 1$ is that of nonpropagation in an unperturbed guide, *i.e.*, $\beta = 0$. For the leaky-wave structure of Fig. IV-2, this frequency region also corresponds to nonpropagation. However, the value of the normalized attenuation constant, αa, was found to be increased over that of the unperturbed case. The region $1 < (2a/\lambda) < \infty$ corresponds to the region of propagation in an unperturbed waveguide, *i.e.*, $\beta > 0$, $\alpha = 0$. For the leaky-wave structure of Fig. IV-2 β was found to be slightly more than the unperturbed waveguide value for θ less than approximately 1.2, and slightly less than the unperturbed value for θ greater than approximately 1.2, while α differed from zero. The variation of α with frequency and its dependence on ϵ, σ, δ, and h will now be discussed.

Figures IV-3 and IV-4 are typical results which relate to Cases 1 and 2. Figure IV-3 considers the example of the slot width occupying 50 percent of the slot period, and Fig. IV-4 the case of the waveguide periodic *E*-plane *T*-junction (*i.e.*, $\delta = \sigma$). In both cases, δ, the ratio of the absorbing waveguide height to the slot period, is a variable parameter that ranges from the minimum permissible value (*i.e.*, $\delta = \sigma$) to the limiting value 1. The theoretical results obtained suggest the following conclusions:

(1) The attenuation constant increases as the absorbing waveguide height increases. An approximation to the dependence of αa on δ for the maximum values of αa is

$$\frac{(\alpha a)_1}{(\alpha a)_2} \approx \frac{\delta_1}{\delta_2} .$$

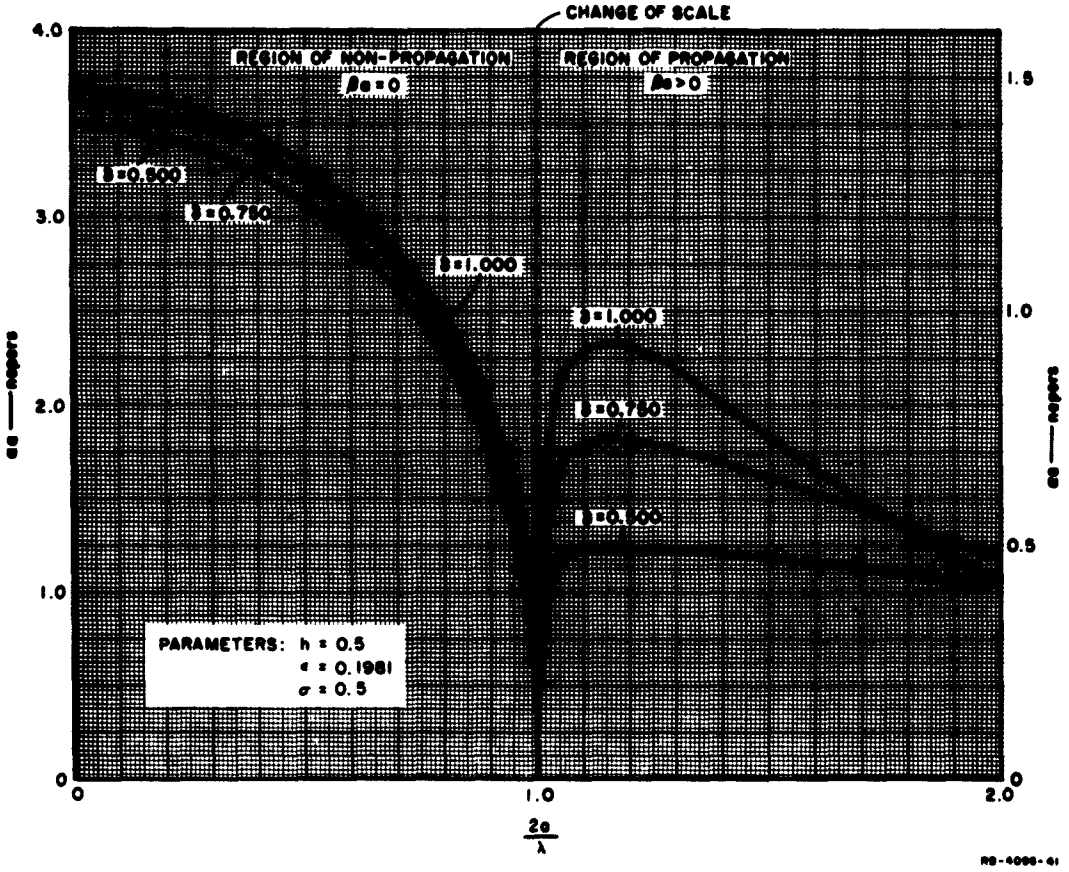

FIG. IV-3 NORMALIZED ATTENUATION CONSTANT γa AS A FUNCTION OF $2a/\lambda$ FOR VARIOUS VALUES OF β (σ = 0.500)

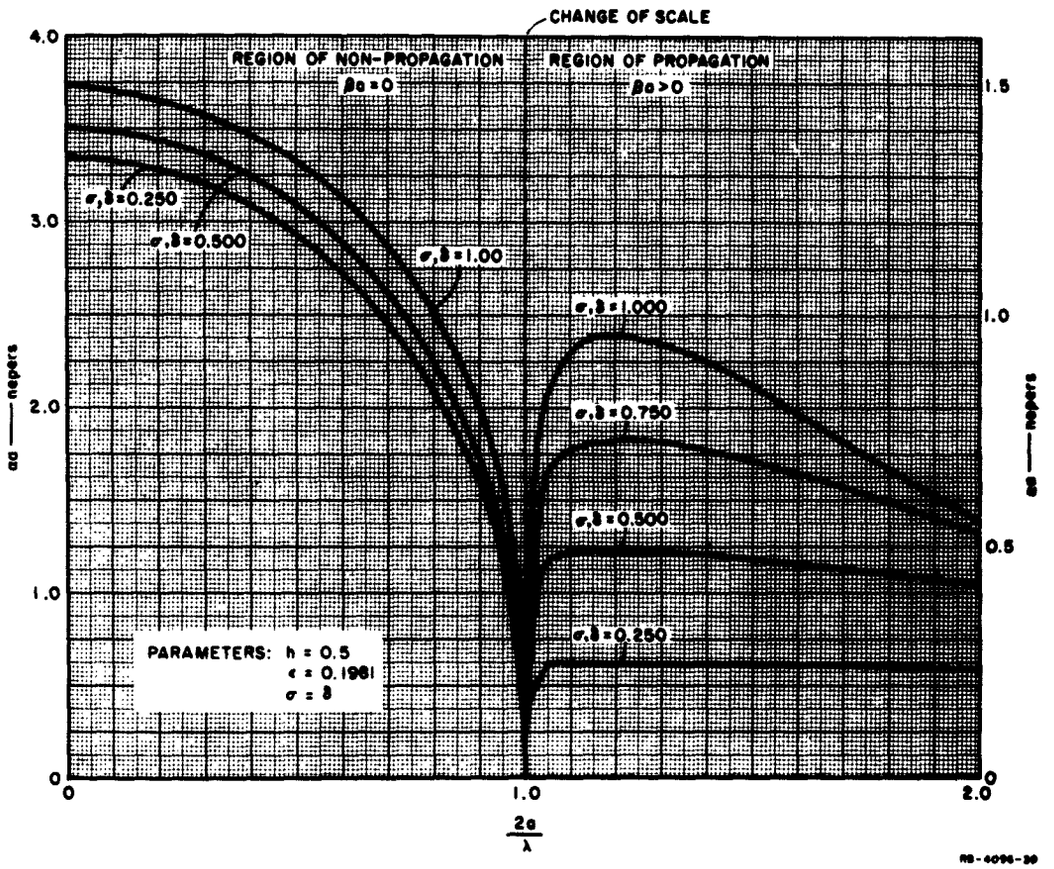

FIG. IV-4 NORMALIZED ATTENUATION CONSTANT γa AS A FUNCTION OF $2a/\lambda$ FOR VARIOUS VALUES OF σ AND $\delta(\sigma = \sigma)$

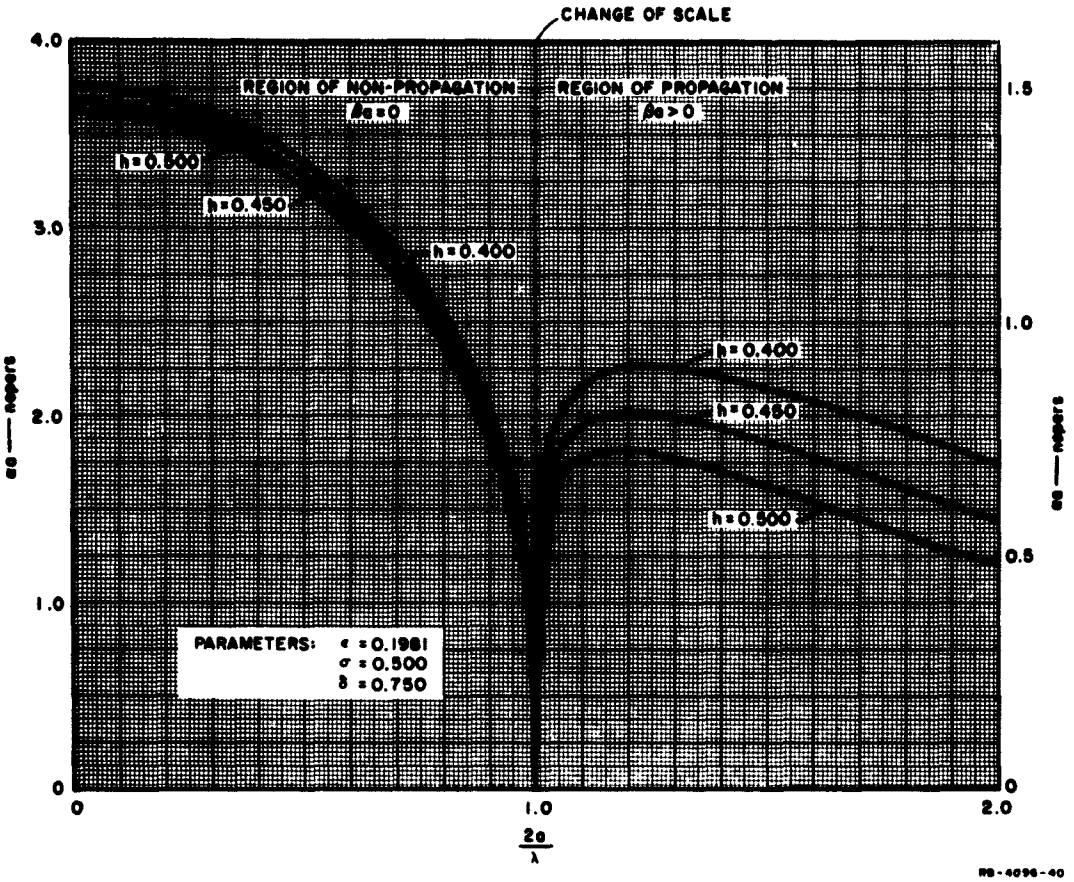

FIG. IV-5 NORMALIZED ATTENUATION CONSTANT αa AS A FUNCTION OF $2a/\lambda$ FOR VARIOUS VALUES OF h(σ = 0.500, δ = 0.750)

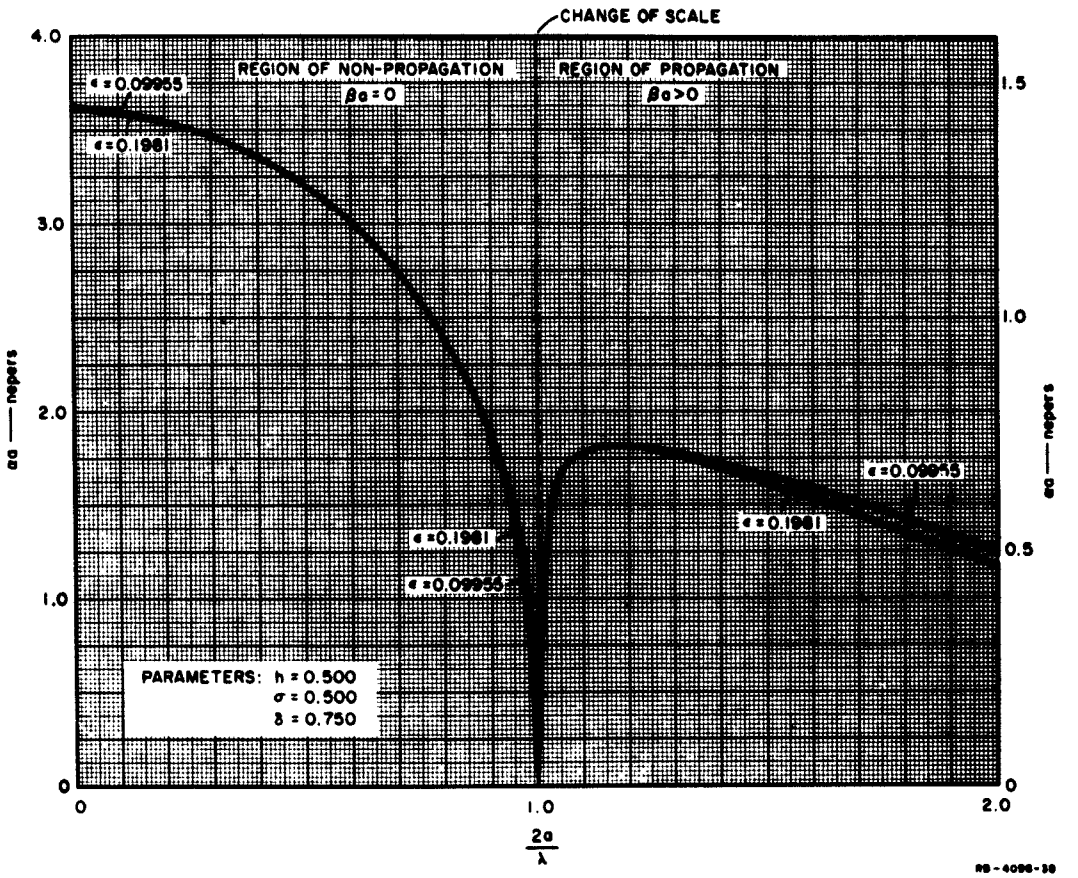

FIG. IV-6 NORMALIZED ATTENUATION CONSTANT γa AS A FUNCTION OF $2a/\lambda$ FOR VARIOUS VALUES OF ϵ (σ = 0.500, δ = 0.750)

(2) The frequency sensitivity of αa increases as the absorbing waveguide height increases. Whereas, over most of the frequency band the absolute value of the slope of the αa versus θ curves is relatively small for small values of δ, it increases monotonically with increasing δ. For a given σ, the least-frequency-sensitive case is when $\delta = \sigma$, *i.e.*, the waveguide periodic T-junction.

Figures IV-5 gives a typical result which shows the effect upon the attenuation constant of varying the main waveguide height while holding all other parameters constant. The particular case shown is for $\sigma = 0.500$, $\delta = 0.750$. However, the results are quite similar for the other cases investigated. The effect of reducing the main waveguide height is to increase the attenuation constant without affecting its frequency sensitivity. This particular result has been experimentally verified in the case of coaxial leaky-wave filters* (where the inner conductor diameter was increased, thus reducing the line impedance) and has also been noted in the waveguide case.[13] For the range of parameters investigated in this work, an approximate relationship between various h curves was found to be

$$\frac{(\alpha a)_2}{(\alpha a)_1} = c\left(\frac{h_1}{h_2}\right); \quad (h_2 < h_1)$$

where c is a number that lies between 1.0 and 1.3.

Figure IV-6 shows the effect of varying the slot period when all other ratios are held constant. The change in αa due to the variation in ϵ is relatively small throughout most of the frequency band but reaches a maximum of 6 percent at $\theta = 2.0$. The example represented by Fig. IV-6 considers reducing the slot period by 50 percent. In most leaky-wave filters, this is about the practical limit of period reduction. Figure IV-6 shows that the smaller period tends to increase α slightly and to make it a little less frequency sensitive; however, this advantage is completely offset by the additional number of absorbing waveguides (twice as many, in this example) required by the reduction in the slot period.

In the introduction it was stated that the analysis presented in this report could easily be extended to include the case of slots on both broad walls.* This extension is made for a given set of parameters, ϵ, σ, δ,

* Experimental results are presented in Sec. III.

and h by replacing h of the set by $h/2$ and solving Eqs. (IV-1) and (IV-2). This is physically equivalent to placing a conducting wall in the H-plane at the half-height position of the main waveguide. Assuming that the approximations made in the derivation of Eq. (IV-2) are then not invalidated, one sees that, qualitatively, all of the results of this study remain unchanged for the case of the leaky-wave waveguide structure with slots on both broad walls.

D. EXPERIMENTAL WORK

In Fig. IV-2, denote an arbitrary absorbing waveguide as the ith guide and any subsequent absorbing waveguide as the jth guide ($j > i$). Then the ratio of power in the ith guide to power in the jth guide is given by

$$\frac{P_i}{P_j} = e^{2(\alpha a)\epsilon(j-i)} \quad . \tag{IV-4}$$

Solving Eq. (IV-4) for αa gives

$$\alpha a = \frac{1}{20\epsilon(j-i)\log_{10} e}\left(10 \log_{10}\frac{P_i}{P_j}\right) \quad . \tag{IV-5}$$

Equation (IV-5) states that αa is equal to the difference in db of the power in the jth and ith guides divided by $8.68(j-i)\epsilon$.

Using Eq. (IV-5) to calculate αa, experimental measurements were made on a waveguide structure that was designed so that it could be easily modified to incorporate the following four cases:

CASE I	
ϵ	= 0.198
h	= 0.472
σ = δ	= 0.555

CASE II	
ϵ	= 0.198
h	= 0.428
σ = δ	= 0.555

CASE III	
ϵ	= 0.198
h	= 0.465
σ	= 0.200
δ	= 0.555

CASE IV	
ϵ	= 0.198
h	= 0.421
σ	= 0.200
δ	= 0.555

Cases I and II are those of the periodic waveguide T-junction wherein the main waveguide height assumes two values. Cases III and IV represent

the case where the coupling slot occupies 20 percent of the slot period and the main waveguide height assumes two values.

The experimental filter structure was constructed of aluminum jig plate to have WR-284 (*S*-band) dimensions. However, this geometry was chosen for convenience in making experimental measurements and does not affect the results, which are determined as dimensionless quantities. A photograph of the finished structure (representing Case IV) is shown in Fig. IV-7. The photograph shows the view seen when looking obliquely at the narrow walls of the main and absorbing waveguides. The cover plate, which acts as the narrow wall for all absorbing waveguides and also the main waveguide, is partially removed in order to show the absorbing waveguides.

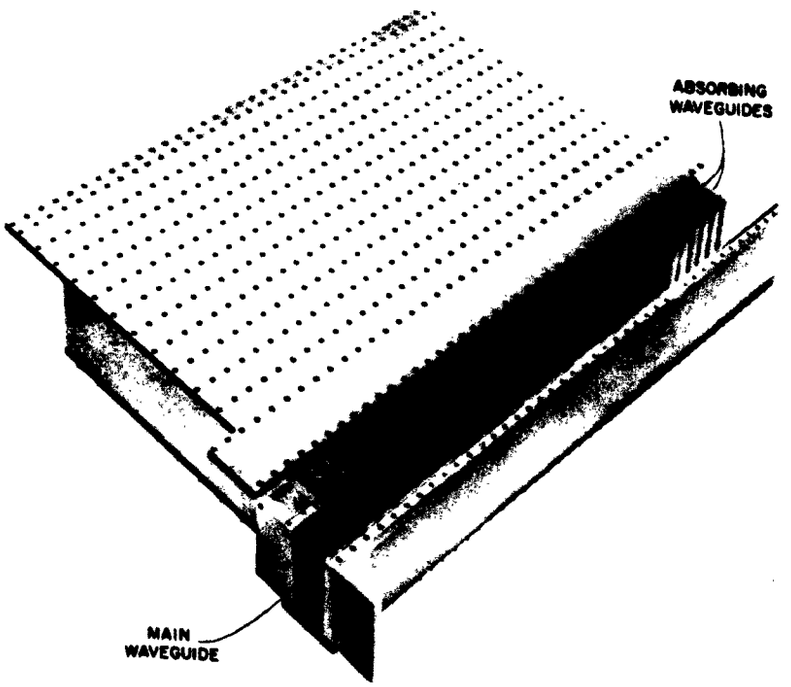

RP-4096-94

FIG. IV-7 PHOTOGRAPH OF THE EXPERIMENTAL WAVEGUIDE LEAKY-WAVE FILTER STRUCTURE

The power in several absorbing waveguides was measured* and the value of αa was then calculated by Eq. (IV-5) using several combinations for j and i of the absorbing waveguides. Since the resulting αa values varied slightly for different values of j and i, their average value is used in the final result. The variation of the values that were calculated from the power measurements results from the variation of VSWR of the loads in the side waveguides. A check of several loads showed that the VSWR's varied from 1.05 to 1.35 over the measured frequency interval. Hence, because of the reflections caused by these loads the coupling varied slightly from guide to guide.

Figure IV-8 gives the computed and measured values of αa for the case of the periodic T-junction for two values of main waveguide height; Fig. IV-9 gives the results for the case where the slot width occupies 20 percent of the slot period for two values of waveguide height. In the latter case, the slot thickness was 0.003 inch and the small thickness correction term was neglected in the theoretically computed values of αa. The additional 0.004-inch reduction in height (compare h in Figs. IV-8 and IV-9) resulted from the particular fabrication technique used in attaching the slot strips to the end of the absorbing waveguides. The four experimental cases give good agreement with the theoretically computed values.

* The measurement techniques are discussed in Ref. 10, pp. 35-37.

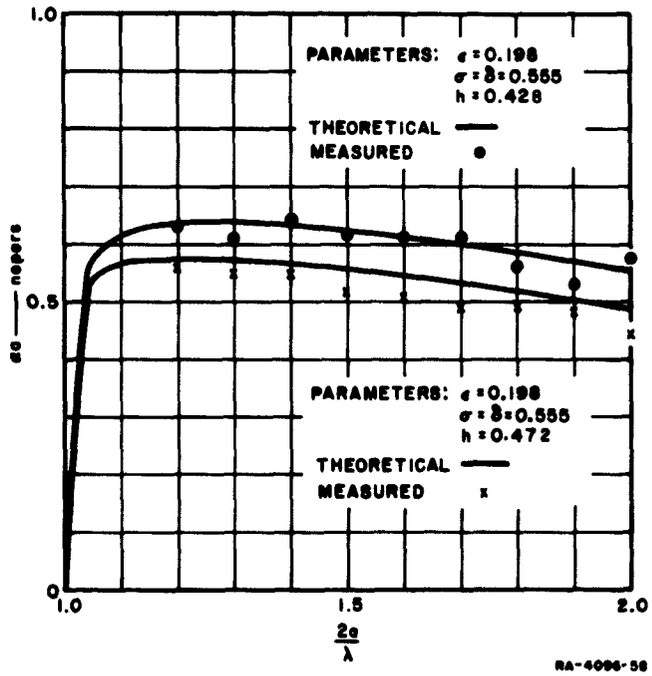

FIG. IV-8 THEORETICALLY COMPUTED AND EXPERIMENTALLY MEASURED NORMALIZED ATTENUATION CONSTANT αa AS A FUNCTION OF $2a/\lambda$ FOR TWO VALUES OF h(ϵ = 0.198, σ = δ = 0.555)

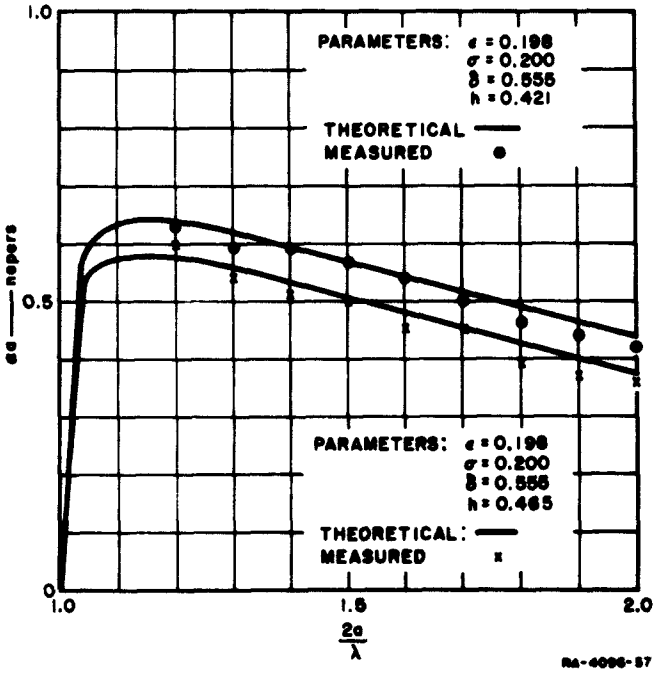

FIG. IV-9 THEORETICALLY COMPUTED AND EXPERIMENTALLY MEASURED NORMALIZED ATTENUATION CONSTANT αa AS A FUNCTION OF $2a/\lambda$ FOR TWO VALUES OF h(ϵ = 0.198, σ = 0.200, δ = 0.555)

REFERENCES

1. N. Marcuvitz, "On Field Representations in Terms of Leaky Modes or Eigenmodes," *IRE Trans. PGAP*, Electromagnetic Wave Theory Symposium, pp. 192-194 (July 1956).

2. K. G. Budden, *The Wave-Guide Mode Theory of Wave Propagation*, pp. 4, 134(Prentice-Hall Inc., Englewood Cliffs, New Jersey, 1961).

3. V. Met, "Absorptive Filters for Microwave Harmonic Power," *Proc. IRE* 47, pp. 1762-1769 (October 1959).

4. V. Price, R. Stone, and V. Met, "Harmonic Suppression by Leaky-Wall Waveguide Filter," *1959 IRE Wescon Convention Record, Part I*, p. 116 (18-21 August 1959).

5. E. G. Cristal, "Some Preliminary Experimental Results on Coaxial Absorption Leaky-Wave Filters," IRE-PGRFI Fourth Annual Symposium, San Francisco, California (29 June 1962).

6. O. M. Salati, "Recent Developments in RF Interference," *IRE Trans. RFI*, pp. 24-32 (May 1962).

7. E. G. Cristal, *op. cit.*

8. V. G. Price, J. P. Rooney, and C. Milazzo, "Measurement and Control of Harmonic and Spurious Microwave Energy, Final Report for Phase II," Report TIS R58ELM 112-1, Contract AF 30(602)-1670, G.E. Microwave Laboratory, Palo Alto, California (8 July 1958).

9. V. G. Price, J. P. Rooney, and R. H. Stone, "Measurement and Control of Harmonic and Spurious Microwave Energy, Final Report Change A," Report TIS 60ELM 112-4, Contract AF 30(602)-1670, G.E. Microwave Laboratory, Palo Alto, California (22 March 1960).

10. E. G. Cristal, L. Young, and B. M. Shiffman, "Suppression of Spurious Frequencies," Quarterly Progress Report 3, pps. 9-18, SRI Project 4096, Contract AF 30(602)-2734, Stanford Research Institute, Menlo Park, California (January 1963).

11. R. Courant, *Differential and Integral Calculus*, Vol. I, pp. 355-359 (Interscience Publishers, Inc., New York, 1952).

12. E. G. Cristal, L. Young, and B. M. Schiffman, *op. cit.* pps. 117-120.

13. V. Met, *op. cit.*

V WAVEGUIDE 0-db AND 3-db DIRECTIONAL COUPLERS AS HARMONIC PADS*

A. GENERAL

Waffle-iron filters (Sec. II) are very compact and effective rejection filters for harmonic frequencies and other spurious frequencies above the transmitter pass-band. However, the unwanted frequencies are reflected rather than absorbed, as would be preferable when either the generator or the load is severely mismatched. Such mismatches can affect:

(1) The over-all attenuation, since the mismatches can be phased so that they reduce the intrinsic attenuation of the rejection filter, and

(2) The power-handling capacity, since (under approximately the same phasing conditions that reduce the attenuation) a resonance may be set up, which may cause arcing in the transmission line.

Both these effects, which are associated with rejection filters, may be overcome by placing a "low-pass attenuator" on the mismatched side of the rejection filter (to be quite safe, one may be placed on each side of the filter). By a "low-pass attenuator" we mean a device that would be matched and dissipation-free in the fundamental pass-band, and that should be matched but absorbing at least from the second harmonic on up in frequency, for all waveguide modes that may propagate. A device with these properties will henceforth be referred to as a *harmonic pad*.

Harmonic pads may, for instance, consist of short sections of leaky-wave filters, either in coaxial line (see Sec. III) or in waveguide.[1,2]* Since leaky-wave filters have been and are being investigated in their own right at SRI (with higher attenuations being sought, and obtained, than are necessary for harmonic padding), this avenue was not explored further in connection with rejection filters. (Short sections of leaky-waveguide filters have indeed been combined in this manner with waffle-iron filters, although no test data have been published.)

---

* This work is reported in more detail in Quarterly Progress Reports 3 and 4.

† References are listed at the end of the section.

Two approaches are taken here. In one approach we investigate the suitability of various 0-db directional couplers (that is, directional couplers having 0-db coupling in the fundamental pass-band) as harmonic pads (Fig. V-1). There are many types of coupler, and only a few could be investigated at this preliminary stage. The choice was influenced largely by (1) a desire for a suitable geometrical configuration which might appear promising for our purpose, (2) possibilities for appropriate modifications at a later stage, and (3) ease of design or commercial availability. Two types of branch-guide couplers and two types of short-slot couplers were investigated.

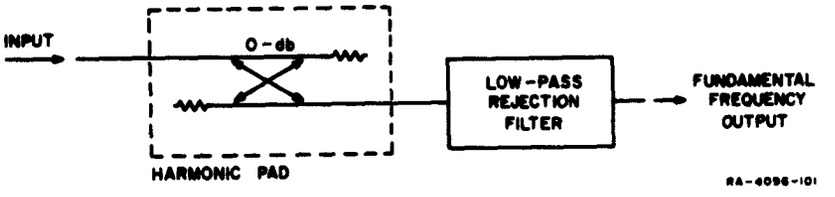

FIG. V-1 0-db HARMONIC PAD AND REJECTION FILTER

In the second approach, we investigate 3-db directional couplers (that is, directional couplers having 3-db coupling in the fundamental pass-band). The 3-db coupler (unlike the 0-db coupler) cannot act as a harmonic pad on its own, but requires two high-pass or band-stop filters to make it into a harmonic pad (Fig. V-2). In rectangular waveguide, a taper into a section of waveguide of reduced width forms a high-pass filter, which will pass most (but not all) modes at frequencies above the pass-band, while reflecting all pass-band frequencies. This circuit has been found to generally perform better than a 0-db coupler configuration as a harmonic pad for those modes passed by the high-pass filter;

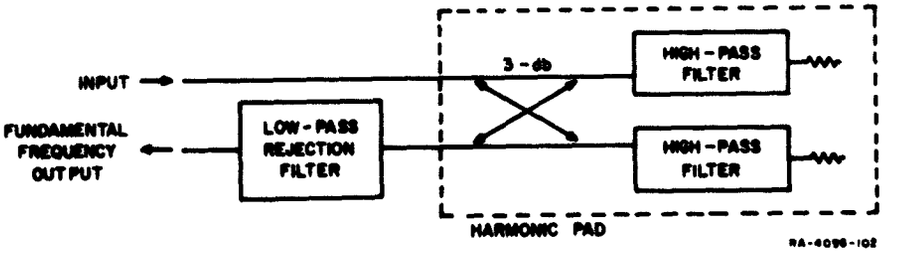

FIG. V-2 3-db HARMONIC PAD AND REJECTION FILTER

however, it cannot function as a pad for those frequencies propagating in modes reflected by the "high-pass" filter (such as occur with a rectangular waveguide of reduced width), and thus the over-all performance of a 0-db coupler harmonic pad will probably be more acceptable, at least until such time as a suitable high-pass filter will have been developed.

It can be shown[3,4] that satisfactory performance can be expected from a harmonic pad provided that the reflected power is at least in the order of 5 or 6 db below the incident power, when a short circuit is placed at the fundamental frequency output. This provides a criterion for judging the performance of a harmonic pad.

B. BRANCH-GUIDE COUPLER

A branch-guide 0-db coupler was designed and constructed, with waffle-iron filters in its branches. A photograph of this new directional coupler is shown in Fig. V-3. It is based on an eight-branch periodic 0-db coupler. There was room for three waffle-iron sections plus a short length of waveguide to add up to a branch length of 270 electrical degrees (three-quarter wavelength) at a center frequency of 1.3 Gc. The mechanical construction of the coupler follows closely the construction of the previous couplers.[5,6]

The pass-band performance was computed on a digital computer and the design was finally optimized by computing the effect of small changes in the branch impedances. The coupler was then built and tested experimentally. Excellent agreement was again obtained between computed and measured curves.[4]

The stop-band performance of the coupler was measured for both the (lowest) TE_{10} and the (cross-polarized) TE_{01} modes, using long tapers from smaller waveguides. A large number of recordings were taken. The greatest reflection coefficient in the TE_{10} mode at all frequencies from the beginning of the second harmonic (2.5 Gc) to the end of the fifth harmonic (6.25 Gc) is better than 7 db (and is, in fact, generally much better). The attenuation is much more than is required of a harmonic pad, and is at least 28 db.

The performance of branch guide couplers as harmonic pads deteriorates at a few frequencies,[4] even though it is satisfactory at most frequencies. The performance of the 0-db coupler with waffle-iron filters in the branches

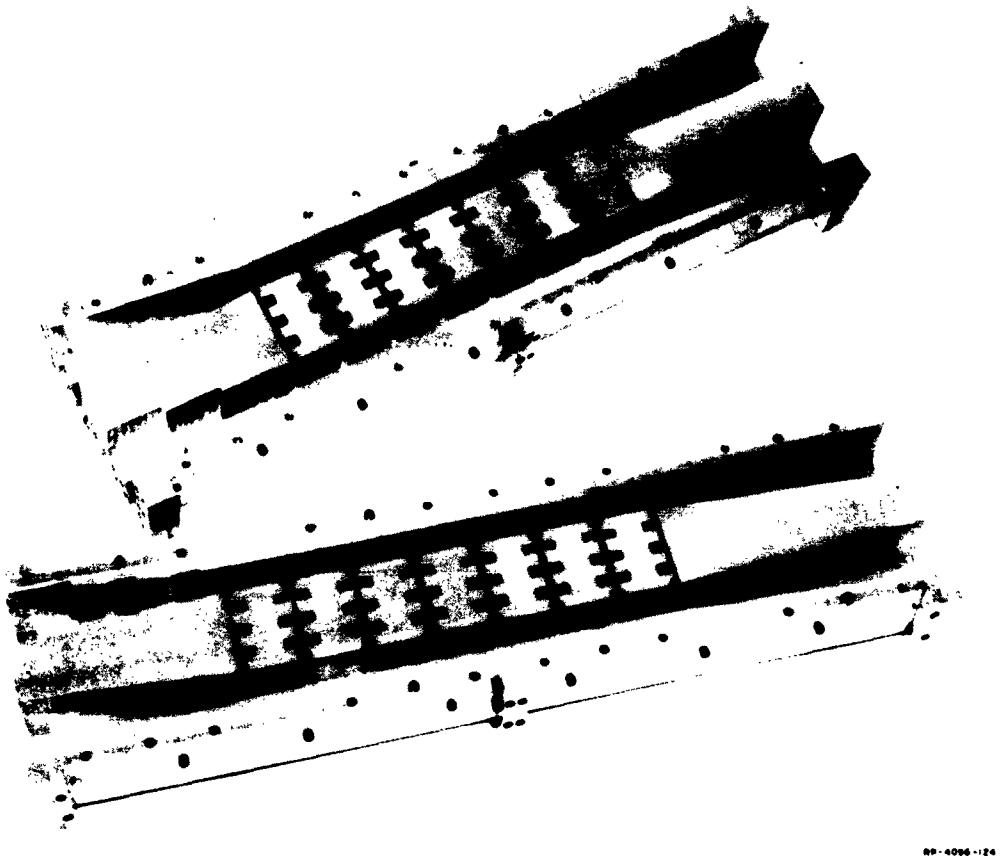

FIG. V-3 EXPLODED VIEW OF 8-BRANCH 0-db BRANCH-GUIDE DIRECTIONAL COUPLER WITH A WAFFLE-IRON FILTER IN EACH BRANCH

was the best of the branch-guide couplers tested.[5] It is especially superior as regards attenuation, because of the filters in the branches. However, the particular model constructed had reduced-height waveguides in order to utilize an existing waffle-iron filter design, and thus reflects the TE_{01} mode up to 4.32 Gc, and would be bound to reflect certain other modes which might be incident in the WR-650 input waveguide.

C. SHORT-SLOT DIRECTIONAL COUPLERS

There are many possible directional couplers which appear suitable for use as harmonic pads either as 0-db couplers in the manner of Fig. V-1,

or as 3-db couplers in the manner of Fig. V-2. Riblet short-slot couplers are particularly compact, are readily available, and have the right kind of geometrical configuration. Two *S*-band sidewall couplers, and two *S*-band topwall couplers in WR-284 waveguide were purchased from Microwave Development Laboratories (Model Numbers 284 HS 22 and HT-1332). Each type was tested as a 3-db coupler harmonic pad (Fig. V-2), and also each pair was cascaded to form two 0-db couplers, shown assembled in Fig. V-4. Each 0-db coupler was then tested as a harmonic pad (Fig. V-1). The spacing between the two 3-db couplers in both cases shown in Fig. V-4 is not critical in the pass-band, and does not appear to be critical in the stop-band. Two one-inch-long pieces of waveguide were used between the flanges of the two side-wall couplers (upper photo in Fig. V-4), and two 1-inch-long guides were used between the topwall couplers (lower photo in Fig. V-4). Two *E*-plane bends were used (Fig. V-4), but the input was always connected to a straight waveguide port.

In the pass-band of 2.7 Gc to 2.9 Gc, the VSWR and dissipation loss were measured for both 0-db couplers, including *E*-plane bends, as shown in the photograph, Fig. V-4. The sidewall 0-db coupler had a VSWR of 1.05 or better, and a dissipation loss of less than 0.07 db at 2.7, 2.8 and 2.9 Gc; the topwall 0-db coupler had a VSWR of 1.03 at all three frequencies, and a dissipation loss rising to 0.13 db at 2.9 Gc.

Four combinations (sidewall 0-db, topwall 0-db, sidewall 3-db, and topwall 3-db) were tested in the stop-band as described for the branch-guide couplers. The reflection coefficient was recorded, using a bank of swept signal generators and a chart recorder, when a short circuit was placed in an arbitrary position at the output. Measurements were made on the TE_{10}, the TE_{01}, and the TE_{20} modes.[4,7]

A large number of recordings was taken,[4,7] and a typical one is shown in Fig. V-5. This shows the reflection coefficient for the TE_{10} and TE_{01} modes from 4.0 to 15.5 Gc, for the short-slot sidewall coupler. In this case the reflected power was always at least 5 db (but mostly about 10 db) below the incident power.

A compact spurious-frequency suppression filter is suggested in Fig. V-6. This would use two 0-db sidewall couplers, one two-layer waffle-iron filter (Sec. II), and two dummy loads to absorb the spurious power. It could be placed in any straight waveguide run, since the input and output waveguides are in line. The complete spurious-frequency suppression filter need be no higher than the waveguide, and only twice as wide.

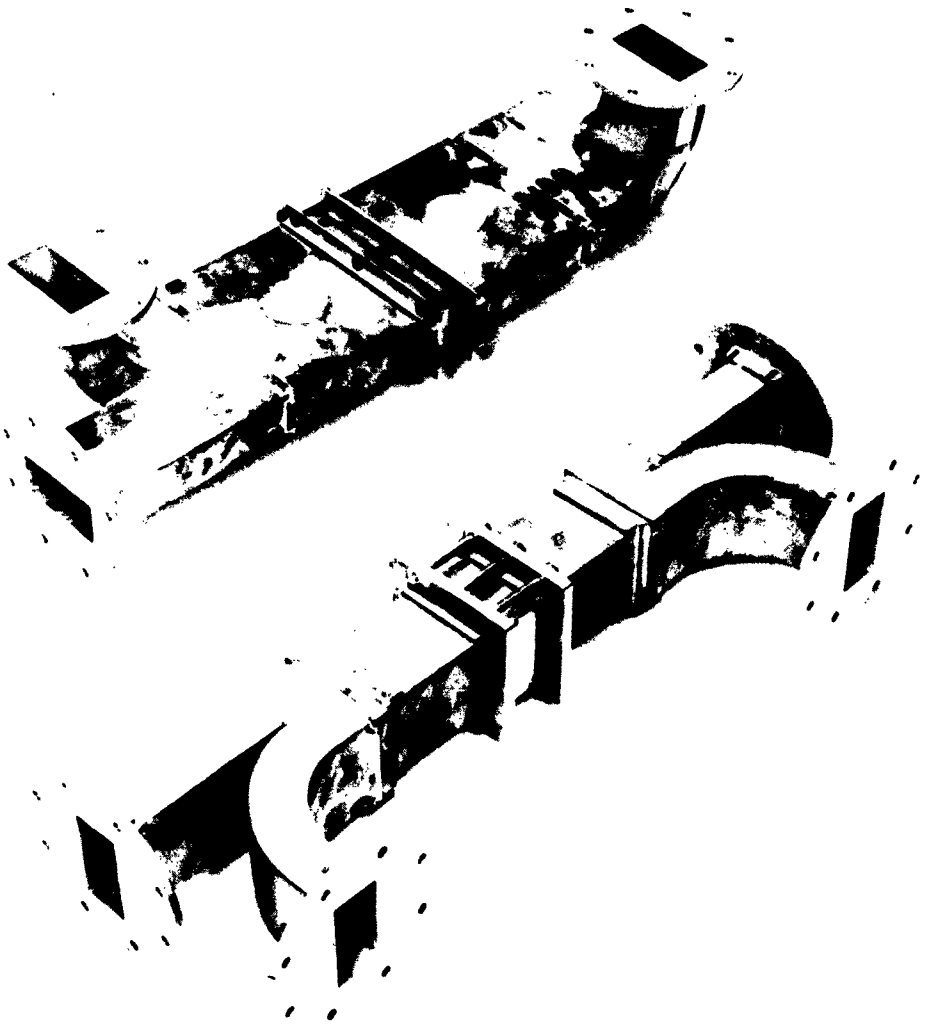

RP-4096-116

FIG. V-4 PHOTOGRAPH OF 0-db SHORT-SLOT DIRECTIONAL COUPLERS

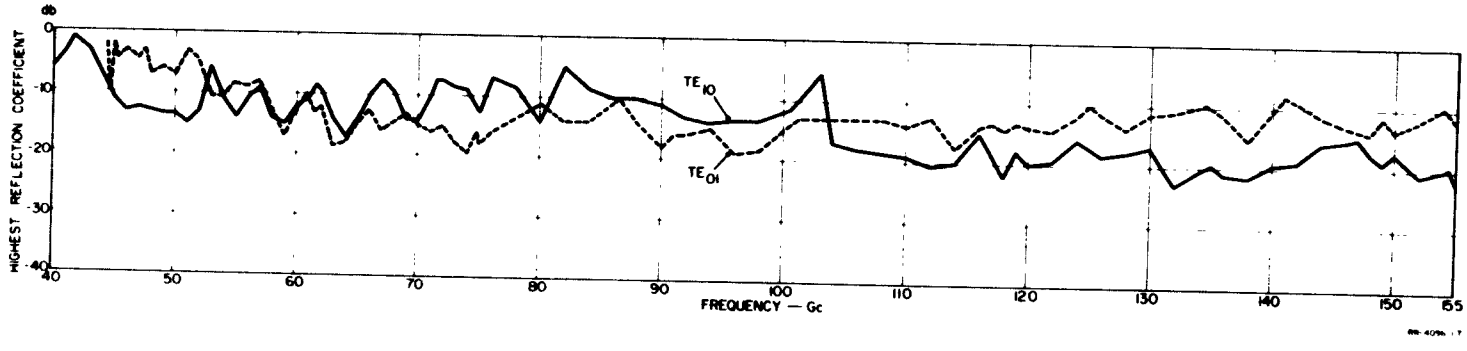

FIG. V-5 REFLECTION COEFFICIENT IN THE STOP-BAND OF THE 0-db SIDEWALL COUPLER

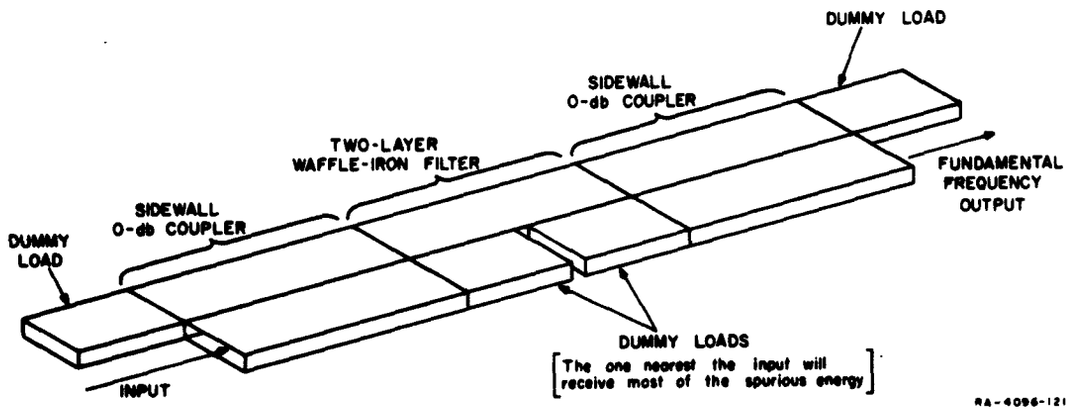

FIG. V-6 SUGGESTED SPURIOUS-FREQUENCY-SUPPRESSION FILTER USING TWO 0-db SIDEWALL COUPLERS, ONE ON EACH SIDE OF A TWO-LAYER WAFFLE-IRON FILTER

REFERENCES

1. V. G. Price, R. H. Stone, and V. Met, "Harmonic Suppression by Leaky-Wall Waveguide Filters," WESCON Convention Record, Part 1, Vol. 3, pp. 112-118 (1959).

2. V. Met, "Absorptive Filters for Microwave Harmonic Power," *Proc. IRE* 47, pp. 1762-1769 (October 1959).

3. L. A. Robinson, E. G. Cristal, B. M. Schiffman, and L. Young, "Suppression of Spurious Frequencies," Quarterly Progress Report 2, SRI Project 4096, Contract AF 30(602)-2734, Stanford Research Institute, Menlo Park, California (October 1962).

4. E. G. Cristal, Leo Young, and B. M. Schiffman, "Suppression of Spurious Frequencies," Quarterly Progress Report 3, SRI Project 4096, Contract AF 30(602)-2734, Stanford Research Institute, Menlo Park, California (January 1963).

5. L. Young, "The Application of Branch-Guide Couplers to the Suppression of Spurious Frequencies," Fourth IRE-PGMTT Symposium, San Francisco, California (June 1962). For further details, see Technical Note 3, SRI Project 3478, Contract AF 30(602)-2392, Stanford Research Institute, Menlo Park, California (February 1962), RADC-TDR-62-130.

6. L. Young, "Synchronous Branch Guide Directional Couplers for Low and High Power Applications," *IRE Trans.* PGMTT-10, pp. 459-475 (November 1962).

7. L. Young, E. G. Cristal, L. A. Robinson, and B. M. Schiffman, "Suppression of Spurious Frequencies," Quarterly Progress Report 4, SRI Project 4096, Contract AF 30(602)-2734, Stanford Research Institute, Menlo Park, California (June 1963).

VI STRIP-LINE BAND-STOP FILTERS*

A new and relatively simple method of designing transmission-line band-stop filters that are well matched in the pass-band was shown to be suitable for the suppression of the second harmonic band, and is believed to be applicable to the design of a band-stop filter with several selected stop-bands, such as the second-, third- and fourth-harmonic stop-bands.[1,2] A convenient method of realizing such filters is by strip-line techniques.

Band-stop filters with narrow stop-bands have been developed before,[3] and general design formulas for this case have been given. The band-stop filters described here are suitable for wider stop-bands, and are thus more suitable for eliminating one or more complete harmonic bands of a high-power transmitter which covers bandwidths of about 10 percent. A typical filter consists of quarter-wavelength, open-circuited stubs separated by quarter-wavelength connecting lines (all lengths are referred to the center frequency of the stop-band). The design method consists of first choosing a suitable low-pass prototype, say an equal-ripple type for which design tables are available,[4-8] and then applying formulas that convert the low-pass network to a band-stop transmission-line network.[9,10] Through an appropriate choice of design parameters, the trough of the equal-ripple response is made to fall in the pass-band and the points of infinite attenuation are made to fall on harmonic frequencies that are to be rejected.[1,2] The design method is exact and the band-stop filter response is a precise mapping of that of the low-pass prototype.

A strip-line realization of a second-harmonic rejection filter is shown in Fig. VI-1. The transmission-line impedances are given in Fig. VI-2, as are the measured and theoretical response of the filter.

The peak power carrying ability of a filter of this type is limited by plate-to-plate spacing of the ground planes. This in turn is limited by the need to minimize any parasitic junction effects in order to fully

* This investigation is reported in more detail in Refs. 1 and 2. (References are listed at the end of the section.)

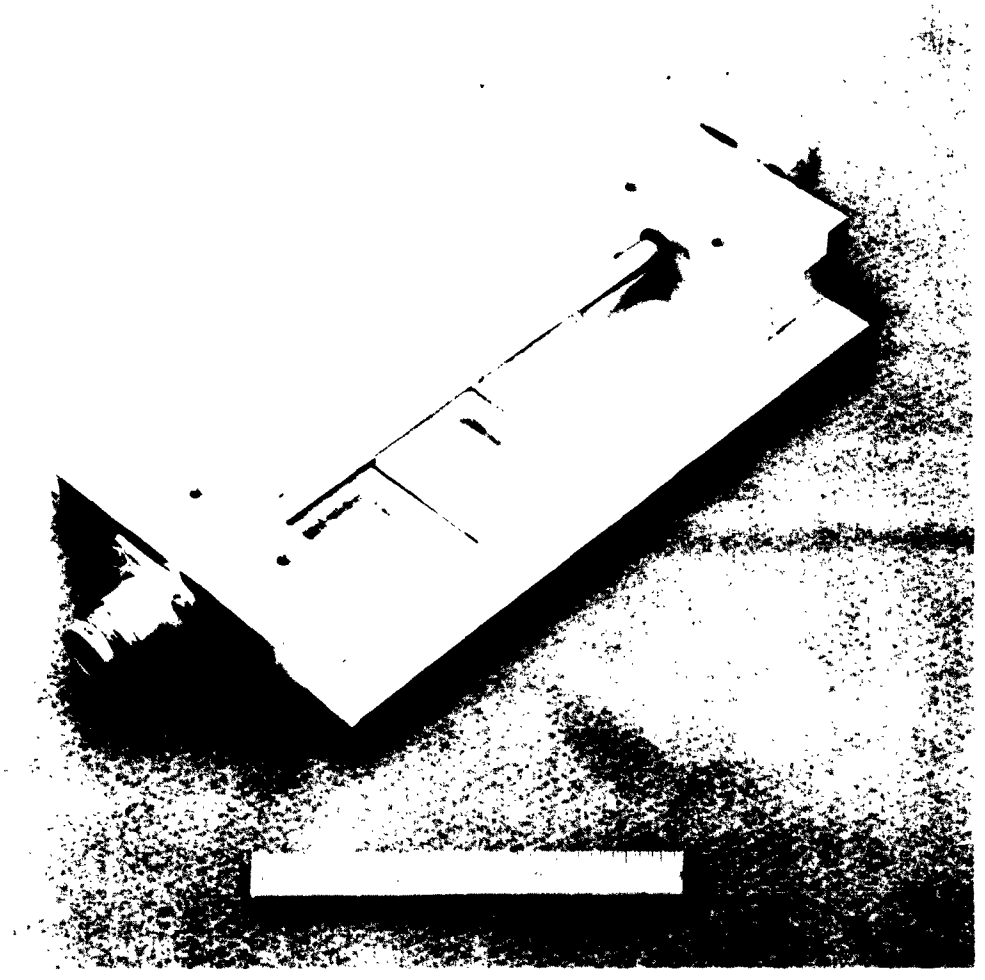

FIG. VI-1 PHOTOGRAPH OF SECOND-HARMONIC-FREQUENCY REJECTION FILTER WITH ONE GROUND PLANE REMOVED

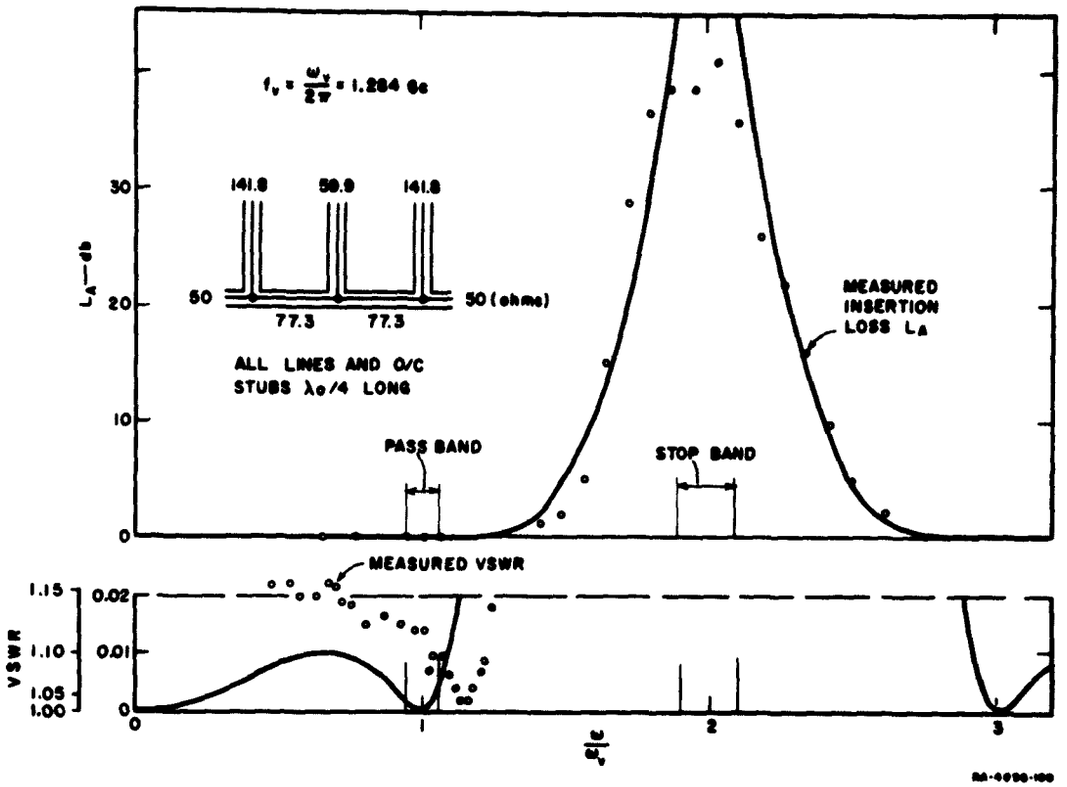

FIG. VI-2 MEASURED AND THEORETICAL RESPONSE OF FILTER OF FIG. VI-1

realize the benefits of the exact design method. Thus it was estimated that a coaxial-line second-harmonic rejection filter of the type described would be capable of transmitting 50 kw peak power at 250 Mc into a matched load.[2] A strip-line filter would have a slightly lower peak power capacity.

REFERENCES

1. L. A. Robinson, E. G. Cristal, B. M. Schiffman, and L. Young, "Suppression of Spurious Frequencies," Quarterly Progress Report 2, pp. 61-71, SRI Project 4096, Contract AF 30(602)-2734, Stanford Research Institute, Menlo Park, California (July 1962).

2. E. G. Cristal, Leo Young, and B. M. Schiffman, "Suppression of Spurious Frequencies," Quarterly Progress Report 3, pp. 99-103, SRI Project 4096, Contract AF 30(602)-2734, Stanford Research Institute, Menlo Park, California (January 1963).

3. L. Young, G. L. Matthaei and E. M. T. Jones, "Microwave Band-Stop Filters with Narrow Stop-Bands," *IRE Trans. PGMTT*-**10**, 6, pp. 416-427 (November 1962). This work first appeared in Quarterly Progress Report 3, SRI, Contract DA 36-039 SC-87398, October 1961.

4. L. Weinberg, "Network Design by Use of Modern Synthesis Techniques and Tables," Tech. Memo 427, Hughes Aircraft Company, Research Laboratories, Culver City, California (April 1956); also *Proceedings of the National Electronics Conference*, **12** (1956).

5. L. Weinberg, "Additional Tables for Design of Optimum Ladder Networks," *Journal of the Franklin Institute*, **264**, Nos. 1 and 2 (July and August 1957).

6. R. Saal, *Der Entwurf von Filtern mit Hilfe des Kataloges normierter Tiefpasse*, Telefunken, G.M.B.H., Backnang/Württemburg, Western Germany (1961) [Part of these tables are contained in the paper: R. Saal and E. Ulbrich, "On the Design of Filters by Synthesis," *IRE Trans. PGCT*-**5**, pp. 284-327 (December 1958)].

7. G. L. Matthaei, *et al.*, "Design Criteria for Microwave Filters and Coupling Structures," Chapter 13, Final Report, SRI Project 2326, Contract DA 36-039 SC-74862, Stanford Research Institute, Menlo Park, California (January 1961).

8. G. L. Matthaei, L. Young, and E. M. T. Jones, "Design of Microwave Filters, Impedance Matching Networks, and Coupling Structures," Vol. I, Sec. 4.05, SRI Project 3527, Contract DA 36-039 SC-87398, Stanford Research Institute, Menlo Park, California (January 1963).

9. B. M. Schiffman, *et al.*, "Microwave Filters and Coupling Structures," Quarterly Progress Report 7, Sec. II, SRI Project 3527, Contract DA 36-039 SC-87398, Stanford Research Institute, Menlo Park, California (November 1962).

10. G. L. Matthaei, L. Young, and E. M. T. Jones, "Design of Microwave Filters, Impedance Matching Networks, and Coupling Structures," Vol. II, Sec. 12.09, SRI Project 3527, Contract DA 36-039 SC-87398, Stanford Research Institute, Menlo Park, California (January 1963).

VII ATTENUATION AND TIME DELAY OF FILTERS*

The connection between attenuation and time delay of band-pass filters is of some interest,[1†] and was treated in detail in Quarterly Progress Report 1.[2] That report considers mainly transmission-line stepped-impedance filters,[3,4] such as quarter-wave transformers or half-wave filters. It is shown[2,4] that the transmission-line filters reduce to lumped-constant filters in the limit as the parameter R (the output-to-input impedance ratio in the case of a quarter-wave transformer) tends to infinity.

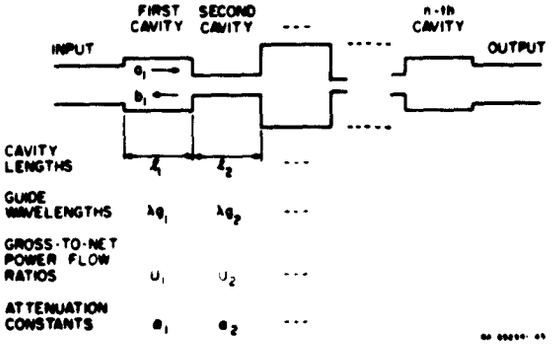

FIG. VII-1 STEPPED-IMPEDANCE FILTER

Consider a stepped-impedance filter (Fig. VII-1). At first, suppose the filter to be free of dissipation loss. Let $|a_1|^2$ be the power carried by the forward wave in the first cavity, and $|b_1|^2$ the power carried by the reflected wave. Similarly for other cavities up to the nth cavity. Let[5]

---

* These results are developed in considerably more detail in Quarterly Progress Report 1.

† References are listed at the end of the section.

$$U_i = \frac{|a_i|^2 + |b_i|^2}{|a_i|^2 - |b_i|^2} = \frac{\text{Gross Power Flow in the } i\text{th Cavity}}{\text{Net Power Flow in the } i\text{th Cavity}} \qquad \text{(VII-1)}$$

Then it can be shown[2] that the group delay $(t_d)_0$ at center frequency f_0 and with the notation of Fig. VII-1 is given by

$$f_0(t_d)_0 = \sum_{i=1}^{n} \left(\frac{\lambda_{gi}}{\lambda}\right)_0^2 \left(\frac{l_i}{\lambda_{gi}}\right)_0 U_i \qquad \text{(VII-2)}$$

where λ is the free-space wavelength. The ratio $(l_i/\lambda_{gi})_0$ is therefore the length of the ith cavity measured in guide wavelengths at center frequency (assumed to be an integral multiple of 1/4), and $(\lambda_{gi}/\lambda)_0^2$ is the dispersion factor[6,7] at center frequency (equal to unity for non-dispersive filters).

It has been shown[5] that the dissipation loss $(\Delta L_i)_0$ of the filter at center frequency, when small, is given by

$$(\Delta L_i)_0 = (1 - |\rho_0|^2) \sum_{i=1}^{n} \alpha_i l_i U_i \qquad \text{(VII-3)}$$

where ρ_0 is the input reflection coefficient. This can be shown[5] to reduce to Cohn's formula[8] for lumped-constant filters when R tends to infinity [except that Cohn omitted the factor $(1 - |\rho_0|^2)$ so that his formula is less accurate for reflecting filters].

When the filter is matched at center frequency ($|\rho_0| = 0$), and when the filter is homogeneous (all the λ_{gi} the same), and when all the attenuation constants α_i are equal, then it follows from Eqs. (VII-2) and (VII-3) that

$$(\Delta L_i)_0 = \alpha\lambda_g(\lambda/\lambda_g)^2 f_0(t_d)_0 \qquad \text{(VII-4)}$$

which can also be written[6]

$$(\Delta L_A)_0 = \frac{\pi}{Q_u} f_0 (t_d)_0 \qquad \text{(VII-5)}$$

where Q_u is the unloaded Q of each cavity.

A series of "universal" curves was plotted[2] for the attenuation and group delay of maximally flat, Chebyshev, maximally flat time-delay, and periodic filters for 1, 2, 3, 4, 8, and 12 resonators. Although these curves were computed for quarter-wave transformers, they were plotted in normalized form so as to be applicable to lumped-constant filters as well.

REFERENCES

1. T. R. O'Meara, "Band-Center Group-Delay and Incidental Dissipation," *IRE Trans. on Circuit Theory* PGCT-9, p. 192 (June 1962).

2. Leo Young, "Suppression of Spurious Frequencies," Quarterly Progress Report 1, RADC Contract AF 30(602)-2734, Stanford Research Institute, Menlo Park, California (July 1962). (Section III: "Group-Delay and Dissipation-Loss Characteristics of Maximally Flat, Tchebycheff, Maximally Flat Time Delay, and Periodic Filters").

3. Leo Young, "The Quarter-Wave Transformer Prototype Circuit," *IRE Trans. on Microwave Theory and Techniques*, PGMTT-8, pp. 483-489 (September 1960).

4. Leo Young, "Stepped Impedance Transformers and Filter Prototypes," *IRE Trans. on Microwave Theory and Techniques* (to be published). Also, Leo Young and G. L. Matthaei, "Microwave Filters and Coupling Structures," Quarterly Progress Report 4, SRI Project 3527, Contract DA 36-039 SC-87398, Stanford Research Institute, Menlo Park, California (January 1962).

5. Leo Young, "Prediction of Absorption Loss in Multilayer Interference Filters," *Jour. Opt. Soc. Am.* 52 (to be published July 1962).

6. Leo Young, "Q-Factors of a Transmission Line Cavity," *IRE Trans. on Circuit Theory* CT-4, pp. 3-5 (March 1957).

7. Leo Young, "Analysis of a Transmission Wavemeter," *IRE Trans. on Microwave Theory and Techniques*, PGMTT-8, pp. 436-439 (July 1960).

8. S. B. Cohn, "Dissipation Loss in Multiple-Coupled-Resonator Filters," *Proc. IRE* 47, pp. 1342-1348 (August 1959).

VIII TRANSIENT RESPONSE OF FILTERS TO RECTANGULAR AND SINE-SQUARED PULSES*

A. GENERAL

One of the most pressing communication problems of today is the scarity of available radio frequency bandwidth in relation to the steadily growing demand. Intimately related to this situation is the general problem of radio spectrum conservation and the reduction and ultimate prevention of radio-frequency interference. With regard to these problems, it is apparent that the operation of radar and communication systems at minimum bandwidth (consistent with the required information rate) is of fundamental importance. Consider, as an example of the necessity of operating a communication system at minimum bandwidth, a hypothetical pulse radar that transmits pulses whose time envelope has an approximately rectangular shape. The resulting frequency spectrum of a single pulse has a $(\sin x)/x$ shape. Approximately 90 percent of the total energy of the pulse is contained in the "main lobe" of the $(\sin x)/x$ spectrum. Hence, about 10 percent of the energy remains in the side lobes. In the case of high-power radars having peak power levels of several megawatts, the energy in the side lobes can be considerable. Although much of the side-lobe energy is never utilized by the receiver, because of receiver selectivity, systems operating at different frequencies may be severely hampered by the intensity of this side-lobe energy. Because of this interference problem, techniques to reduce the width of the transmitted spectrum are of considerable interest. One method is to use a very narrow band-pass filter to suppress the unwanted side lobes. At microwave frequencies, assuming rectangular pulse lengths of the order of a microsecond, this would require filter band-widths of approximately one percent, depending on the carrier frequency. A second method is to shape the pulse envelope in the time-domain by appropriate modulation of the transmitter power amplifier. This method reduces the side-lobe energy content directly, and increases the energy density of the main lobe. A third method that has been proposed by some is to use a pulse-shaping filter; *i.e.*, a filter with a prescribed frequency response such that the spectrum of an input pulse is modified by the filter to give

* This work is reported in more detail in Quarterly Progress Reports 2 and 4.

a particular shaped pulse in the time domain.[1*] This type of filter differs from an ordinary band-pass filter which merely attenuates frequencies outside the pass-band.

During this study, the effects on pulse shape of using narrow-band filters to reduce the spectrum side lobes has been considered for rectangular pulses and for sine-squared pulses. (With the latter pulse shape, of course, the side-lobe energy has already been reduced considerably by means of the pulse shaping in the time domain.) In such use of filters, the question arises as to how much of the pulse energy, *i.e.*, how many side lobes, can be suppressed without appreciable distortion of the pulse. As is well known, even with an ideal filter, (*i.e.*, constant amplitude and linear phase throughout the pass-band) the suppression of any side lobe energy at all causes some distortion of the pulse shape.[2] This result is inherent in the physical problem. What is more important in practical situations is the effect of the amplitude and phase characteristics of actual filters on the transmission of radar pulses. For this reason, the transfer functions of several practical filter types were used in the calculations. The transient responses were obtained using Laplace and Fourier transform methods.[3] Details of the methods are given elsewhere.[4,5]

B. LOW-PASS PROTOTYPES AND RELATIONSHIPS TO BAND-PASS FILTERS

The actual problem of interest is the distortion of pulsed microwave signals as they are passed through narrow-band, band-pass filters. However, the calculations are simplified by using video pulses and low-pass prototypes whose element values are closely related to those of the band-pass filters, rather than pulse-modulated RF carriers (whose envelope is the same as the video pulse) and band-pass filters. Mathematical justification for using this simplified method of obtaining the transient responses is given elsewhere.[4] Only a single pulse is used here, but the results apply to a train of pulses where the spacing between pulses is sufficiently long that the transient due to one pulse is damped out before the next pulse occurs. Four types of prototypes were used in this study: (1) the equal-ripple filter, (2) the maximally flat filter, (3) the maximally flat time-delay filter, and (4) the equal-element filter. The characteristics of the first three of these filters may partially be described by their attenuation or phase response in the pass-band. Briefly, the equal-ripple filter has equal-ripple attenuation peaks in the pass-band;

* References are listed at the end of the section.

the maximally flat filter has an attenuation characteristic that is maximally flat at zero frequency in the low-pass prototype; and the maximally flat time-delay filter exhibits a time-delay characteristic that is maximally flat at zero frequency in the low-pass prototype. For all the low-pass prototypes, zero frequency corresponds to mid-band frequency of the band-pass filters. The equal-element filter can be distinguished from the others primarily by its element values. The low-pass prototype for the equal-element consists of a ladder network of series inductances and shunt capacitances whose normalized series and shunt elements are all of equal numerical value.[6] (The generator and load terminations of the equal-element filter are equal to each other, but are not necessarily equal numerically to the normalized reactive elements.) Of the four filters, the equal-element filter can be shown to have the following characteristics for a given degree of selectivity:[6,7]

(1) Maximum power-handling capability

(2) Minimum midband dissipation loss (when the loss is small)

(3) Simplified construction and alignment procedures, since all internal coupling elements and spacings are identical.

For these reasons microwave filters designed from equal-element prototypes may be of increased importance in the future.

In order to compare the transient properties of the various filter types, it is necessary to specify bandwidth. The definition that appeared best suited for this particular study is the following:

(1) *For low-pass filters*--The bandwidth is defined as the frequency at which the transducer loss* rises to 30 db.

(2) *For band-pass filters*--The bandwidth is defined as the difference of the frequencies at which the transducer loss rises to 30 db.

Since filter specifications usually require that the transducer loss exceed some given value at a given freuqency in the stop-band, the above definition permits comparison on the basis that the four types of filters have equal bandwidths to some point in the stop-band. Although the choice

* Transducer loss is defined as $10 \log_{10}(P_{avail}/P_L)$, where P_{avail} is the power available from the generator when the load presents a conjugate match to the generator, and P_L is the power delivered to the load resistance when the filter is in place. The transducer loss is always greater than or equal to zero db. In the case of equal and purely real generator and load impedances, transducer loss is the same as the more commonly used insertion loss.

of the 30-db frequencies is somewhat arbitrary in defining band-width, it is believed that the value of 30-db transducer loss is a suitable compromise between smaller and larger values.

Direct comparison of the various filter types is often made difficult by the fact that bandwidth is commonly defined in a different way for each filter type. For the equal-ripple prototype bandwidth is usually measured to a point on the response skirts that has the same transducer loss as the transducer loss existing at the ripple peaks. For the maximally flat prototype, the bandwidth is usually measured to the frequency where the transducer loss is 3 db. For the maximally flat time-delay prototype, the radian bandwidth is usually considered to be the reciprocal of the zero-frequency time delay. No convention has been established for defining the bandwidth of equal-element prototypes. As explained previously, all of the filters considered in this study are compared on the basis of having equal bandwidth to some point in the stop-band--specifically, to the frequency of 30-db transducer loss when no dissipation loss is present. The ratios of the more conventional bandwidths to the 30-db bandwidth are shown in Figs. VIII-1 and VIII-2 to aid the reader in relating the 30-db bandwidth to quantities with which he may be more familiar. A comment is in order concerning the six-reactive-element, equal-element prototype. For this prototype, the last ripple in the pass-band is slightly higher than 3 db; the 3-db bandwidth plotted in Fig. VIII-1 is measured to the last 3-db frequency.

All low-pass prototypes used in this study are in the form of ladder networks, as shown in Fig. VIII-3. The g_i, $i = 1, 2, \ldots, n$, are capacitance in farads for the shunt reactive elements, and are inductance in henries for the series reactive elements. The h_i are conductance in mhos for the shunt elements, and are resistance in ohms for the series elements. For filters with zero dissipation loss within the filter elements, all of the h_i are zero. Each termination is a pure resistance in ohms if the adjacent reactive element is a shunt element, or a pure conductance in mhos if the adjacent reactive element is a series element. Several tables are available for the g_i required to give equal-ripple, maximally flat, and maximally flat time-delay types of transfer functions for dissipationless prototypes.[8,9,10] The h_i are made greater than zero to take dissipation loss into account. In introducing dissipation loss into the prototypes used in this study, the same values of g_i are used in both the

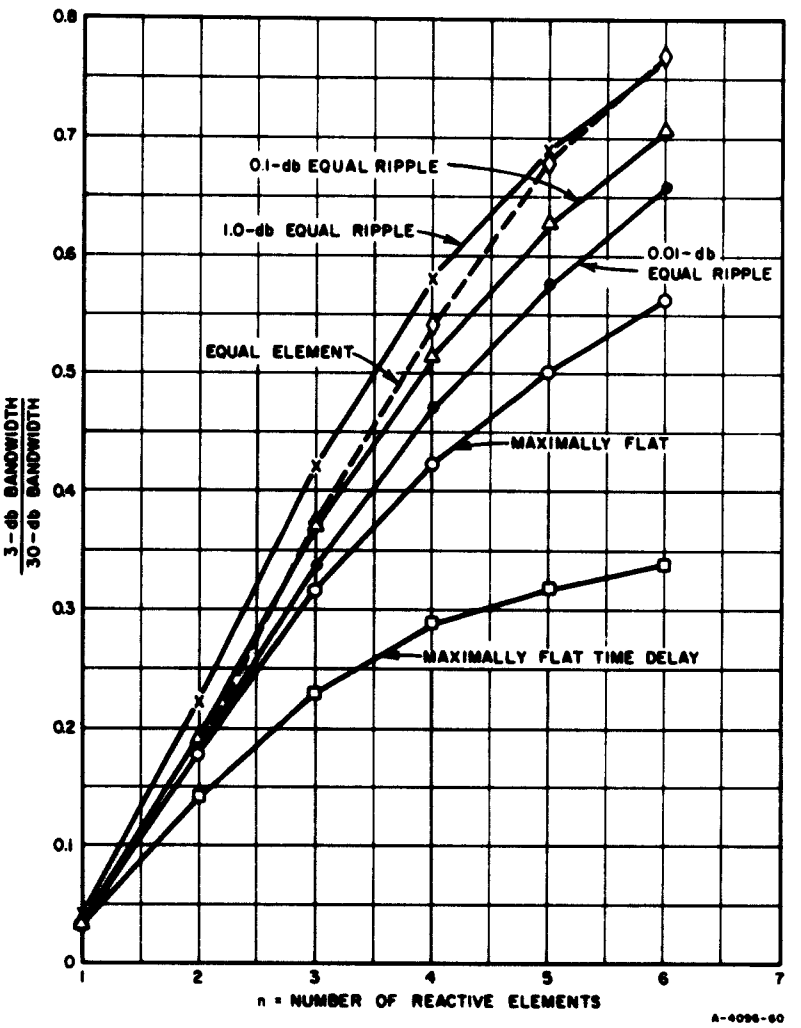

FIG. VIII-1 RATIO OF 3-db AND 30-db BANDWIDTHS FOR FOUR FILTER TYPES

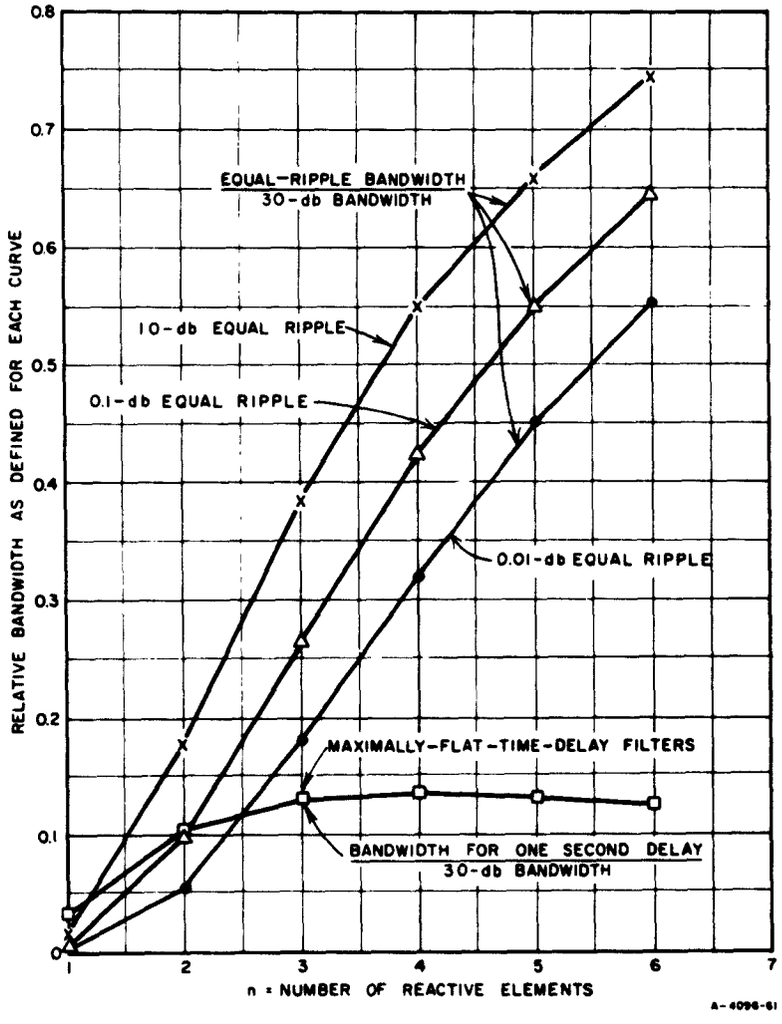

FIG. VIII-2 ADDITIONAL BANDWIDTH COMPARISONS FOR EQUAL RIPPLE AND MAXIMALLY FLAT-TIME-DELAY FILTERS

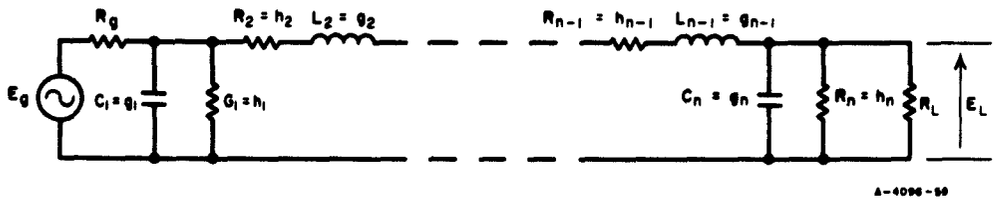

FIG. VIII-3 LOW-PASS PROTOTYPE WITH LOSS ELEMENTS INCLUDED

the lossless and the corresponding lossy case. Note, therefore, that the descriptions *equal-ripple* and *maximally flat* used in this report describe the filter characteristics when there is no dissipation loss. Dissipation loss will obliterate the ripples in the transfer function of the equal-ripple filter, and the maximally flat filter will no longer have the flattest possible transfer function at midband. Filters having true maximally flat or equal-ripple responses when dissipation loss is present have not been considered in this study, since it has been shown that these filter types have higher dissipation loss for a given resonator unloaded Q.[6,11]

The study of the effects of dissipation loss on the transient response of filters has been limited to the typical situation in microwave filters where all of the resonators in a given filter have equal values of unloaded Q. The corresponding low-pass prototypes have equal values of the ratio h_i/g_i for each of the pairs of reactive and lossy elements. Thus, for each filter, a parameter that will be called *dissipation factor* can be defined as

$$d = \frac{h_i}{g_i}, \quad i = 1,2,\ldots, n \qquad \text{(VIII-1)}$$

where n is the number of reactive elements in the prototype. For most types of microwave filters, n will also be the number of resonators in the filter. For the prototypes considered in this report, the parameter d was chosen to correspond with 3-db increase in transducer loss at midband for the band-pass filter as a result of dissipation. (The prototypes than have 3-db increase in transducer loss at zero frequency.) Also, the midband dissipation loss can be related to the product of band-pass filter fractional bandwidth, $w_{3\,db}$, and the unloaded Q of the resonators, Q_u.

The specific definition of bandwidth is given by

$$w_{30\ db} = \frac{\omega_2 - \omega_1}{\omega_0} \qquad \text{(VIII-2)}$$

where ω_1 and ω_2 are the lower and upper frequencies, respectively, where the transducer loss of the dissipationless, band-pass filter is 30-db, and $\omega_0 = 0.5(\omega_1 + \omega_2)$ is the midband frequency of the band-pass filter. The values of $w_{30\ db}Q_u$ corresponding to the transient responses presented in this report are tabulated in Table VIII-1 for reference. The value 3 db was chosen as a probable upper limit on the amount of dissipation loss that could be tolerated for the proposed application, where the filter would follow a high-power radar transmitter tube.

Table VIII-1

PRODUCT OF 30-DB FRACTIONAL BANDWIDTH AND UNLOADED Q FOR BAND-PASS FILTERS WITH 3-DB MIDBAND DISSIPATION LOSS

	0.1-DB-EQUAL-RIPPLE FILTER	EQUAL-ELEMENT FILTER	MAXIMALLY FLAT FILTER	MAXIMALLY FLAT TIME-DELAY FILTER
Three-resonators filters	17.4	17.4	18.2	21.4
Six-resonator filters	19.6	20.4	19.9	22.8

To orient the reader with respect to the differences in the filter types considered in this report, the magnitude of the voltage transfer functions are plotted in Fig. VIII-4 for the four prototypes having six reactive elements each. In this report, transfer function refers to the ratio of the voltage across the load, E_l, to the generator voltage, E_g, with the transfer function normalized to unity maximum value. Note that there is considerable difference in the shapes of the transfer functions for the four prototypes. Also shown in Fig. VIII-4 is the voltage spectrum of a rectangular and of a sine-squared pulse. For the rectangular pulse the expression for the voltage spectrum normalized to unity at zero frequency is[12]

$$\frac{\sin\left(\frac{\omega' T}{2}\right)}{\left(\frac{\omega' T}{2}\right)} \qquad \text{(VIII-3)}$$

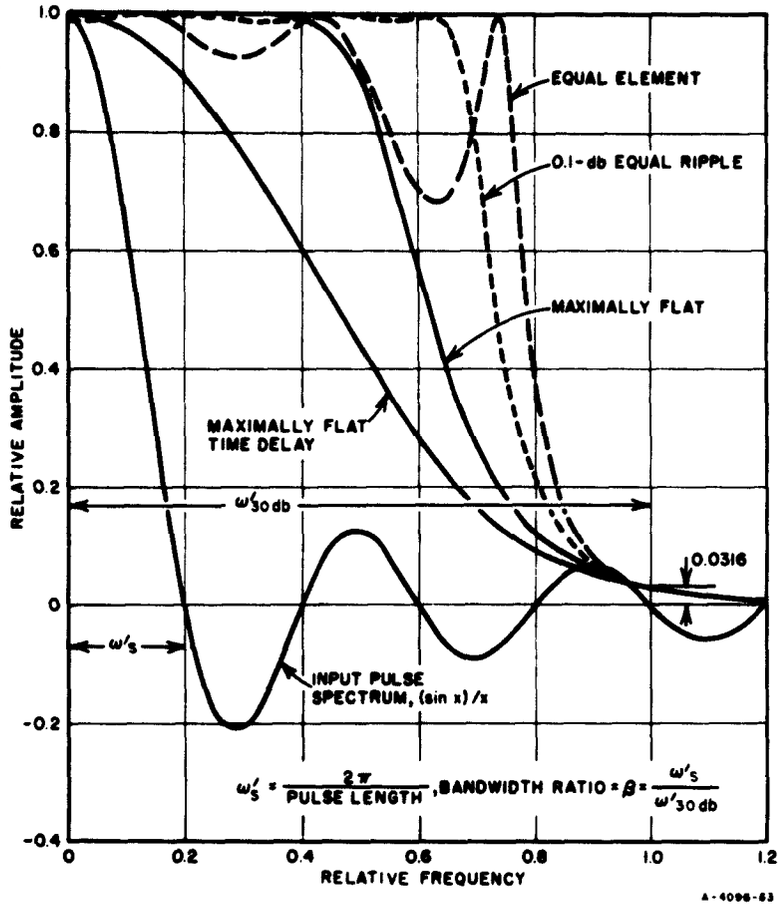

FIG. VIII-4 TRANSFER FUNCTIONS OF SIX-REACTIVE-ELEMENT PROTOTYPES AND SPECTRUM OF INPUT RECTANGULAR AND SINE-SQUARED PULSE

For the sine-squared pulse the expression for the voltage spectrum normalized by unity at zero frequency is[13]

$$\frac{\sin\left(\frac{\omega' T}{2}\right)}{\left(\frac{\omega' T}{2}\right)\left[1 - \left(\frac{\omega' T}{2\pi}\right)^2\right]} \quad . \qquad \text{(VIII-4)}$$

The width ω'_s of the input-pulse spectrum is defined here as the frequency of the first zero-crossing. A parameter that will be used throughout this

report is the ratio β of the spectrum bandwidth to the filter bandwidth, as defined by

$$\beta = \frac{\omega_s'}{\omega_{30\ db}'} \quad , \tag{VIII-5}$$

where $\omega_{30\ db}'$ is the frequency at which the transfer function of the low-pass prototype is down 30 db, as shown in Fig. VIII-4. This ratio can also be written directly in terms of the pulse length T, in seconds, and the filter bandwidth, in cycles per second:

$$\text{Rectangular Pulse} \qquad \beta = \frac{1}{Tf_{30\ db}'} = \frac{2}{T(f_2 - f_1)} \tag{VIII-6}$$

$$\text{Sine-Squared Pulse} \qquad \beta = \frac{2}{Tf_{30\ db}'} \qquad \frac{4}{T(f_2 - f_1)} \tag{VIII-7}$$

where $f_{30\ db}' = \omega_{30\ db}'/2\pi$ is the 30-db frequency for the low-pass prototype, and f_1 and f_2 are the lower and upper 30-db frequencies, respectively, of the corresponding band-pass filter. For each filter type, the ratio β is defined assuming no dissipation loss within the filter. In comparing the curves presented in Parts C and D, note that β increases as either pulse length, or filter bandwidth, or both are decreased.

C. TRANSIENT RESPONSES TO RECTANGULAR PULSE SIGNALS

The transient responses to rectangular pulse signals are given graphically in this part for two representative values of β. (A more detailed presentation and several more responses are given in Ref. 4). Also, quantitative data of *relative peak overshoot, rise-time, delay-time,* and *ringing time* are presented in Table VIII-2 for the cases of $\beta = 0.1$. These parameters are useful for describing and comparing the responses to rectangular pulses of the four filter types investigated in this study.

The responses of the four filter types to a rectangular pulse having a pulse-spectrum-to-filter-bandwidth ratio of $\beta = 0.1$ are given in Figs. VIII-5 and VIII-6. Figure VIII-5 shows the responses of the four filter types having three reactive elements with and without dissipation

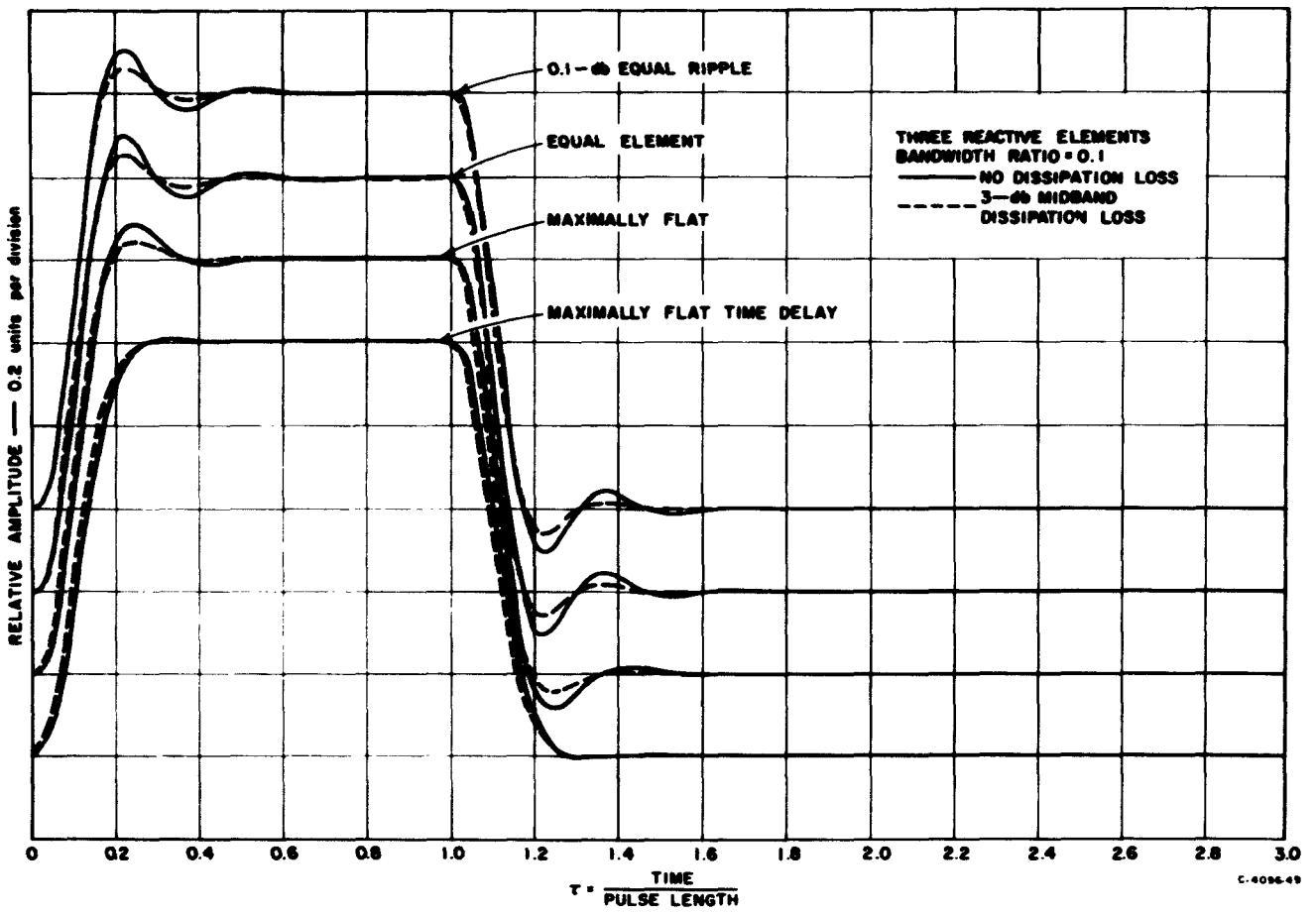

FIG. VIII-5 TRANSIENT RESPONSE CURVES FOR FOUR FILTER TYPES WITH AND WITHOUT LOSS HAVING THREE REACTIVE ELEMENTS (Pulse-Bandwidth-to-Filter-Bandwidth Ratio β = 0.1)

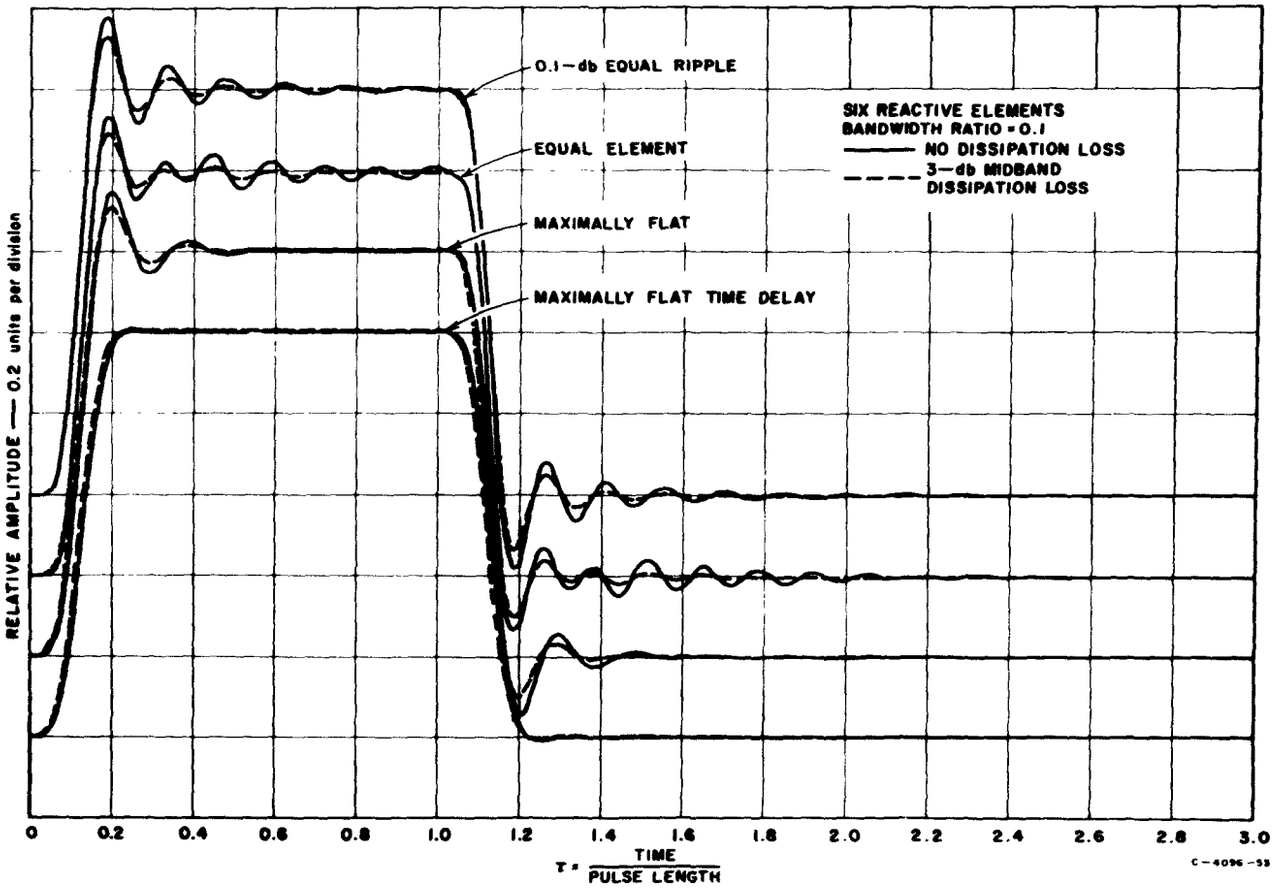

FIG. VIII-6 TRANSIENT RESPONSE CURVES FOR FOUR FILTER TYPES WITH AND WITHOUT LOSS HAVING SIX REACTIVE ELEMENTS (Pulse-Bandwidth-to-Filter-Bandwidth Ratio β = 0.1)

Table VIII-2

CHARACTERISTICS OF TRANSIENT RESPONSES TO RECTANGULAR PULSES FOR THREE- AND SIX-REACTIVE-ELEMENT FILTER PROTOTYPES

(Pulse-bandwidth-to-filter-bandwidth ratio $\beta = 0.1$)

	0.1-db-EQUAL-RIPPLE FILTER		EQUAL-ELEMENT FILTER		MAXIMALLY FLAT FILTER		MAXIMALLY FLAT TIME-DELAY FILTER	
	$N = 3$	$N = 6$	$N = 3$	$N = 6$	$N = 3$	$N = 6$	$N = 3$	$N = 6$
Overshoot, percent:								
(a) Lossless cases	10%	18%	10%	13%	8%	14%	0.6%	0.6%
(b) 3-db-loss cases	6%	13%	6%	10%	4%	10%	0.3%	0.4%
Ten-to-90-percent rise time, fraction of pulse length:								
(a) Lossless cases	0.105	0.0688	0.102	0.0687	0.115	0.0762	0.152	0.102
(b) 3-db-loss cases	0.108	0.0712	0.106	0.0712	0.118	0.0787	0.144	0.102
Delay time, fraction of pulse length:								
(a) Lossless cases	0.102	0.118	0.102	0.120	0.108	0.118	0.118	0.127
(b) 3-db-loss cases	0.098	0.116	0.098	0.118	0.100	0.113	0.105	0.120
Number of ripple extremes deviating from unity by more than ±1%:								
(a) Lossless cases	3	8	3	>13	2	4	0	0
(b) 3-db-loss cases	2	4	2	9	1	2	0	0

Note: N = number of reactive elements.

loss; Fig. VIII-6 shows the responses of the four filter types having six reactive elements with and without dissipation loss. The curves in these figures are displaced from each other by one graph division to reduce overlap. However, they are still close enough to permit easy visual comparison. The solid curves are for the cases with no dissipation loss within the filters, and the dashed curves are for the cases with an increase in transducer loss of 3 db at zero frequency due to dissipation loss within the filter. For convenience in making visual comparisons of overshoot, the amplitude for the transient responses to rectangular pulses has been normalized so that the top of the pulse approaches unity as the ringing is damped out. Significant characteristics of the responses of each curve in Figs. VIII-5 and VIII-6 are summarized in Table VIII-2. Since the transient curves are normalized to unity amplitude as the ringing is damped out, amplitudes are expressed in Table VIII-2 as a fraction of unity. Also, all time scales are normalized with respect to the length of the input pulse, so that the times in Table VIII-2 are expressed as fractions of the input pulse length. The quantity labeled *overshoot* is the amount by which the first peak of the transient exceeds unity, and is expressed in percent. The 10-to-90 percent *rise time* is measured from the time at which the output pulse equals 0.1 to the time that it first

equals 0.9. The *delay-time* is measured from the time that the input pulse is applied to the filter to the time that the output pulse reaches a value of 0.5. (This definition of delay time is conveniently read from the time-response curves, but is not the same as the definition of group delay time discussed in Sec. III of Quarterly Progress Report 1 on this contract.[14]) Ringing of the different filter types is described here by the number of ripple extremes that exceed plus or minus one percent. For example, the next to last row in Table VIII-2 shows that the transient for the equal-element filter goes past 1.01 once, then goes below 0.99, and then above 1.01 again before the top of the pulse stays within the limits 0.99 to 1.01.

The effect on the transient response of narrowing the filter bandwidth relative to the pulse-spectrum-bandwidth is demonstrated by the curves of Figs. VIII-7 and VIII-8, in which the cases $\beta = 0.4$ are given.

D. TRANSIENT RESPONSES TO SINE-SQUARED PULSE SIGNALS

The transient responses to sine-squared pulse signals are given graphically in this part for two representative values of β. (A more detailed presentation and several more responses are given in Ref. 5.) Also, quantitative data of relative energy transmission, relative peak amplitude transmission, relative peak undershoot, and delay-time are presented in Table VIII-3 for $\beta = 0.2$, 0.4, 0.6, and 0.8. These parameters are useful for describing and comparing the responses to sine-squared pulses of the four filter types investigated in this study.

The responses of the four filter types having three and six reactive elements to a sine-squared pulse for $\beta = 0.2$ are given in Figs. VIII-9 and VIII-10, respectively; those for $\beta = 0.8$ are given in Figs. VIII-11 and VIII-12, respectively. The curves of these figures have been normalized by multiplying the transient responses by a constant that makes the maximum value of the transfer function equal to unity. This normalization procedure is equivalent to that used for rectangular pulses except in the cases of the six-reactive-element, equal-ripple filter. However, this particular normalization procedure ensures that the relative energy transmission will be less than or equal to 100 percent.

In Figs. VIII-9 through VIII-12, the transient responses are for the cases in which the filters have no internal dissipation loss. Responses

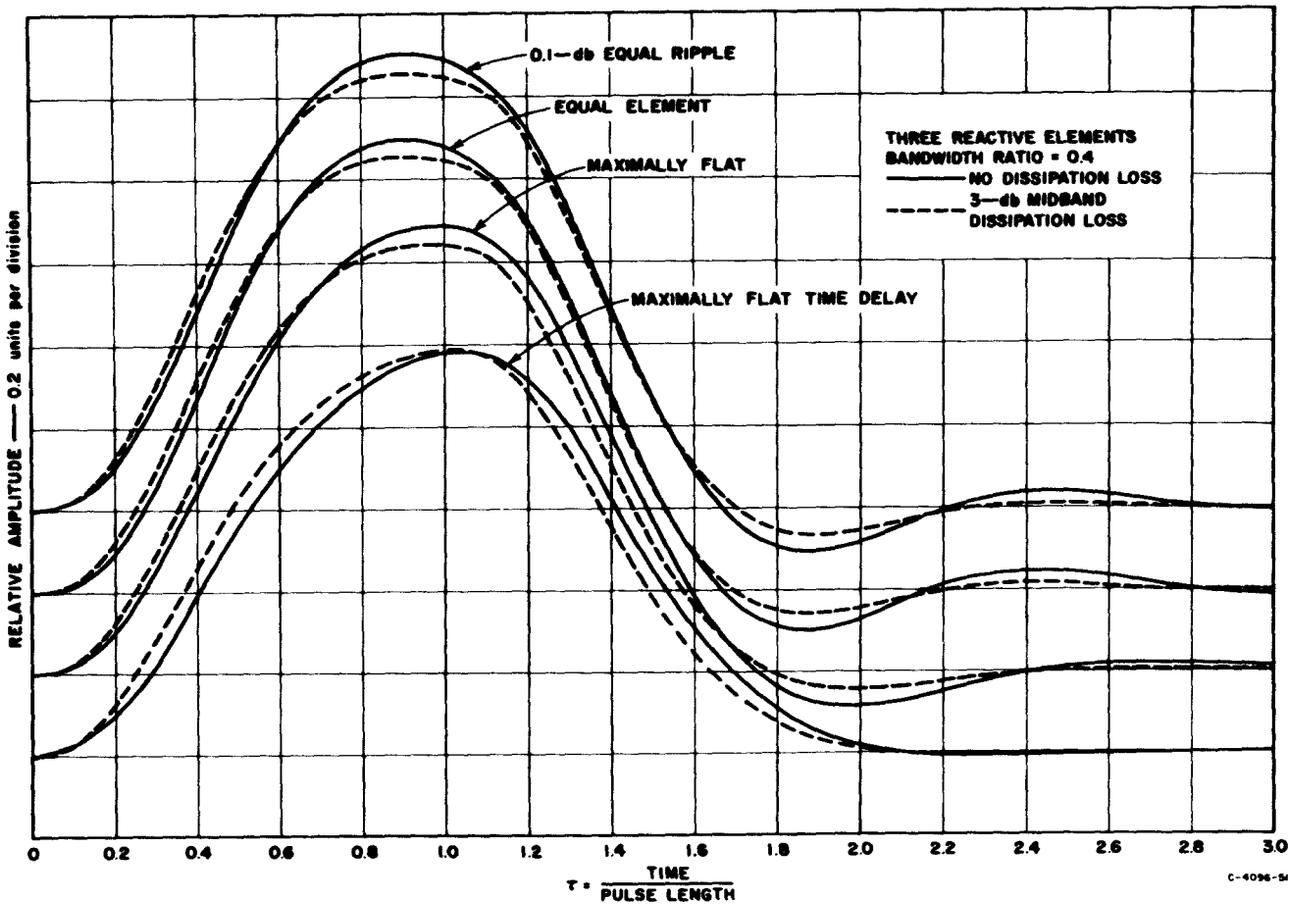

FIG. VIII-7 TRANSIENT RESPONSE CURVES FOR FOUR FILTER TYPES WITH AND WITHOUT LOSS HAVING THREE REACTIVE ELEMENTS (Pulse-Bandwidth-to-Filter-Bandwidth Ratio β = 0.4)

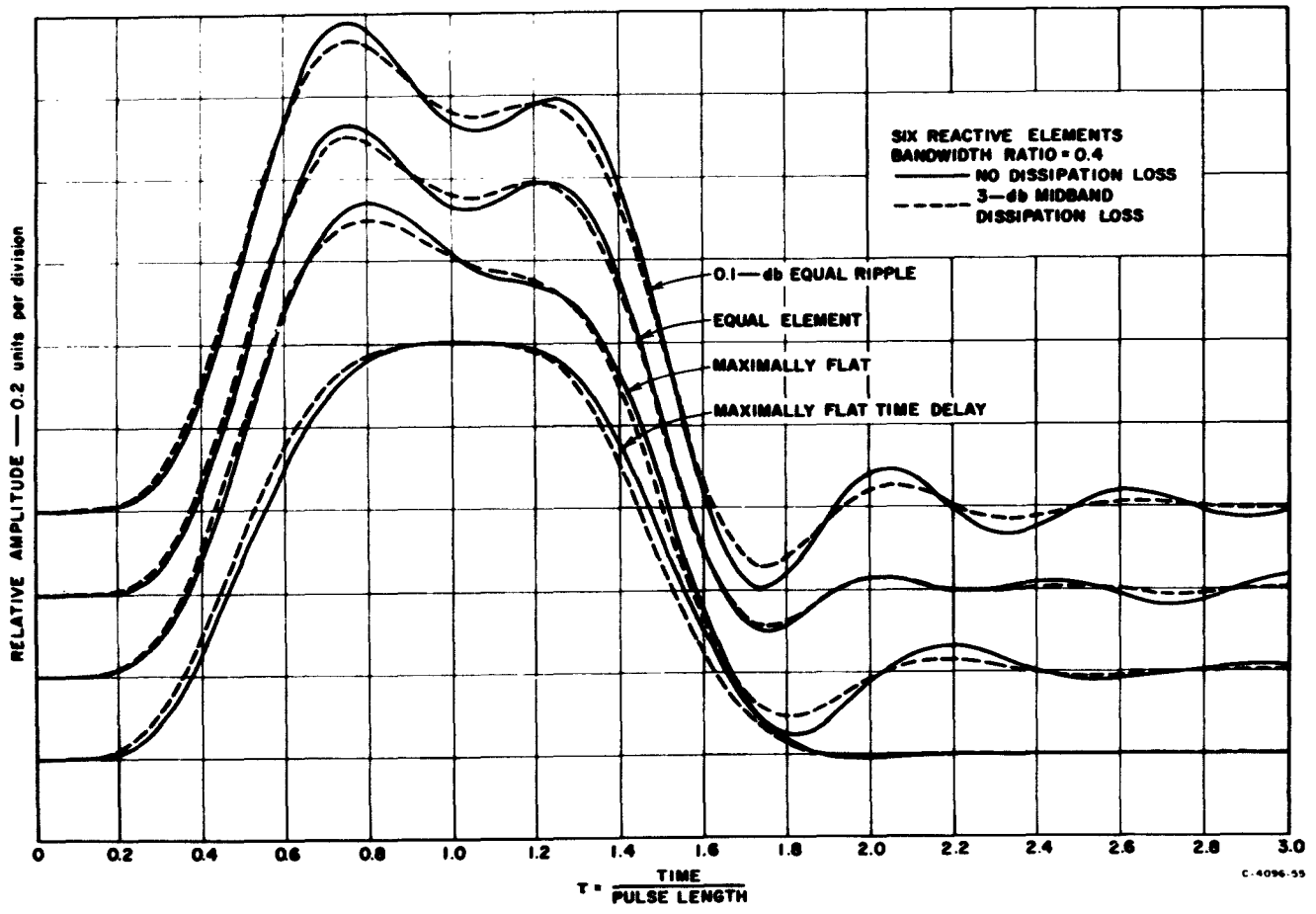

FIG. VIII-8 TRANSIENT RESPONSE CURVES FOR FOUR FILTER TYPES WITH AND WITHOUT LOSS HAVING SIX REACTIVE ELEMENTS (Pulse-Bandwidth-to-Filter-Bandwidth Ratio = 0.4)

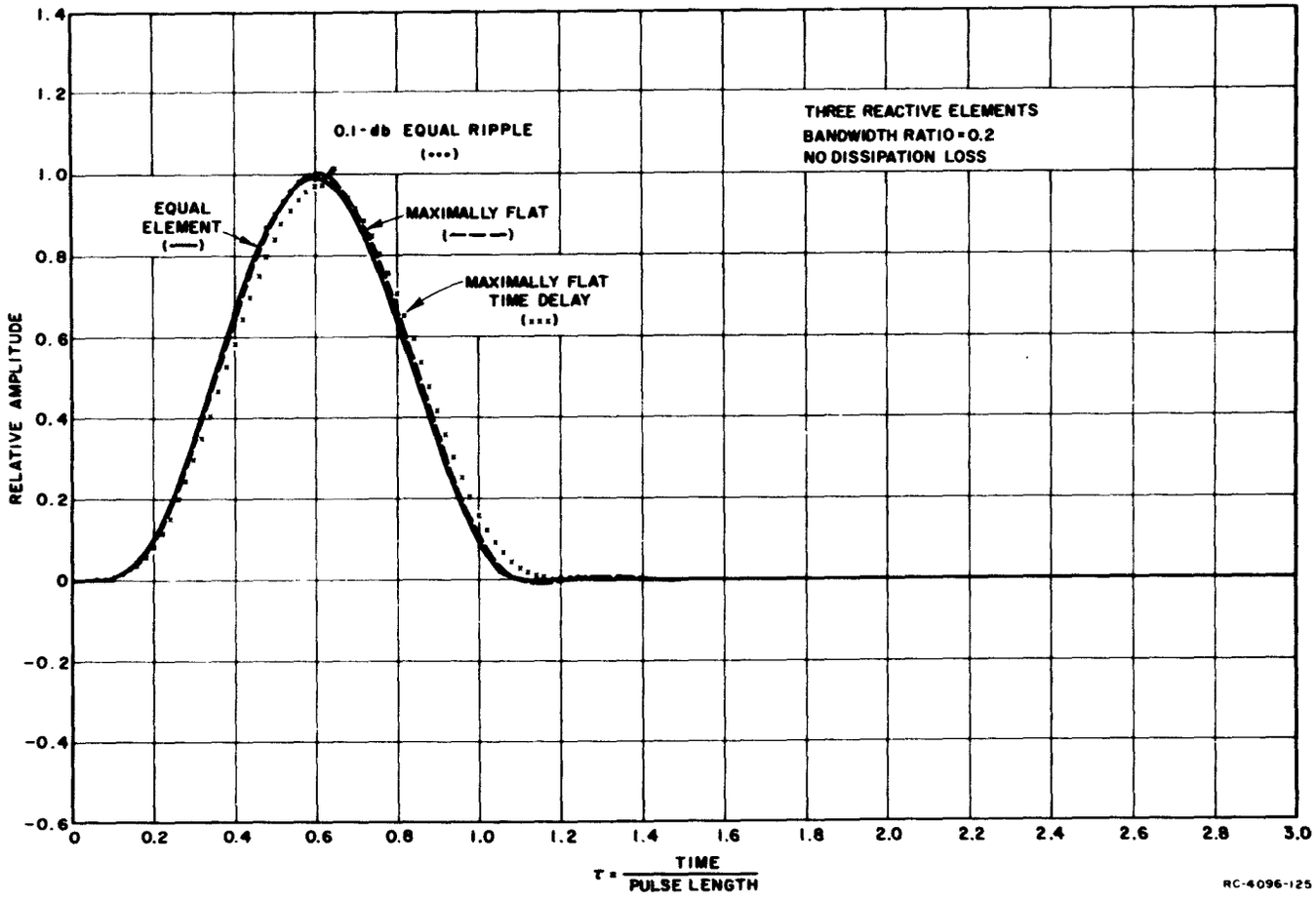

FIG. VIII-9 TRANSIENT RESPONSE CURVES FOR FOUR FILTER TYPES WITHOUT LOSS HAVING THREE REACTIVE ELEMENTS (Pulse-Bandwidth-to-Filter-Bandwidth Ratio = 0.2)

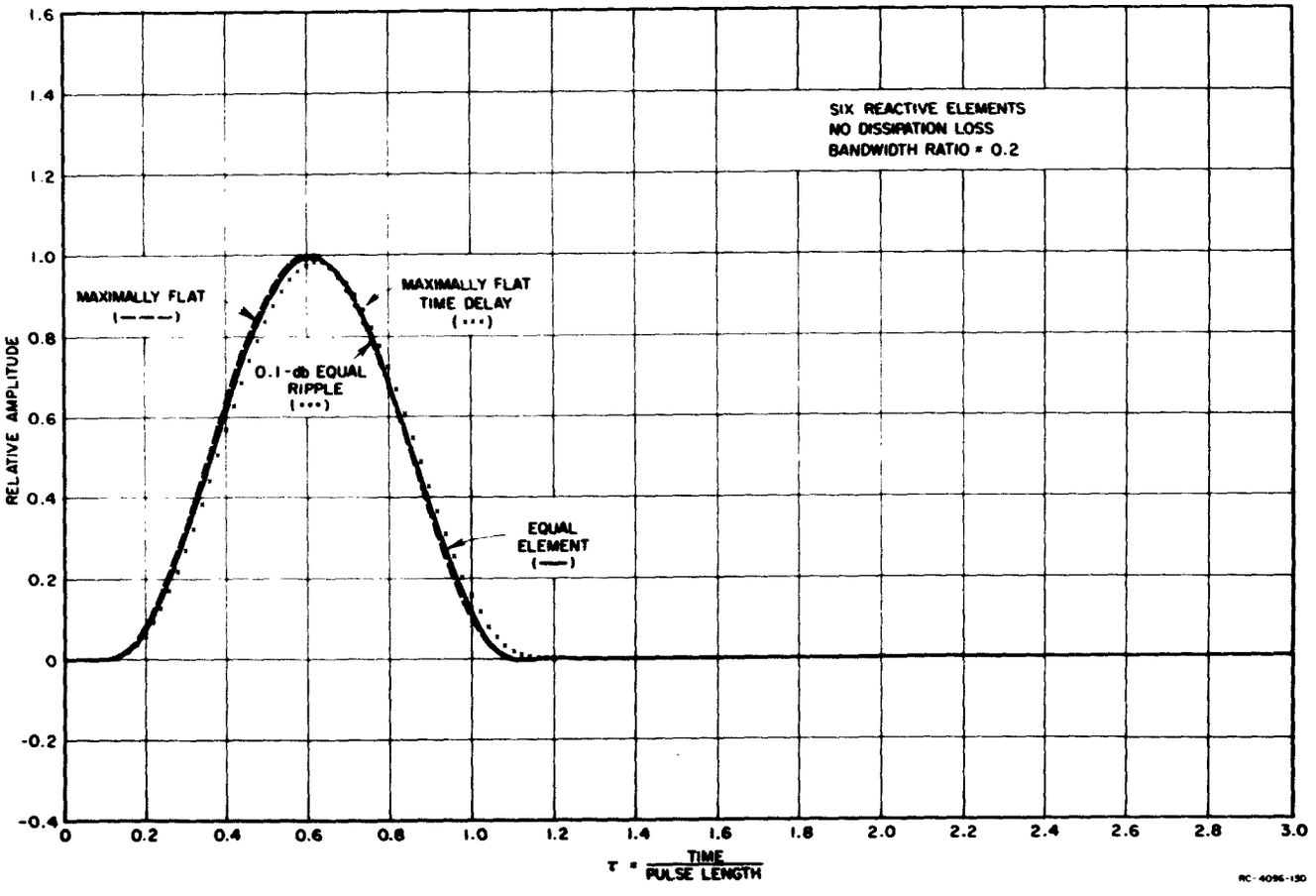

FIG. VIII-10 TRANSIENT RESPONSE CURVES FOR FOUR FILTER TYPES WITHOUT LOSS HAVING SIX REACTIVE ELEMENTS (Pulse-Bandwidth-to-Filter-Bandwidth Ratio = 0.2)

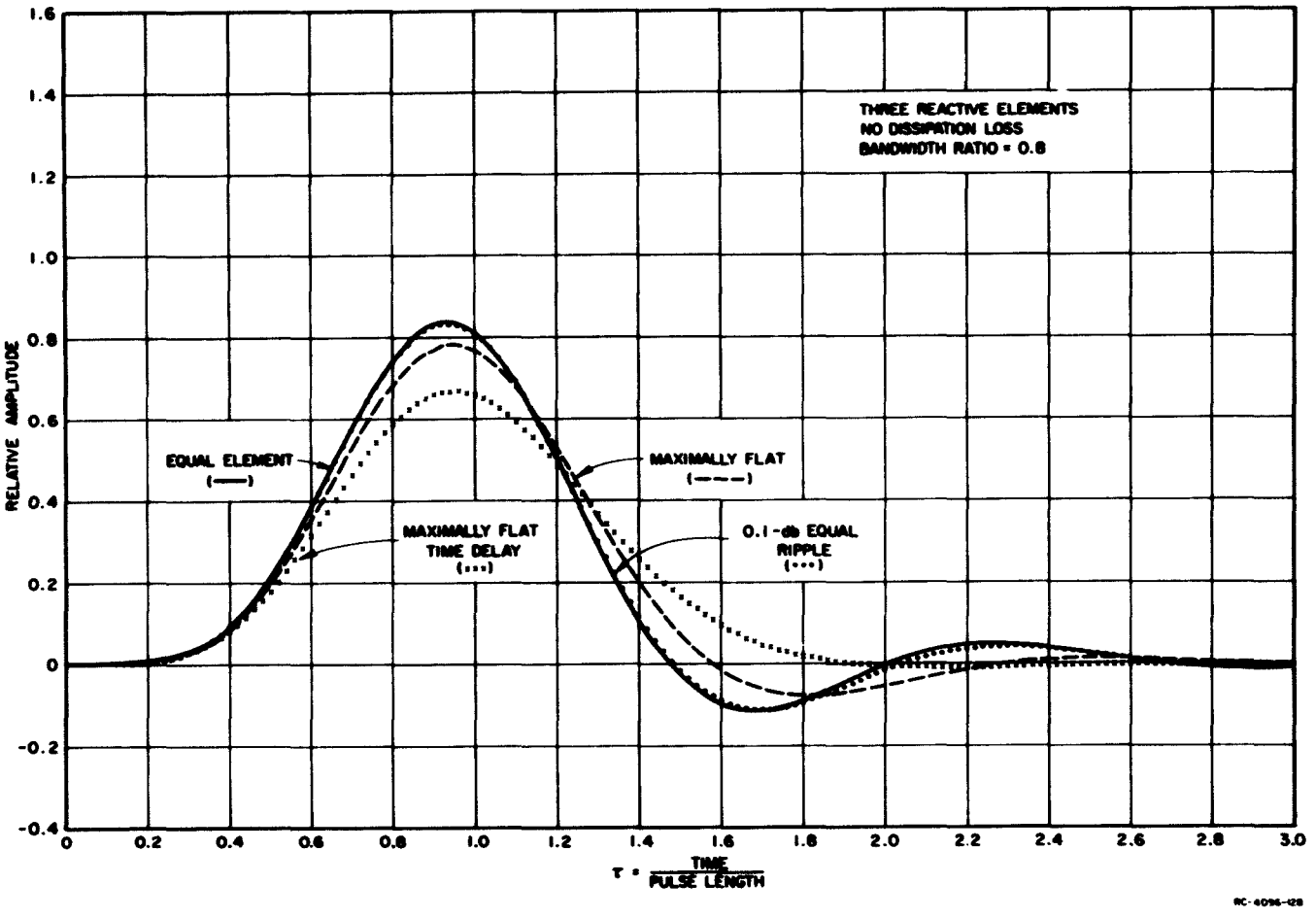

FIG. VIII-11 TRANSIENT RESPONSE CURVES FOR FOUR FILTER TYPES WITHOUT LOSS HAVING THREE REACTIVE ELEMENTS (Pulse-Bandwidth-to-Filter-Bandwidth Ratio = 0.8)

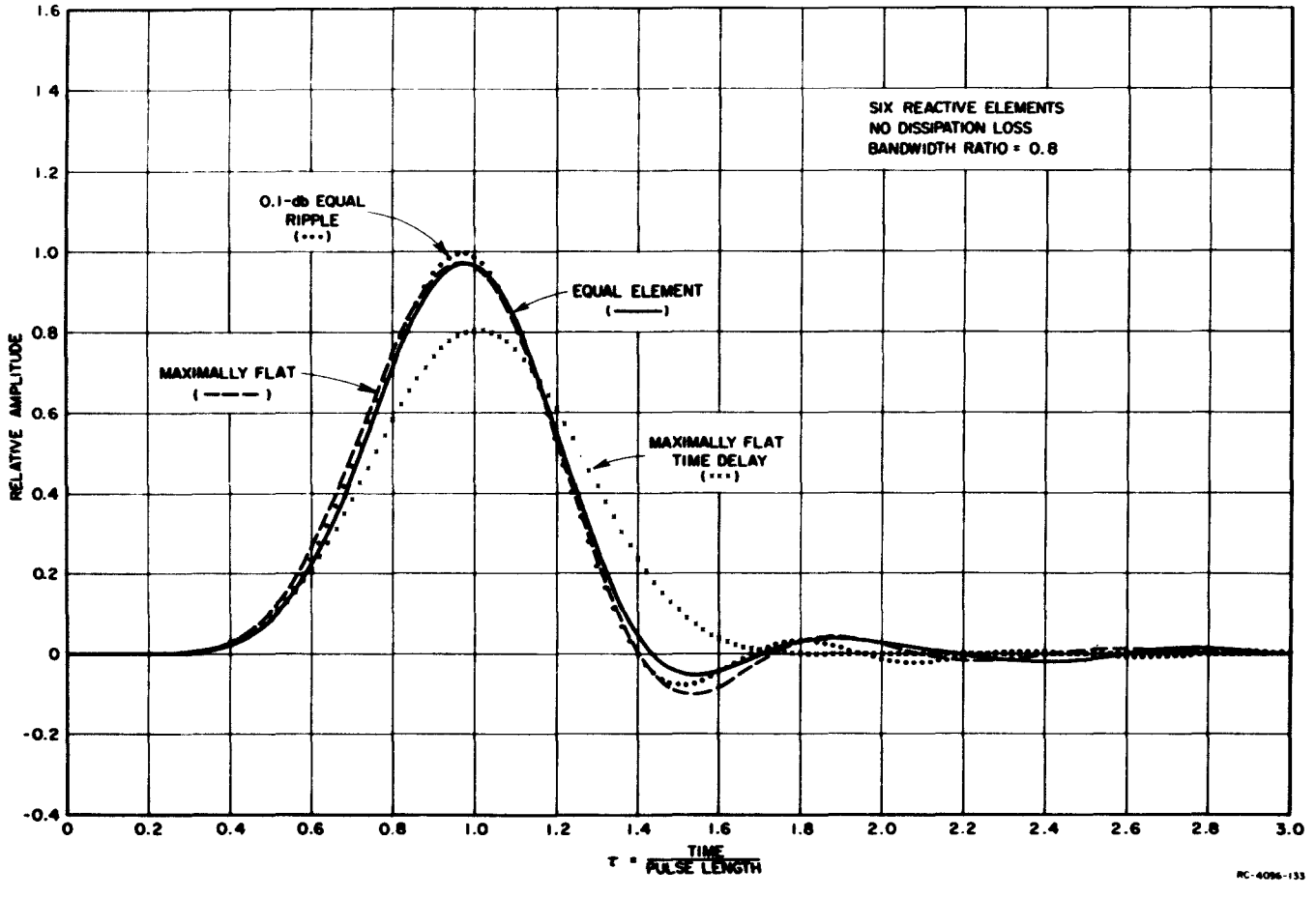

FIG. VIII-12 TRANSIENT RESPONSE CURVES FOR FOUR FILTER TYPES WITHOUT LOSS HAVING SIX REACTIVE ELEMENTS (Pulse-Bandwidth-to-Filter-Bandwidth Ratio = 0.8)

Table VIII-3

CHARACTERISTICS OF TRANSIENT RESPONSES TO SINE-SQUARED PULSES FOR THREE- AND SIX-REACTIVE ELEMENT LOSSLESS FILTER PROTOTYPES

	β	0.1-db EQUAL-RIPPLE FILTER		EQUAL-ELEMENT FILTER		MAXIMALLY FLAT FILTER		MAXIMALLY FLAT TIME-DELAY FILTER	
		$N = 3$	$N = 6$	$N = 3$	$N = 6$	$N = 3$	$N = 6$	$N = 3$	$N = 6$
Relative energy transmission, percent	0.2	99.3	98.2	99.0	99.8	99.9	100	96.2	98.1
	0.4	98.7	98.7	98.1	98.6	98.1	100	86.5	92.9
	0.6	95.2	98.8	95.1	97.4	90.9	99.9	74.7	85.7
	0.8	87.4	98.7	87.8	95.9	80.9	98.9	63.9	77.6
Relative peak amplitude transmission, percent	0.2	99.5	98.2	99.2	99.8	100	100	97.1	98.5
	0.4	99.4	98.7	99.3	98.9	97.7	99.9	88.7	94.4
	0.6	93.1	98.8	93.4	98.6	88.9	99.9	77.4	88.1
	0.8	83.2	98.7	83.8	97.0	78.0	97.1	66.7	80.4
Relative peak undershoot, percent	0.2	0.4	0.7	0.2	0.3	1.2	0.4	0.1	0.0
	0.4	3.8	2.2	3.3	0.5	4.7	1.8	0.4	0.0
	0.6	9.5	4.0	9.5	2.0	7.2	4.4	0.6	0.1
	0.8	11.3	7.6	11.6	5.5	7.5	10.0	0.6	0.2
Delay time, fraction of a pulse length in percent	0.2	10	11	10	11	10	10	12	13
	0.4	20	22	20	22	22	22	24	26
	0.6	32	34	31	34	34	33	35	38
	0.8	43	46	43	46	43	46	46	51

Note: N = number of reactive elements.

of the equal-element filter with 3-db dissipation loss at zero frequency are given elsewhere,[5] as typical examples of the effects of internal dissipation loss on the transient responses. In general the effects were qualitatively the same as those for rectangular pulses. That is, overshoot was decreased, ringing was damped and the delay-time was decreased.

The parameters relative energy transmission, relative peak amplitude transmission, relative peak undershoot and delay-time are tabulated in Table VIII-3 for $\beta = 0.2$, 0.4, 0.6, and 0.8. *Relative energy transmission* is defined as the ratio of energy that is delivered to the load resistor with a filter inserted between it and the generator, divided by the energy delivered to the load resistor when it is matched to the generator by an ideal transformer. *Relative peak amplitude transmission* is defined as the ratio of the peak amplitude of the output pulse and the peak amplitude of the input pulse. *Relative peak undershoot* is defined as the ratio of the maximum undershoot at the trailing edge of the output pulse and the maximum amplitude of the input pulse. For the cases of sine-squared pulse signals, *delay-time* is defined as the value of τ for which the cross-correlation of the input and output pulse is a maximum. It is shown elsewhere[5] that the delay-time obtained from this definition is the time for which the output pulse energy, measured over an interval of a pulse length, is a maximum provided that the output pulse is not badly distorted.

E. DISCUSSION

A few observations remain to be made concerning the various filters. From the standpoint of faithful reproduction of either rectangular or sine-squared pulses, there are only small differences between the equal-element, the 0.1-db equal-ripple, and the maximally flat filter types. (Recall that this comparison is made on the basis that each filter has the same bandwidth measured between frequencies of 30-db transducer loss.) The maximally flat time-delay filter has the characteristic, which may be useful for some applications, that there is essentially no overshoot at the leading edge for rectangular pulse inputs, and essentially no undershoot at the trailing edge for either rectangualr or sine-squared pulse inputs. On the other hand, this same filter transmits less of the total input energy than the other three types of filter, and has somewhat slower rise and fall times for rectangular pulse inputs.

In comparing filters with different numbers of resonators, it is seen that a larger pulse-spectrum-to-filter-bandwidth ratio can be used for six-resonator filters than for three-resonator filters before the output pulse shape is seriously degraded. By *seriously degraded*, we mean that the rectangular pulse becomes rounded off, and the sine-squared pulse is stretched in time and has ringing introduced at the trailing edge. The superiority of filters with a larger number of resonators is in part due to the fact that the pass-band more nearly approaches a rectangular shape, although the phase characteristics probably are also important.

The main effects of dissipation loss within the filter elements, aside from the reduction in output amplitude, are to reduce the magnitude of overshoot and undershoot when they occur, and to shorten the length of time during which ringing occurs. These effects tend to even further reduce the small differences in the transient responses of the equal-element, the 0.1-db equal-ripple, and the maximally flat filter types.

It is also of interest to compare some of the characteristics of the two pulse shapes used in this study. For all filters it is found that the main lobe of the input pulse spectrum can fill a larger fraction of the filter bandwidth before serious degradation of the pulse shape occurs when the input pulse has sine-squared shape rather than rectangular shape. This is related to the fact that the sine-squared pulse has less than 0.2 percent of its energy in the side lobes of the frequency spectrum,

whereas the rectangular pulse has approximately 10 percent. Thus, attenuation or incorrect phase delay of the spectrum side-lobe energy will have less effect on the sine-squared pulse than on the rectangular pulse.

There are several practical questions related to the use of narrow-band filters for the suppression of spurious frequencies near the carrier frequency of pulsed radars. One of these is what the shape is, in the time domain, of the pulse reflected back to the RF power amplifier. A related question is whether this reflected pulse will interfere with proper operation of the power amplifier. Also, it is well known that high-power RF amplifier tubes such as are commonly used in pulsed radar have highest efficiency when operating at their maximum rated power output. If the RF power amplifier is driven or modulated to produce a shaped output pulse, the amplifier is not working at peak efficiency at all instants in time during the pulse, and thus the average efficiency will be reduced. Another way to obtain a rounded pulse would be to feed a rectangular pulse from the RF power amplifier into a narrow-band filter to suppress the spectrum side lobes, thus losing part of the pulse energy. It would be of interest to compare the over-all efficiencies of these two methods of obtaining a rounded output pulse.

REFERENCES

1. W. H. Kautz, "Transient Synthesis in the Time Domain," *IRE Trans. PGCT*-1, pp. 29-39 (September 1954).

2. S. Goldman, *Frequency Analysis, Modulation, and Noise*, p. 83 (McGraw-Hill Book Co., Inc., New York, N.Y., 1948).

3. M. F. Gardner and J. L. Barnes, *Transients in Linear Systems*, Vol. I, Chapter 3 (John Wiley and Sons, Inc., New York, N.Y., 1953).

4. L. A. Robinson, *et al*, "Suppression of Spurious Frequencies," Quarterly Progress Report 2, SRI Project 4096, Contract AF 30(602)-2734, Stanford Research Institute, Menlo Park, California (September 1962).

5. L. Young, *et al*, "Suppression of Spurious Frequencies," Quarterly Progress Report 4, SRI Project 4096, Contract AF 30(602)-2734, Stanford Research Institute, Menlo Park, California (June 1963).

6. S. B. Cohn, "Dissipation Loss in Multiple-Coupled-Resonator Filters," *Proc. IRE* 47, pp. 1342-1348 (August 1959).

7. S. B. Cohn, "Design Considerations for High-Power Microwave Filters," *IRE Trans. PGMTT*-7, pp. 149-153 (January 1959).

8. G. L. Matthaei, *et al.*, "Design Criteria for Microwave Filters and Coupling Structures," Final Report, SRI Project 2326, Contract DA 36-039 SC-74862, Stanford Research Institute, Menlo Park, California (January 1961).

REFERENCES

9. L. Weinberg, "Network Design by Use of Modern Synthesis Techniques and Tables," Tech. Memo. 427, Hughes Aircraft Company, Research Laboratories, Culver City, California (April 1956); also *Proceedings of the National Electronics Conference*, Vol. 12 (1956).

10. L. Weinberg, "Additional Tables for Design of Optimum Ladder Networks," Tech. Memo. 434, Hughes Aircraft Company, Research Laboratories, Culver City, California (31 August 1946); also *Journal of the Franklin Institute*, Vol. 264, pp. 7-23 and 127-138 (July and August 1957).

11. E. G. Fubini and E. A. Guillemin, "Minimum Insertion Loss Filters," *Proc. IRE* 47, pp. 37-41 (January 1959).

12. "Reference Data for Radio Engineers," p. 1012, 4th Edition, (American Book-Stratford Press, Inc., New York 1949).

13. *Ibid*, p. 1014.

14. Leo Young, "Suppression of Spurious Frequencies," Quarterly Progress Report 1, SRI Project 4096, Contract AF 30(602)-2734, Stanford Research Institute, Menlo Park, California (July 1962).

IX A THIN-FILM BOLOMETER*

A. GENERAL

A first step in reducing RFI emission from a microwave transmitter is the accurate determination of the total power in all the undesired frequency components traveling in the waveguide transmission line. A power meter that operates over an extremely broad band and does not discriminate against power in any mode that might exist within the measurement band would be a very useful RFI monitoring device. This section describes work done on developing a thin-film bolometer for that purpose.[1] In practice it would be used to measure the power in a waveguide from which the main output had been filtered out.[1,2]

Thin-film and wire bolometers of various forms have been used in the past as single-mode, waveguide, power-measuring devices.[3-7] These earlier forms, which did not cover the full cross-section of the waveguide, were inherently less sensitive to power in higher modes, the TE_{20} mode for example.

A film bolometer that covers the full waveguide cross-section, on the other hand, must intercept and therefore measure the flow of power, no matter what the mode or frequency. The ability of the film bolometer to measure the combined power in two modes at different frequencies, with minor loss of accuracy, was shown by the experiments described herein. Also separate power measurements were made on the TE_{10}, the TE_{01}, and the TE_{20} modes.

B. MATERIALS AND METHODS

A variety of different conductive film materials and substrates were used in experiments to devise a stable, sensitive bolometer film for S-band waveguide (2.840 × 1.340 inch I.D.). Figure IX-1 shows some sample films; the upper left film is silver paint on tracing paper, the upper right is gold on mica, the two center films are gold on glass mounted on

* This work is reported in more detail in Ref. 1. (References are listed at the end of the section.)

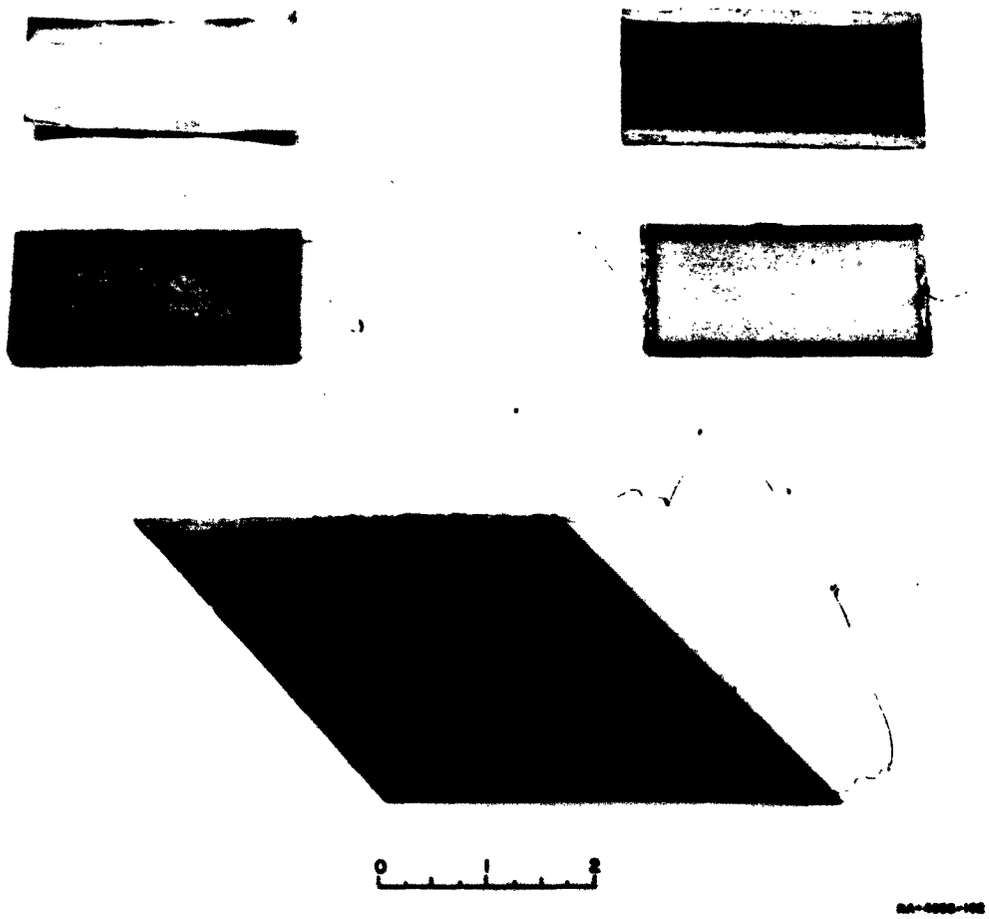

FIG. IX-1 FILM BOLOMETERS OF SEVERAL SHAPES AND MATERIALS

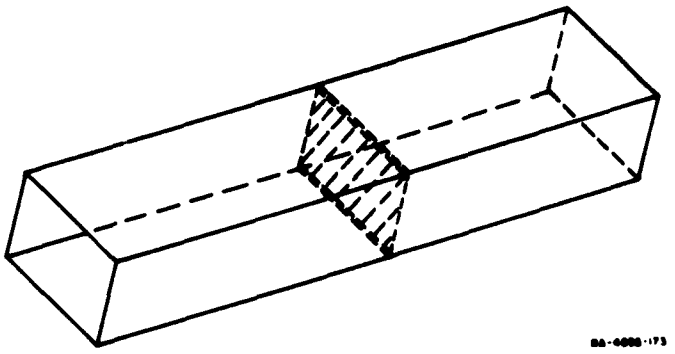

FIG. IX-2 TRANSVERSE FILM BOLOMETER

(but insulated from) metal frames and the lower film is gold on mica. The rectangular films were mounted as shown in Fig. IX-2, while the rhombic film was mounted as shown in Fig. IX-3. Both film shapes intercept, but do not completely absorb, the power flowing in the waveguide.

The conductive film was insulated from the waveguide in each case. A dc-substitution bridge that was constructed for the purpose was used to measure the microwave power absorbed by the film. (A commercial microwave power meter was used at first but was later found to be less accurate.) The bridge arms consisted of small adjustable wire-wound

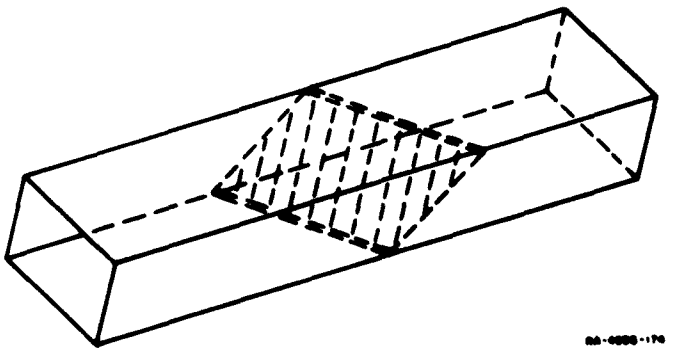

FIG. IX-3 RHOMBIC FILM BOLOMETER

power resistors. Film resistivities were of the order of 400 ohms per square for transverse films, which is approximately equal to the wave impedance (far from cutoff). The optimum film resistance for maximum power transfer to the film bolometer, with a matched source, is equal to the waveguide impedance when the film is backed by a properly spaced short circuit, and half the waveguide impedance when the film is backed by a matched load. Lower resistance values were found to be desirable for the rhombic film. Transfer of power to the bolometer was calculated from the measured forward power flow, the VSWR, and the measured or calculated power transmitted to the load (if any) behind the bolometer.

Tests were performed on waveguide film-bolometers at frequencies from *S*- through *X*-band and for the TE_{10}, TE_{01}, and TE_{20} modes, both for single frequencies and for combinations of two frequencies in cross-polarized modes. Mode suppressing septums were used for mixing the power in two frequencies and modes in a single film. The fraction of power absorbed by the film from each mode was calculated after first measuring the forward power in each mode and the VSWR of that mode. The total power absorbed by the film is the sum of the two calculated powers. This sum was then compared with the dc substitution power required to again balance the bridge.

C. POWER MEASUREMENTS WITH THIN-FILM BOLOMETERS

The most accurate results were obtained with a film mounted transversely across the waveguide. The average error was less than 1 db for all modes tested (the TE_{10}, TE_{01} and TE_{20} modes, either singly or in various combinations). The disadvantage of the transverse film is the relatively high VSWR (about 3:1) required for fairly efficient power transfer to the film.[1] The rhombic film permits matching into the waveguide (better input VSWR) but was found to measure rf power less accurately.

All measurements that were taken on one mode at a time with the aid of the dc bridge were finally sorted out according to mode and consolidated, with the following results. The average error for the TE_{10} was -1.8 db* (46 measurements). The average error for the TE_{01} mode was -1.0 db* (16 measurements). The average error for the TE_{20} mode was $+0.5$ db* (7 measurements).

* This value was obtained by averaging the results obtained with a variety of films and waveguide mounts at several frequencies.

The range of VSWR in all measurements was typically under 1.7 for rhombic films backed up by a matched load; some films showed a much better VSWR than that. Transverse films were typically less than 3.2 VSWR with matched load, although maximum power is transferred to the bolometer at 3.0 VSWR.

A simplified mathematical analysis of rectangular bolometer films with uniform and non-uniform dc and microwave power absorption patterns (in all combinations) leads to the conclusion,[1] that rhombic films are probably inherently less accurate because of the non-uniform absorption patterns for both dc and microwave power.

REFERENCES

1. Leo Young, E. G. Cristal, L. Robinson, and B. M. Schiffman, "Suppression of Spurious Frequencies," Quarterly Progress Report 4, Project 4096, Contract AF 30(602)-2734, Stanford Research Institute, Menlo Park, California (June 1963).
2. E. G. Cristal, Leo Young, and B. M. Schiffman, "Suppression of Spurious Frequencies," Quarterly Progress Report 3, pp. 63-98, SRI Project 4096, Contract AF 30(602)-2734, Stanford Research Institute, Menlo Park, California (January 1963).
3. J. Collard, "The Enthrakometer, An Instrument for the Measurement of Power in Rectangular Wave Guides," *Proc. IEE* (London) *93*, Part III-A, pp. 1399-1402 (1946).
4. J. A. Lane, "Transverse Film Bolometers for the Measurement of Power in Rectangular Waveguides," *Proc. IEE* (London) *105*, Part B, pp. 77-80 (January 1958).
5. I. Lenco and B. Regal, "Resistive Film Milli-Wattmeters for the Frequency Bands 8.2-12.4 Gc/s and 26.5-40 Gc/s," *Proc. IEE* (London) *107*, Part B, pp. 427-430 (September 1960).
6. J. A. Lane and D. M. Evans, "The Design and Performance of Transverse-Film Bolometers in Rectangular Waveguides," *Proc. IEE* (London) *108*, Part B, pp. 133-135 (January 1961).
7. L. E. Norton, "Broad-Band Power-Measuring Methods at Microwave Frequencies," *Proc. IRE* 37, pp. 759-766 (July 1949).

X CONCLUSIONS

Considerable progress has been made in the various studies which together make up the research described in this report. As some components reach a stage where they can be passed on to industry for production, other components remain at the experimental stage and require more research to turn them into practical devices. The waffle-iron filter is an example of the first kind, while the thin-film bolometer may be cited as an example of the second kind. Even as progress is made in the laboratory, other ideas evolve and new designs take shape and wait their turn to be tested experimentally. In parallel with the work on components, analytical studies yield new insights and a better understanding of the principles involved.

Work on the project has resulted in a waffle-iron filter with a wide, low-VSWR pass-band as well as a wide stop-band (see Sec. II). For instance, one filter had a pass-band VSWR of better than 1.20 over almost the whole of *L*-band. (The VSWR is better than 1.10 over a large portion of the band.) The power-handling capacity has been improved. For instance, one filter passes 8 megawatts of pulse power at *L*-band without pressurization. The stop-band remains as good as for the earlier filters, so that, for instance, one filter had a stop-band extending from the second to the tenth harmonic inclusive, while its pass-band VSWR was better than 1.15 over a 30-percent frequency band.

The coaxial leaky-wave filter described in Sec. III was found to be inherently wide-band; to be absorptive rather than reflective (generally less than 0.1 db reflection loss) in the stop-band; to have low VSWR and low attenuation in the pass-band (less than 1.08 VSWR and less than 0.2 db attenuation using the normal center conductor); and to provide high attenuation per unit length for an incident TEM wave (greater than 3.7 db/inch at its peak value using the normal center conductor) and for an incident TE_{11} wave of $\theta = \pi/2$ polarization* (greater than 4.9 db/inch at its peak value using the normal center conductor). The attenuation of both the TEM and TE_{11} modes can be increased without increasing the filter VSWR

* See Sec. III-C for the definition of polarizations of the TE_{11} mode.

or derating the peak power capacity of the filter, by using tapered center conductors that lower the filter impedance.

Under the specific conditions of the high-power tests that were made, the filter did not de-rate the peak power capacity of the coaxial line for filter impedances of from 50 to 20 ohms.

The attenuation of the filter has a relatively low rate of rise in the first octave above cutoff for the TEM mode. Also, the filter does not provide sufficient attenuation for the TE_{11} mode of $\theta = 0$ polarization (typically 10 db). If the coaxial leaky-wave filter is to be generally applicable for suppressing spurious energy of high-power transmitters, these defects must be corrected. One simple method that removes both defects simultaneously is to place two coaxial leaky-wave filters in tandem, oriented so that the slot-pairs of one filter are rotated 90 degrees relative to the slot-pairs of the other filter. This method would approximately double the attenuation for TEM waves, while the resultant attenuation of TE_{11} waves, for both $\theta = 0$ and $\pi/2$ polarizations, would be the sum of the attenuation of the $\theta = 0$ and $\pi/2$ polarizations given by Fig. III-6.

A second method of correcting the defects of slow attenuation rise and insufficient TE_{11} attenuation is to use a leaky-wave filter of a given cutoff frequency followed in tandem by a reflection filter having a slightly higher cutoff frequency. Because the leaky-wave filter acts as a matched pad in the stop-band, the reflection filter would be effectively isolated from the transmitter. In this method, the resulting attenuation in the stop-band would be approximately the sum of the attenuation of the reflection filter and leaky-wave filters when acting individually. In order for this method to be generally effective, the reflection filter should be wide-band, and should also be a multi-mode filter, although it could be a band-pass filter that is designed to attenuate a particular frequency band.*

Other methods might include (1) re-orienting the coupling slots so that they couple to the H_z field of the TE_{11} mode, and (2) using more sophisticated high-pass filters in place of the (absorbing) waveguides in order to improve the rate of rise of attenuation of TEM waves in the first octave above cutoff.

* This method was demonstrated experimentally at low power levels using the 1-5/8 inch coaxial leaky-wave filter and a 1-5/8 inch low pass coaxial reflection filter having a cutoff frequency of 2.5 Gc. Details are given in Quarterly Progress Report 3 on this contract.

The analysis of a waveguide leaky-wave filter structure over a limited frequency range (Sec. IV) has shown how the normalized attenuation constant (*i.e.*, the attenuation constant per unit length multiplied by the main waveguide width) depends on various design parameters. The dependence of the attenuation constant upon these parameters may be expected to follow the same general pattern in waveguide leaky-wave filters attenuating incident TE_{10}-mode energy. For the case of incident TE_{n0} modes ($n > 1$), the analysis should provide useful quantitative design data.

The results of the analysis are summarized in the following statements:

(1) The peak value of the normalized attenuation constant is approximately directly proportional to the absorbing waveguide height, and to the coupling slot width. For the range of design parameters investigated, the constant of proportionality varied only slightly.

(2) The frequency sensitivity of the normalized attenuation constant increases with increasing height of the absorbing waveguide.

(3) For a given slot width, the periodic *T*-junction is the least frequency-sensitive filter configuration.

(4) The normalized attenuation constant is approximately inversely proportional to the main waveguide height. For the range of design parameters investigated, the "constant" of proportionality was found to vary up to approximately 30 percent.

(5) The attenuation per unit length is very insensitive to small changes in the slot period. Thus, increasing the number of slots per unit length is not an effective method of increasing the attenuation of the filter. However, there is a tendency to increase the attenuation per unit length very slightly for smaller slot periods.

Leaky-wave filters absorb unwanted power while waffle-iron filters reflect it. Reflection filters may cause harmonic resonances and arcing in the presence of other mismatches, their attenuation may be reduced at the same time, and damage may even result to the transmitter. To avoid this, a harmonic pad should be inserted. A novel approach that has been explored with some success (Sec. V) is to use 0-db (at the fundamental frequency) directional couplers. Commercial short-slot sidewall couplers have been tested in the TE_{10}, TE_{01}, and TE_{20} modes, and offer a relatively inexpensive and effective solution.

A new "exact" design technique for band-stop filters was adapted for the design of a filter that is very well-matched in its pass-band and that highly attenuates specific harmonics of the pass-band center frequency. A harmonic suppression filter was constructed using stripline techniques, and it was found to bear out the theory (Sec. VI).

The dissipation loss in the pass-band of a filter is proportional to the group delay through the filter. Useful formulas have been derived, and "universal curves" were plotted, which should prove useful to the designer interested in time delay or dissipation loss, and will also help in estimating power-handling capacity (Sec. VIII).

At microwave frequencies, the method of suppressing pulse-spectrum side-lobe energy by means of narrow-band filters appears to be limited to very short pulses. This limitation results from the very narrow bandwidths, and thus the very high resonators Q's, that would be required for pulses of moderate length.

Study of the transmission of pulses through narrow-band filters indicates that transient-response characteristics do not provide a criterion for generally recommending any one filter type over others. The small differences between the filters, however, may make some filter types more suitable than others for specific applications. The transient responses of the equal-element, the 0.1-db equal-ripple, and the maximally flat filters to a rectangular input pulse are characterized by each having about the same overshoot, rise time, and delay time. On the other hand, the transient response of the maximally flat time-delay filter to a rectangular pulse has essentially no overshoot, but has somewhat slower rise time, and transmits less of the total available energy. For a sine-squared input pulse, none of the filters considered here have ringing at the peak of the output pulse. The equal-element, the 0.1-db equal-ripple, and the maximally flat filters do have ringing at the trailing edge of the pulse when the filter bandwidth is about the same as the width of the main lobe in the spectrum of the input sine-squared pulse. Under these same conditions, the maximally flat time-delay filter has essentially no ringing, but has a lower peak output amplitude.

Dissipation of energy within the filter has very little effect on the over-all shape of the output pulse for either rectangular or sine-squared input pulses. (These conclusions apply at least for the cases

where all resonators have equal unloaded Q's, and for dissipation loss sufficient to increase the mid-band transducer loss by 3 db, which were the situations investigated here.) Dissipation loss does, however, tend to reduce overshoot and undershoot, and to damp the ringing whenever these features are present in the output pulse.

If retention of the shape of a rectangular pulse is desired, the filter bandwidth must be several times the width of the main lobe of the input pulse spectrum, regardless of the type of filter used. Good retention of the shape of a sine-squared pulse is possible, however, with filter bandwidths only slightly greater than the width of the main lobe of the input pulse spectrum.

Microwave power measurements were made on thin-film bolometers over a very broad frequency range using several modes singly and in combinations (Sec. IX). The results of these measurements indicate that such bolometers are or can be made to be simple power-measuring devices that do not discriminate against any mode or frequency traveling in the waveguide.

ACKNOWLEDGMENTS

Many individuals contributed their ideas and technical skill to this project. Dr. G. L. Matthaei discussed the work frequently and provided many helpful ideas. Mr. M. Di Domenico assisted greatly with the early work on the new waffle-iron filters. Mr. R. B. Larrick and Mr. P. R. Reznek made most of the experimental measurements, and helped considerably in the design of the thin-film bolometer.

Mr. P. H. Omlor, Mrs. Suzanne B. Philp, Mr. Vahe Sagherian and Mr. Leonard Leving all helped in programming computations on the Burroughs Datatron 220. Mr. Jack Jennings supplied most of the evaporated metal films for use in the microwave bolometer.

The high-power tests were made at the Eitel-McCullough plant in San Carlos, with the continued cooperation of Dr. George Caryotakis.

SUBCONTRACT TO EITEL McCULLOUGH

In addition to the research at Stanford Research Institute, work was carried out at Eitel McCullough in San Carlos, California, on a subcontract to SRI, to investigate techniques for the suppression of the spurious emission within high-powered tubes. These investigations are described in four technical reports by Eitel McCullough.

The project leader at Eitel McCullough is Mr. Donald H. Preist.

APPENDIX

CONTENTS OF FOUR QUARTERLY PROGRESS REPORTS

APPENDIX

CONTENTS OF FOUR QUARTERLY PROGRESS REPORTS

QUARTERLY PROGRESS REPORT 4 (June 1963)

STANFORD RESEARCH INSTITUTE

MENLO PARK
CALIFORNIA

Regional Offices and Laboratories

Southern California Laboratories
820 Mission Street
South Pasadena, California

Washington Office
808–17th Street, N.W.
Washington 6, D.C.

New York Office
270 Park Avenue, Room 1770
New York 17, New York

Detroit Office
1025 East Maple Road
Birmingham, Michigan

European Office
Pelikanstrasse 37
Zurich 1, Switzerland

Japan Office
911 Iino Building
22, 2-chome, Uchisaiwai-cho, Chiyoda-ku
Tokyo, Japan

Representatives

Toronto, Ontario, Canada
[illegible]
Toronto 1, Ontario, Canada

Milan, Italy
Via Macedonio Melloni, 49
Milano, Italy